REPUBLIC OF IRAQ

MINISTRY OF HIGHER EDUCATION AND SCIENTIFIC RESEARCH
AL-FURAT AL-AWSAT TECHNICAL UNIVERSITY
ENGINEERING TECHNICAL COLLEGE NAJAF

EXPERIMENTAL STUDY THE EFFECT OF NANOPARTICLE FILL FINS OF HEAT EXCHANGER ON THE PRODUCTIVITY OF ADISTILLATION WATER

AHMED RAHEEM QAID

M.TECH
IN MECHANICAL ENGINEERING TECHNIQUES OF POWER

2022

EXPERIMENTAL STUDY THE EFFECT OF NANOPARTICLE FILL FINS OF HEAT EXCHANGER ON THE PRODUCTIVITY OF ADISTILLATION WATER

A THESIS

SUBMITTED TO THE DEPARTMENT OF MECHANICAL ENGINEERING TECHNIQUES OF POWER
IN PARTIAL FULFILLMENT OF THE REQUIREMENTS FOR
THE DEGREE OF MASTER OF THERMAL TECHNOLOGIES IN MECHANICAL ENGINEERING TECHNIQUES OF POWER
(M.TECH)

BY

AHMED RAHEEM QAID

Supervisor By

Prof. Dr. Ali Shakir Baqir

Asst. Prof Dr. Montadhar Aboodi Muhammed

2022

يَرْفَعِ اللَّهُ الَّذِينَ آمَنُوا مِنْكُمْ وَالَّذِينَ أُوتُوا الْعِلْمَ دَرَجَاتٍ وَاللَّهُ بِمَا تَعْمَلُونَ خَبِيرٌ

صدق الله العظيم

﴿المجادلة(11)﴾

DISCLAIMER

I confirm that the work submitted in this thesis is my own work and has not been submitted to other organization or for any other degree.

Signature:

Name: Ahmed Raheem Qaid

Date: / / 2022

ACKNOWLEDGMENT

All Praise to ALLAH for his uncountable blessings, assistance during the preparation of this work.

I want to submit my profound respects and sincere gratitude to my supervisors, **Prof. Dr. Ali Shakir Baqir** and **Asst. Prof Dr. Montadhar Aboodi Muhammed,** for their support during the research period and guidance to accomplish this work.

Special thanks to the Dean of the College, **Asst. Prof Dr.Hassanain Ghani Hameed**, as well as, a special thanks to the members and head of the Mechanical Power Techniques Engineering department , **Dr. Ahmed Salim Naser** for their support in this work. I would like to thank all lovely, helpful people who support me directly and indirectly to conduct this work. Special thanks to my collagenous for their great assistant and great encouragement.

My deepest thanks and gratitude are due to each family member, especially my dearest parents, and brothers for their patience, support, and encouragement throughout my life.

Ahmed Raheem Qaid
2022

SUPERVISORS CERTIFICATION

We certify that the thesis entitled "**Experimental Study The Effect of Nanoparticle Fill Fins of Heat Exchanger on the Productivity of a Distillation Water**" submitted by **Ahmed Raheem Qaid** has been prepared under our supervision at the Department of Mechanical Engineering Techniques of Power, College of Technical Engineering-Najaf, AL-Furat Al-Awsat Technical University, as partial fulfillment of the requirements for the degree of Master of Techniques in Thermal Engineering.

Signature:

Name: Prof. Dr. Ali Shakir Baqir

(Supervisor)

Date: / / 2022

Signature:

Name: Asst. Prof Dr. Montadhar Aboodi Muhammed

(Supervisor)

Date: / / 2022

In view of the available recommendation, we forward this thesis for debate by the examining committee.

Signature:

Name: Dr. Ahmed Salim Naser

Head mechanical Eng Tech of power Dept.

Date: / / 2022

COMMITTEE CERTIFICATION

We certify that we have read the thesis entitled " **Experimental Study The Effect of Nanoparticle Fill Fins of Heat Exchanger on the Productivity of a Distillation Water** " submitted by **Ahmed Raheem Qaid** and, as examining committee, examined the student's thesis in its contents. And that, in our opinion, it is adequate as a thesis for the degree of Master of Techniques in Thermal Engineering.

Signature:

Name: Prof. Dr. Ali Shakir Baqir

(Supervisor)

Date: / / 2021

Signature:

Name: Asst. Prof Dr. Montadhar Aboodi Muhammed

(Supervisor)

Date: / / 2022

Signature:

Name: Asst. Prof.Dr.Mahdi Hatf Kadhum

(Member)

Date: / / 2022

Signature:

Name: Asst. Prof.Dr.Basim Hameed A.Freegah

(Member)

Date: / / 2022

Signature:

Name: Asst. Prof.Dr.Basim HameedA.Freegah

(Chairman)

Date: / / 2022

Approval of the Engineering Technical College- Najaf

Signature:

Name: Asst. Prof. Dr. Hassanain Ghani Hameed

Dean of Engineering Technical College- Najaf

Date: / / 2022

LINGUISTIC CERTIFICATION

This is to certify that this thesis entitled "**Experimental Study The Effect of Nanoparticle Fill Fins of Heat Exchanger on the Productivity of a Distillation Water**" was reviewed linguistically. Its language was amended to meet the style of the English language.

Signature:

Name:

Date:

ABSTRACT

Solar energy is an important alternative energy source, especially for countries that have a lot of solar radiation intensity such as Iraq. One of the ways to benefit from solar energy is to use parabolic dish concentrators. The current study aims to distill saline water using solar energy through the use of the concentrator of the solar parabolic dish, as well as, working on improving the productivity of the solar water distillation system through the use of an innovative heat exchanger that contains internal fins to increase the surface area exposed to heat transfer. A novel design for solar heat exchanger was proposed and manufactured to produce a lot of amount of distilled water. In this experiment, two models of heat exchangers were used, the first containing internal fins of aluminum, and the second containing internal fins with a nano-filling of multi-walled carbon nanotube (MWCT) which has a superior thermal conductivity. Where an innovative method was employed by inserting nanomaterials inside the fins of the internal heat exchanger. Where the inner fins of the heat exchanger are filled with a nano-material (MWCT) with a very high thermal conductivity 3500W/m.k. The experiments showed that the use of nano-filling contributed significantly to increasing the productivity of the solar water distillation system. The average rate of increase in productivity between these two models for the days in which the experiments were conducted was 57.67%. The greatest productivity when using the heat exchanger (fins without nano) are 10.17 liters / day at average solar radiation was 817.8W/m^2, with the average working hours of the distillation system of 6 hours. The maximum productivity of the distillation system when using the second model of the heat exchanger (fins with nano-filling) is reached 16.11 liters/day, with an average intensity of solar radiation 820.33 W/m^2.

CONTENTS

DISCLAIMER ..... **I**
ACKNOWLEDGMENT ..... **II**
SUPERVISORS CERTIFICATION ..... **III**
COMMITTEE CERTIFICATION ..... **IV**
LINGUISTIC CERTIFICATION ..... **V**
ABSTRACT ..... **VI**
CONTENTS ..... **VII**
LIST OF TABLES ..... **IX**
LIST OF FIGURES ..... **XI**
NOMENCLATURE ..... **XV**
CHAPTER ONE **1**
1.1INTRODUCTION **1**
1.2 History of Concentrated Solar Power **2**
1.3 Solar radiation distribution **4**
1.4 Solar Technologies Type **7**
1.5 Solar Concentrators **7**
1.5.1 Parabolic-trough collectors(PTC) **7**
1.5.2 Linear Fresnel Reflector (LFR) **8**
1.5.3 Heliostate Solar Tower **9**
1.5.4 Parabolic Dish collectors (PDC) **10**
1.6 Problem statement and Objectives Of The Thesis **12**
1.7 Thesis Outline **13**
CHAPTER TWO **14**
LITERATURE REVIEW **14**
INTRODUCTION **14**
2.1 Water desalination **14**
2.2 Nanomaterials and their use in solar water desalination **30**
2.3 Sumary of literature review **31**
2.3 Scope of The Present Work **33**

CHAPTER THREE 35
MATHEMATICAL MODEL 35
3.1INTRODUCTION 35
3.2 Geometrical analysis model of the parabolic dish 35
3.3 Model for optical analysis 37
3.4 Model for thermal analysis 38
3.5 Calculation's procedure 41
CHAPTER FOUR 42
4.1INTRODUCTION 42
4.2 Materials and methods 42
4.2.1 Parabolic Dish collector (PDC) 44
4.2.2 Reflective material 45
4.2.3 Absorber 46
4.2.4 Multi Walled Carbon Nanotubes (MWCT) 52
4.2.5 Frame and Support Structure 53
4.2.6 Solar Tracking system 53
4.2.7 Steam condensing system 56
4.3 Measurement Devices 58
4.3.1 Data Logger 58
4.3.2 Temperature sensors 59
4.3.3 Measurement of the intensity of solar radiation 60
4.3.4 Measuring ambient temperature and wind speed 60
4.3.5 Error analysis 61
4.4 Thermal camera test 61
4.5 Experimental procedure 62
CHAPTER FIVE 64
INTRODUCTION 64
5.1 Sources of Solar heat with fins 64
5.1.1 Water Productivity 64
5.1.2 Temperature of working fluid 69
5.1.3 Surface Temperature of Heat Exchanger absorber 71
5.2 Sources of Solar heat with fins Filling/Nanomaterial 72

5.2.1 Water Productivity **72**
5.2.2 Temperature of working fluid **77**
5.2.3 Surface Temperature of Heat Exchanger absorber **78**
5.3 Effect of Using Nanomaterial on Thermal Performance of Heat Exchanger **80**
5.3.1 Water Productivity **81**
5.3.2 Temperature of working fluid **85**
5.3.3 Surface Temperature of Heat Exchanger absorber **89**
5.4 Heat losses from the heat exchanger **92**
CHAPTER SIX **99**
CONCLUSIONS AND RECOMMENDATIONS **99**
INTRODUCTION **99**
6.2 Recommendations **101**
REFERENCE: **102**
APPENDIXES .....
Appendix (A): Heat loss from heat exchanger .....
Appendix (B): List of Publications .....
الخلاصة .....

LIST OF TABLES

CHAPTER TWO

Table 2.1: Specifications of the three experiments……..……...28
Table 2.2: Summary of the productivity of some solar distillation systems……...32

CHAPTER FOUR

Table 4.1: Summary of the dimensions of the solar parabolic dish distillation system. ……...56

CHAPTER FIVE

Table 5.1: Variation of the productivity of the distillation system during the days of experiments 69

Table 5.2: shows the productivity of the solar distillation system for the different days of experiments and using the heat exchanger (absorber) with nano-filling 77

APPENDIX

Table A.1: Heat loss for the experiment conducted on 3/17/2022(Fins without nano filling).
Table A.2: Heat loss for the experiment conducted on 24/4/2022) Fins without nano filling).
Table A.3: Heat loss for the experiment conducted on 3/5/2022) Fins without nano filling).
Table A.4: Heat loss for the experiment conducted on 13/5/2022) Fins without nano filling).
Table A.5: Heat loss for the experiment conducted on 18/3/2022) Fins with nano filling)
Table A.6: Heat loss for the experiment conducted on 25/4/2022) Fins with nano filling)
Table A.7: Heat loss for the experiment conducted on 6/5/2022) Fins with nano filling)
Table A.8: Heat loss for the experiment conducted on 14/5/2022) Fins with nano filling)

LIST OF FIGURES

CHAPTER ONE

Figure 1.1Archimedes' mirror used to burn Roman ships [13]:. 2
Figure 1.2:Augustin Mouchot'scondensed at the Paris Exhibition in 1878 [14].……..…..3
Figure 1.3: John Ericsson's Solar Engines [14].. 4
Figure 1.4: Earth's horizontal solar radiation map[16].. 5
Figure 1.5: direct solar radiation to the earth[16].. 5
Figure 1.6: Map of global horizontal solar irradiation on Iraq[16].. 6
Figure 1.7: Map of direct normal solar irradiation on Iraq[16].. 6
Figure 1.8: Parabolic trough solar collector[10].. 8
Figure 1.9: Linear Fresnel Reflector[20].. 9
Figure 1.10: Solar tower power generation of Gemasolar plant owned by Torresol Energy, Spain. Picture provided by SENER, Spain, 2018..... 10
Figure 1.11: Parabolic dish concentrates..... 12

CHAPTER TWO

Figure 2.1:Schematic diagram of the developed point-focus solar still [1]……..……15
Figure 2.2: Variation of distillate production rate with weather data (day: 18-10-2013, the salinity of water: 20 g/kg) [1]…….15
Figure 2.3: Production of distilled water (milliliters) at various times of the day (Rig 1) [22]. 16
Figure 2.4: Production of distilled water (milliliters) at various times of the day (Rig 2) [22]. 17
Figure 2.5: The triple basin desalination system [42]. 22
Figure 2.6: In TBSS, numerous parameters vary hourly [42]..... 22
Figure 2.7: For various scenarios, a comparison of daily accumulated freshwater production is made [39]..... 25
Figure 2.8: Productivity during the test period (hourly)[41]..... 27
Figure 2.9: Inlet and outlet temprature of working fluid [41]..... 28
Figure 2.10: Productivity and intensity of solar radiation[43]..... 30

CHAPTER THREE

Figure 3.1: Geometrical parameters[60]. 36
Figure 3.2: Schematic of the parabolic dish thermal powers[58]. 39

CHAPTER FOUR

Figure 4.1: Location of experimental test. 42
Figure 4.2: Schematic diagram of the parts of the experiment. 43
Figure 4.3:. Photograph of the solar distillation system 44
Figure 4.4: Photograph of a parabolic dish (antenna). 45
Figure 4.5: Parabolic dish after covering its surface with glass mirrors 46
Figure 4.6: Heat exchanger (absorber) before thermal insulation. 47
Figure 4.7: Steam generator cover with fins. 48
Figure 4.8: Inner holes for the fins of the heat exchanger (absorber). 49
Figure 4.9: The process of filling nanomaterial into the inner holes of the fin. 50
Figure 4.10: The process of welding the fins after filling them with nanomaterial. 50
Figure 4.11: The final shape of the fin after filling it with nano-material and welding it. 51
Figure 4.12: Heat exchanger cover (absorber) final shape. 51
Figure 4.13: Carbon nanoparticles used in the experiment 52
Figure 4.14: Frame and Support Structure. 53
Figure 4.15: DC motor. 54
Figure 4.16: LDR sensor. 55
Figure 4.17: The electronic circuit of the solar tracking system. 55
Figure 4.18: a steam condensing system. 56
Figure 4.19: Picolog-6 data logger with 8-thermocouples. 58
Figure 4.20: Temperature sensors. 59
Figure 4.21: Solar Transmission & Power meter SP2065. 60
Figure 4.22: Anemometer Plus AR836. 61
Figure 4.23: Thermal camera result. 62

CHAPTER FIVE

Figure 5.1: Variation of the productivity of the solar distillation system with the environmental conditions for a day (17/3/2022). 65
Figure 5.2: Variation of the productivity of the solar distillation system with the environmental conditions for a day (24/4/2022). 66
Figure 5.3: Variation of the productivity of the solar distillation system with the environmental conditions for a day (3/5/2022). 67
Figure 5.4: Variation of the productivity of the solar distillation system with the environmental conditions for a day (13/5/2022). 68

Figure 5.5: Variation of water temperatures inside the heat exchanger (absorber) at the start of the experiment at 9:00 70
Figure 5.6: Variation in the temperature of the heat exchanger cover when the system starts operating at 9:00. 71
Figure 5.7: Variation of the productivity of the solar distillation system with the environmental conditions for a day (18/3/2022). 73
Figure 5.8: Variation of the productivity of the solar distillation system with the environmental conditions for a day (25/4/2022). 74
Figure 5.9: Variation of the productivity of the solar distillation system with the environmental conditions for a day (6/5/2022). 75
Figure 5.10: Variation of the productivity of the solar distillation system with the environmental conditions for a day (14/5/2022). 76
Figure 5.11: Variation of water temperature inside the heat exchanger 78
Figure 5.12: Variation in the temperature of the heat exchanger cover when starting the system. 80
Figure 5.13: Comparison between the outputs of the distillation system using both models of the heat exchanger for the days of 17/3/2022 & 18/3/2022. 81
Figure 5.14: Comparison between the outputs of the distillation system using both models of the heat exchanger for the days of 24/4/2022 & 25/4/2022. 82
Figure 5.15: Comparison between the outputs of the distillation system using both models of the heat exchanger for the days of 3/5/2022 & 6/5/2022. 83
Figure 5.16: Comparison between the outputs of the distillation system using both models of the heat exchanger for the days of 13/5/2022 & 14/5/2022 85
Figure 5.17: Comparison of the water temperature inside the heat exchanger when the system starts operating between 17/3/2022 and 18/3/2022. 86
Figure 5.18: Comparison of the water temperature inside the heat exchanger when the system starts operating between 24/4/2022 and 25/4/2022. 87
Figure 5.19: Comparison of the water temperature inside the heat exchanger when the system starts operating between 3/5/2022 and 6/5/2022. 87
Figure 5.20: Comparison of the water temperature inside the heat exchanger when the system starts operating between 13/5/2022 and 14/5/2022. 88
Figure 5.21: Comparison of the temperatures of the heat exchanger cover during the start of operation of the solar distillation system between 17/3/2022 and 18/3/2022 89
Figure 5.22: Comparison of the temperatures of the heat exchanger cover during the start of operation of the solar distillation system between 24/4/2022 and 25/4/2022. 90

Figure 5.23: Comparison of the temperatures of the heat exchanger cover during the start of operation of the solar distillation system between 3/5/2022 and 6/5/2022. 90
Figure 5.24: Comparison of the temperatures of the heat exchanger cover during the start of operation of the solar distillation system between 13/5/2022 and 14/5/2022. 91
Figure 5.25: The average heat loss for the experiments carried out using the first model of the heat exchanger. 93
Figure 5.26: The average heat loss for the experiments carried out using the second model of the heat exchanger 93
Figure 5.27: Variation of heat loss with environmental conditions for the day 17-3-2022.....94
Figure 5.28: Variation of heat loss with environmental conditions for the day 24-4-2022.....94
Figure 5.29: Variation of heat loss with environmental conditions for the day 3-5-2022. 95
Figure 5.30: Variation of heat loss with environmental conditions for the day 13-5-2022.....95
Figure 5.31: Variation of heat loss with environmental conditions for the day 18-3-2022.....96
Figure 5.32: Variation of heat loss with environmental conditions for the day 25-4-2022.....96
Figure 5.33: Variation of heat loss with environmental conditions for the day 6-5-2022. 97
Figure 5.34: Variation of heat loss with environmental conditions for the day 14-5-2022.....97

NOMENCLATURE

Symbol	Definition	Unit
A_a	Aperture area of a parabolic dish	m^2
A_{abs}	The area of the absorber	m^2
A_t	Area that shaded by the receiver on the concentrator	m^2
C_{RO}	Optical focus	-
C_{pW}	Specific heat of water	kJ/kg K
C_R	Geometrical concentration ratio	-
d	Aperture diameter diameter of dish	m
f	Focal length for parabolic dish	m
h	Depth of the parabolic dish	m
h_{air}	The heat convection coefficient	$W/m^2.K$
I_{abs}	solar radiation absorbed by the heat exchanger	W/m^2
I_b	Beam solar intensity falling on an aperture area of the dish	W/m^2
$I_{b\ av}$	Average solar intensity	W/m^2
k	Thermal conductivity	W/m.K
m_w	Mass of water	Kg
Q_{abs}	The amount of energy received by the absorber	W
Q_s	The amount of energy received by the aperture area	W
Q_{usufl}	The useful heat absorbed	W
Q_l	The rate of thermal losses	W
Q_{rad}	Heat loss by radiation	W
Q_{conv}	Heat loss by convection	W
S	The surface area of this parabola	m^2
t, Δt	Time required to achieve the maximum temperature of the water	Second
T_{abs}	Absorbed surface temperature	K
T_{ambint}	Ambient air temperature	K
T_{w1}	Initial water temperature	K
T_{w2}	Final water temperature	K
Δ_{Tf}	Difference between the maximum water temperature and ambient air temperature	K
Greek Symbols		
η^o	Optical efficiency	-
ρ	Reflectivity of the parabolic dish	-
γ	The receiver intercept factor	-
θ	The angle of incidence of solar radiation	-
λ	The un-shading coefficient or shape factor	-

$\tau\alpha$	The transmittance– absorptance product	-
η_u	Overall thermal efficiency (%)	-

Abbreviations	
Symbols	**Description**
CSP	Concentrators solar power
PVC	Photovoltaic cells
PTC	Parabolic-trough collectors
PVC	Polyvinyl chloride
LFR	Linear Fresnel Reflector
PDC	Parabolic Dish collectors
HDD	Humidification and dehumidification desalination system
TBSS	Triple basin glass solar still
MWCNT	Multi-wall carbon nanotube
TDS	Total Dissolved Solids
LDR	Light Dependent Resistor

Chapter One

Introduction

CHAPTER ONE

INTRODUCTION

1.1 Introduction

Water and energy sources lack are of the most important issues -facing the world especially in the underdeveloped countries. The population increase and the increase of demand for water and power have led to the scarcity of these two essential elements for the sustainability of life on the planet's surface. Water constitutes an estimated 71% of the planet's total area, but most of this water is not suitable for human daily consumption directly because is salty water. The amount of salty water is estimated to be 96.54%, while less than 4% is freshwater, However, Even freshwater is not fully usable because is polluted or inaccessible.[1].

The lack of freshwater inspired the researchers to find techniques in order to obtain a suitable amount of fresh water from the salty water. The term (water desalination) refers to any process that removes salts and other minerals from water and makes it suitable for daily life consumption. Many methods are used in the desalination process, and one of these methods is solar distillation. Which is one of the most appropriate solutions to purify water especially in areas regions that received a high of solar energy [1-9].

Energy supply, in turn, is also of the problems facing humans, where humans currently use a number of fossil fuels, their use causes many economic, environmental, and health problems, as fossil fuels constitute 84.32% of the total energy consumed in the world for the year 2019[10].

It is known that the remnants combustion of fossil fuels contribute to the aggravation of the environmental situation of the planet, and the amount of pollution resulting from the use of this type of fuel, as its combustion produces many gases that cause global warming such as carbon dioxide as well as sulfur dioxide that generates aerosols that are considered highly toxic. Which results in millions of deaths annually [11]

In general, there are two ways to benefit from solar energy, namely, direct transmission by converting solar radiation into electrical energy through the use of photovoltaic cells, indirect use is represented by utilizing solar thermal energy in many areas such as heating, cooking and water desalination processes[12].

1.2 History of Concentrated Solar Power

It is believed that the Greek scientist Archimedes (282 -212) B.C. used sunlight to destroy the invading Roman ships in this manner, as depicted in Figure(1.1) [13]

Figure (1.1): Archimedes' mirror used to burn Roman ships[13]

During the years 1852 through 1871 , Augustin Mouchot working as a secondary school mathematics teacher, has conducted experiments on the conversion of solar energy into usable work. Mouchot's solar energy concepts were so practical that he was able to secure the funding of the French government to pursue them full-time. The apparatus was presented during the 1878 Universal Exhibition in Paris, and it was hailed as the most inspirational demonstration ever (Figure 1.2)[14].

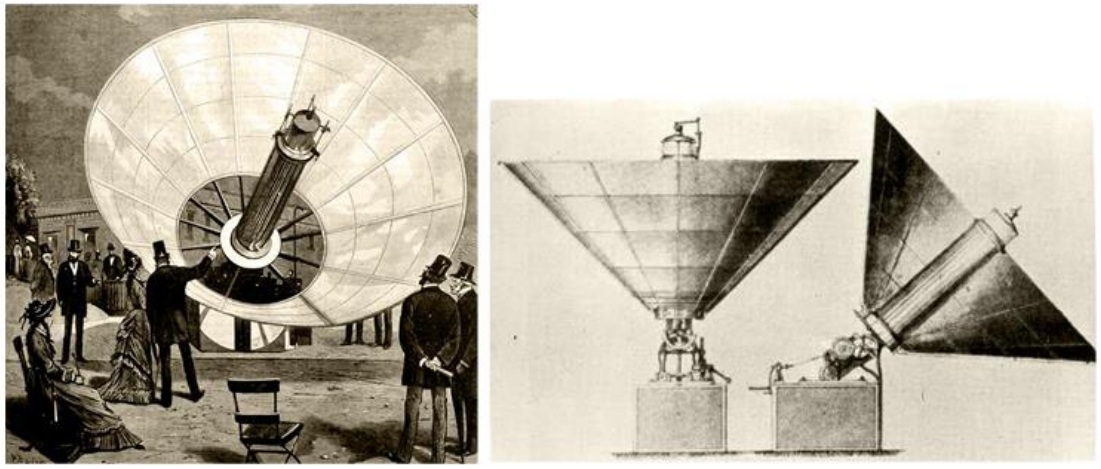

Figure (1.2): Augustin Mouchot'scondensed at the Paris Exhibition in 1878[14].

Because of the low costs of coal mining in that period, support for his project was stopped[14].

During the 1870s and 1880s, the inventor and engineer; John Ericsson; was working on developing a solar-powered heat engine that could be used in conjunction with a traditional gas-fueled power source[14].

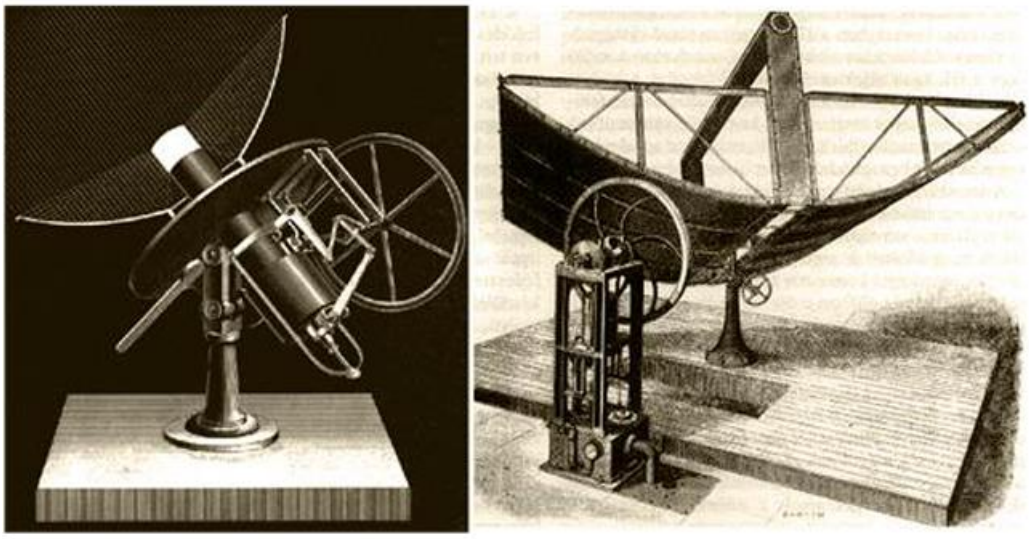

Figure (1.3): John Ericsson's Solar Engines [14].

Both Mouchot and Ericsson were instrumental in developing concentrated solar energy as a renewable energy source. They discovered that the availability of fossil-fuel resources limited the demand for fossil-fuel electricity. Eventually, the globe would look into solar energy as a viable and environmentally friendly source of energy creation. The works of Mouchot, Pierre, and Ericsson served as inspiration for future scientists who designed the modern Concentrating Solar Power (CSP) Technologies that are currently in use[14].

1.3 Solar radiation distribution

Solar radiation distribution varies by location in terms of latitude and longitude. As illustrated in (Figure 1.4), some locations receive an abundance of solar radiation. However, the distribution of worldwide horizontal solar radiation fluctuates annually from (803-2702) kWh/m^2. In addition, the global distribution of direct sun irradiances (Figure 1.5) is around (356-3652) kWh/m^2, this can be represented as a huge irradiance that can be utilized for a variety of applications[15,16].

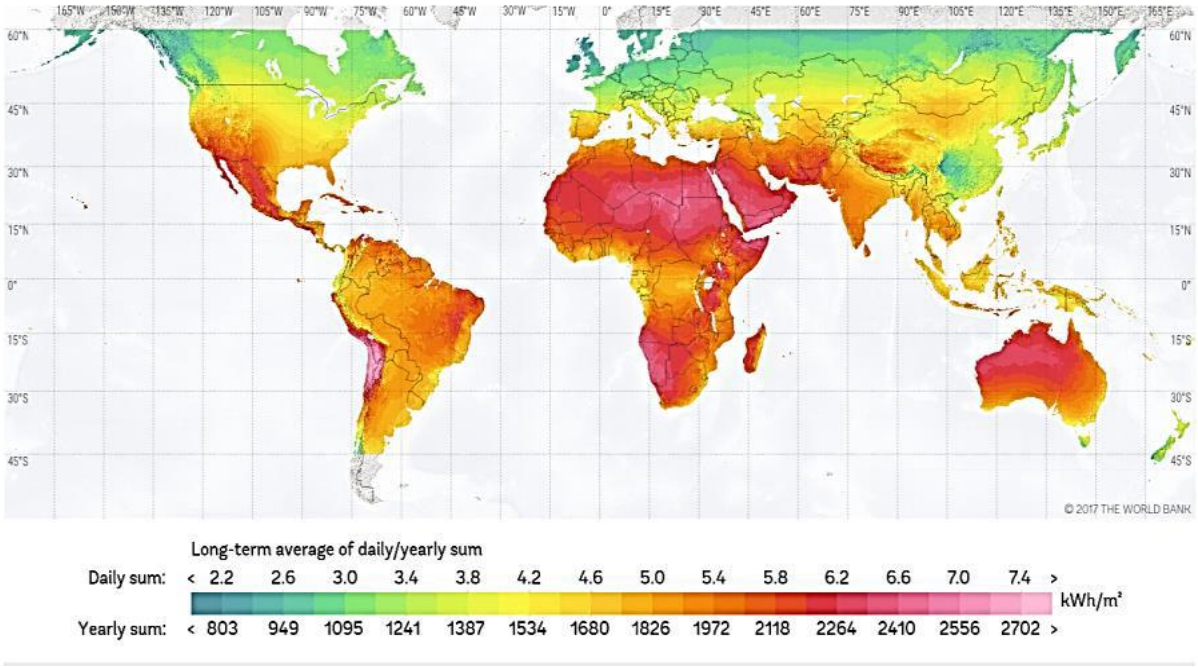

Figure (1.4): Earth's horizontal solar radiation map[16].

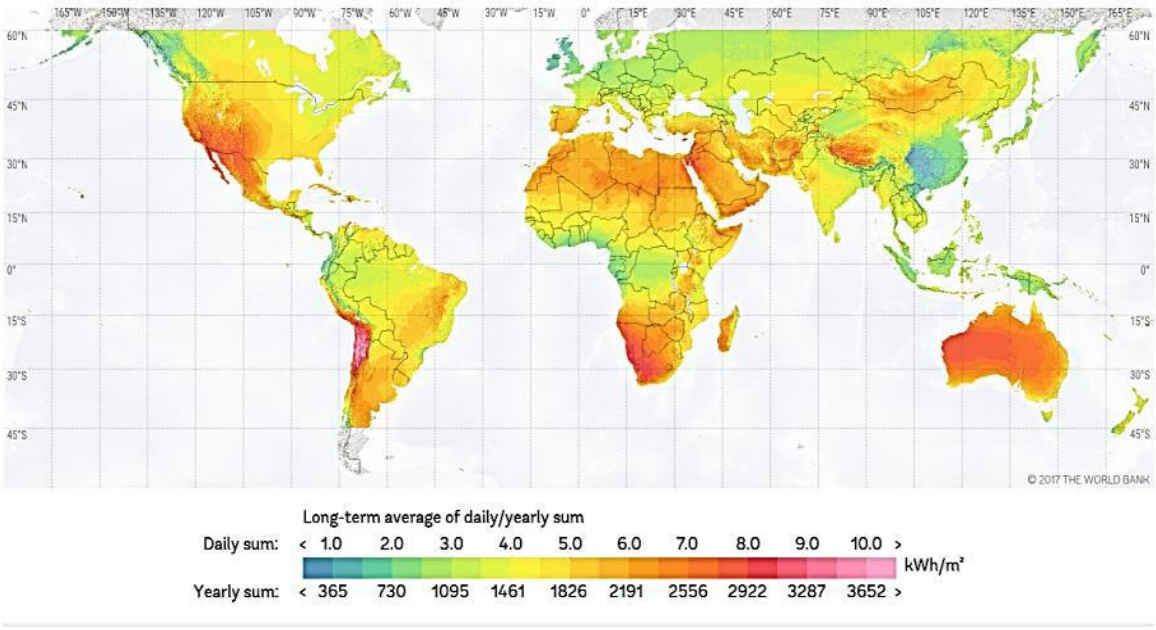

Figure (1.5): direct solar radiation to the earth [16]

Iraq's geographic location (32.1°N / 44.19°E) has enabled it to receive a yearly quantity of horizontal radiation (1753-2191) KWh/m^2 (Figure 1.5), while the annual amount of direct solar radiation is about (1706-2483) KWh/m^2 (Figure1.7), This amount solar radiation, which can be exploited for a variety of applications [17].

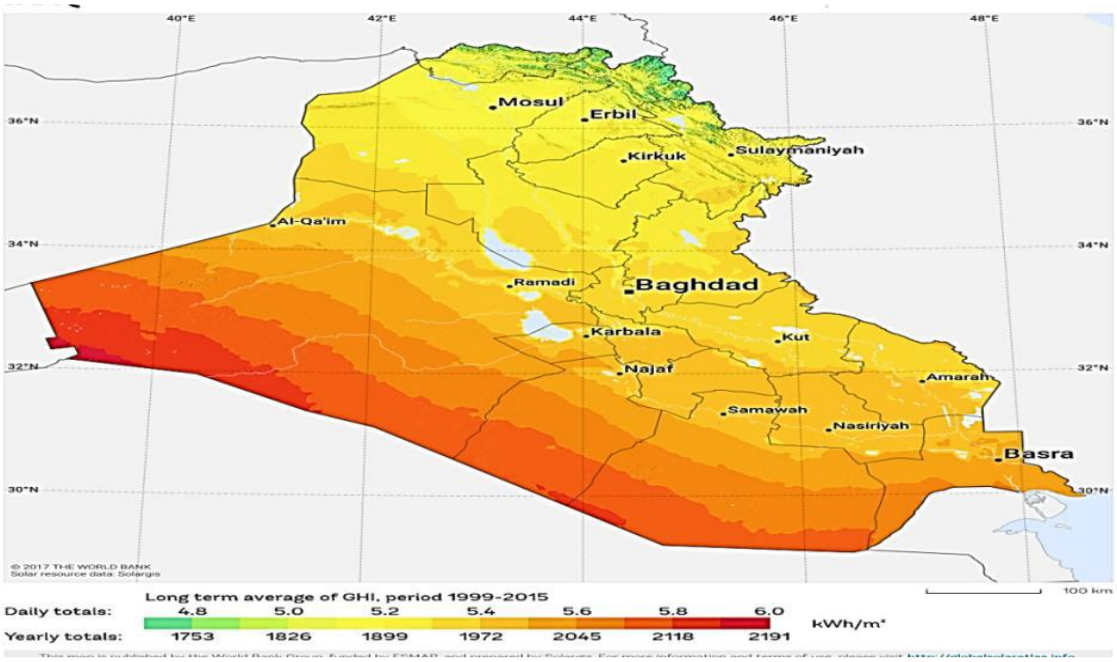

Figure (1.6): Map of global horizontal solar irradiation on Iraq [16]

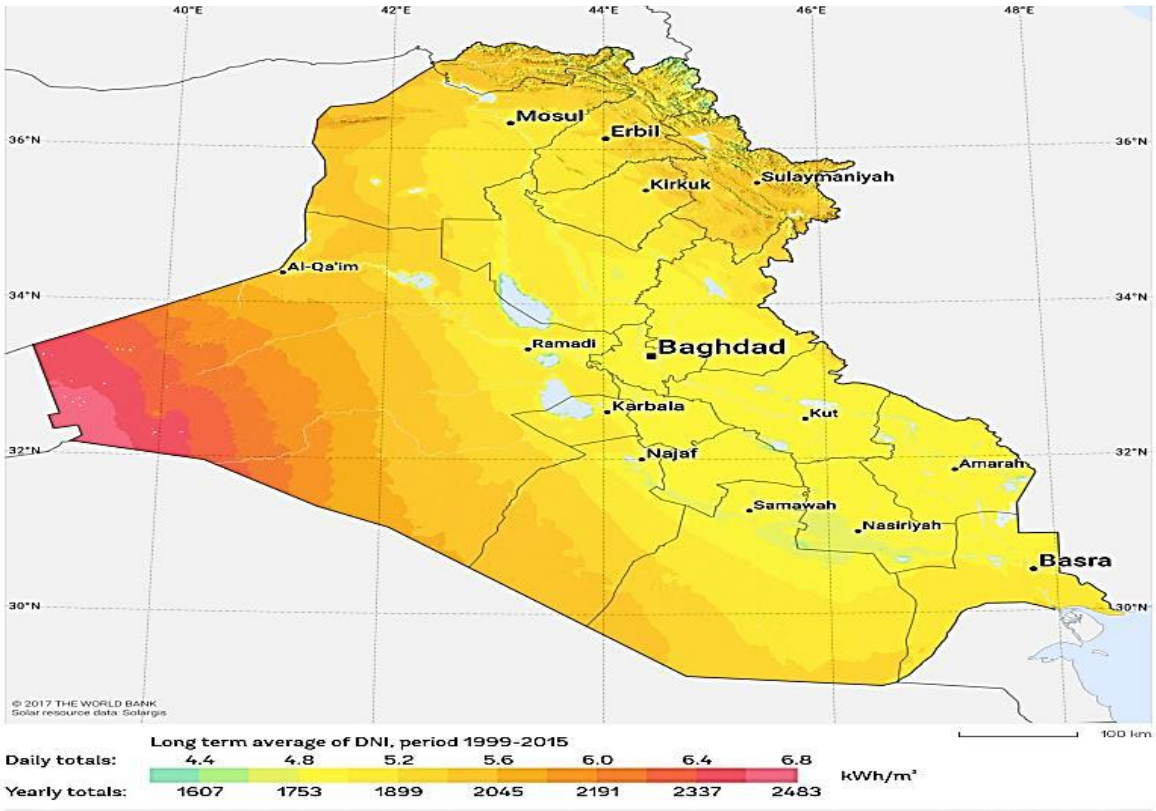

Figure (1.7): Map of direct normal solar irradiation on Iraq [16].

1.4 Solar Technologies Type

There are several solar energy technologies in use, however; the most common use is the photovoltaic cells (PVC) and concentrators of solar energy [18]. Photovoltaic (PV) solar cells are characterized by their small size compared to solar energy concentrators. Still, at the same time, the cost of manufacturing and using them is considered high compared to the energy produced. As for the concentrators of solar energy, they can be used in many fields, such as the production of electric power also and for the process of heating, cooking, and water distillation operations[19].

1.5 Solar Concentrators

The solar concentrator is a system for concentrating solar energy, there are many types of solar concentrators which can be employed in many fields such as electric power generation, water distillation, cooking, heating water. The following types explain solar concentrators:

1.5.1 Parabolic-trough collectors(PTC)

A sheet of a reflective material is bent into a parabolic form to create a parabolic trough collector (PTC). Along the focal line of the receiver, a black metal tube is installed, which is covered with a glass tube to decrease heat losses. It is sufficient to track the sun on a single axis, resulting in lengthy collector modules. The collector can be set up to track the sun from north to south in an east-west orientation[20].

A horizontal north-south trough field gathers significantly more energy than a horizontal east-west collector over the course of a year. The north-south field, on the other hand, collects a lot of energy in the summer and much less in the winter. The east-west field collects more energy in the winter and less in the summer than a north-

south field, resulting in a more consistent annual production. As a result, the best orientation is determined by the application and whether more energy is required in the summer or winter. PTCs are the most developed solar technology for generating heat at temperatures up to $400c^o$ for solar thermal power production or process heat applications, They may also produce heat at temperatures ranging from 50 to 400 c^o.However, today's operational temperatures are limited to 400°C due to the usage of oil-based heat transfer media, resulting in only modest steam quality[20].

Figure(1.8): Parabolic trough solar collector [10].

1.5.2 Linear Fresnel Reflector (LFR)

Linear Fresnel Reflector (LFR) depends on a group of mirrors arranged in a unilateral way that reflects the sun's rays to the receiving tube.

These mirrors are usually placed close to the ground in order to avoid wind loads, and in this type of concentrator, a temperature of 275℃can be achieved.

Figure (1.9): Linear Fresnel Reflector[20].

Among the advantages of a linear Fresnel reflector are the following:

- It can be combined with a fossil-fuel-powered system if the sun does not shine due to weather factors.
- Less expensive in manufacturing than other types of solar concentrators, as the used mirrors are less expensive than those used from concentrators of solar energy.
- Resistant to weather factors (wind), as well as not needing immense structures to install it as it is close to the ground [21].

However, the productivity of this type of solar condensers is low compared to other types of condensers, and this is considered one of the disadvantages[18].

1.5.3 Heliostate Solar Tower

It is one of the ways to benefit from solar energy, as it works to benefit from the thermal energy associated with sunlight. It consists of a group of parabolic mirrors that reflect the sun's rays falling on them to a central receiver (absorber) installed on a high tower.Figure (1.10) shows Heliosteite Tower. There are many liquids that can be used to transfer enthalpy into the central receiver (absorber), such

as water, water and dissolved salt. Where it is possible to benefit from the steam generated in the rotation of steam turbines used in the generation of electric power. The steam generated can be used to rotate the steam turbines used in the generation of electric power, and it is characterized by its ability to generate high temperatures exceeding 1000 Celsius, which helps to integrate it with electric power plants operating in the combined Rankine cycle, which can contribute to reducing the costs of generated electricity.

Figure (1.10): Solar tower power generation of Gemasolar plant owned by Torresol Energy, Spain. Picture provided by SENER, Spain, 2018.

1.5.4 Parabolic Dish collectors (PDC)

A parabolic dish reflector is a point-focus collector that follows the sun in two directions and concentrates solar energy on an endothermic receiver at the dish's focal point. To reflect the solar radiation gathered by the dish onto the receiver, the dish must fully track the sun [21].

The thermal receiver takes the beam solar energy and turns it into thermal energy, which can be used for cooking, heating water, and sterilization, as in the parabolic solar cooker. Alternatively, it can be converted into electrical energy using a generator engine directly linked to the receiver or transported as heat to a centralized power transmission system via tubes. Using equivalent concentration methods, temperatures over 1500 °C can be reached [21].

- It is the most efficient collector system because it always points to the sun.
- They have concentration collectors and thermal receiver units that can operate independently or as part of a lamore extensiveystem of concentrating dishes.

The concentrated solar energy absorbed from the individual thermal receivers is collected and transferred through the heat transfer fluid to the energy conversion systems in parabolic dish systems that generate electricity from a central transducer. The circulation of the heat transfer fluid across the collector field design considerations, such as piping architecture, pumping needs, and thermal losses, must all be taken into account. The Stirling engine is the most common form of heat engine used in dish drive systems, but it has yet to acquire a particular level of dependability and large production [20].

Figure (1.11): Parabolic dish concentration[20].

1.6 Problem statement and Objectives Of The Thesis

Rural and remote areas in the deserts of Najaf, Samawa, Basra, and Anbar, as well as some areas of southern Iraq's governorates, suffer from a lack of drinking water and the difficulty of cars reaching water basins, with the presence of turbidity in the water of deep wells, and these problems can be solved by using solar distillers at a low cost, through which water is produced drink enough for a family of three to four people**.**

This thesis also aims to study each of the following:

1. Proposed a novel manufacturing for heat exchanger to produced distilled water with suitable amount which is a more then of previose worker with the same field.

2. Studying water distillation by solar energy through the use of a parabolic dish in the Iraqi environment.
3. Studying the effect of Nano-materials filling on the water distillation productivity using solar energy.
4. Study the effect of thermal insulation of the heat exchanger and its effect on productivity.

1.7 Thesis Outline

This master's thesis is divided into five chapters and three appendices, as follows:

1. The first chapter includes an introduction to solar energy and the history of its use, as well as the distribution of solar radiation around the world, as well as the types of solar energy concentrates.
2. The second chapter includes previous literature dealing with the use of a parabolic solar dish in cooking, water heating, and water distillation.
3. The third chapter includes the equations from which the heat loss is extracted, the net energy absorbed by the heat exchanger.
4. The fourth chapter includes the materials that were used in the experiment (the practical part) in addition to the measuring devices.
5. The fifth chapter presents a discussion of the experiences obtained from the solar water distillation system and using the two models of the heat exchanger (absorber).
6. The sixth chapter deals with the conclusions obtained from the experimental study and some recommendations for future work .

Chapter Two

Literature Review

CHAPTER TWO

LITERATURE REVIEW

INTRODUCTION

The use of solar energy concentrators is one of the solutions offered to provide the world's energy needs, as it is possible to benefit from the thermal energy associated with the reflected rays. One of the types of solar energy concentrators is the parabolic dish, which can be used in many applications such as solar heater, solar cooker, and solar water desalination systems.This chapter provides a review of the studies on a shell and helically coiled tube heat exchangers to improve their thermal performance through the use of heat transfer enhancement strategies (passive, active, and compound), with an emphasis on the air bubbles injection technique and helical fins coil as the topic of the current thesis.

2.1 Water desalination

Shava Gorjian et al. (2014) [1] have manufactured a desalination system using a parabolic dish collector, as shown in Figure (2.3), the effect of weather conditions on the work of the system was included. They used a 2 m dish diameter covered with small pieces of glass to reflect the sun's rays. The absorber was made of ck45 metal alloy insulated by thermal fleece. The experiment was conducted in Tehran city in October 2013. 5.12 liters/day were produced as an average of 7 working hours per day. Figure (2.4) shows the weather data such as temperature, wind speed, and solar radiation intensity for the days during which the experiments were conducted.

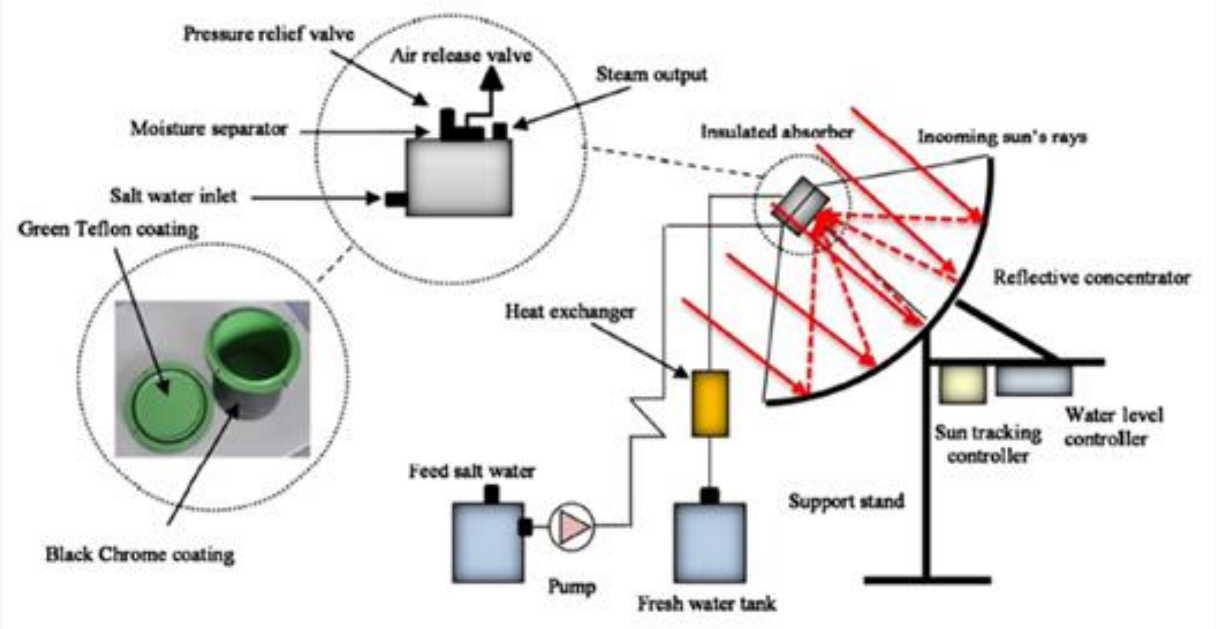

Figure (2.1). Schematic diagram of the developed point-focus solar still[1].

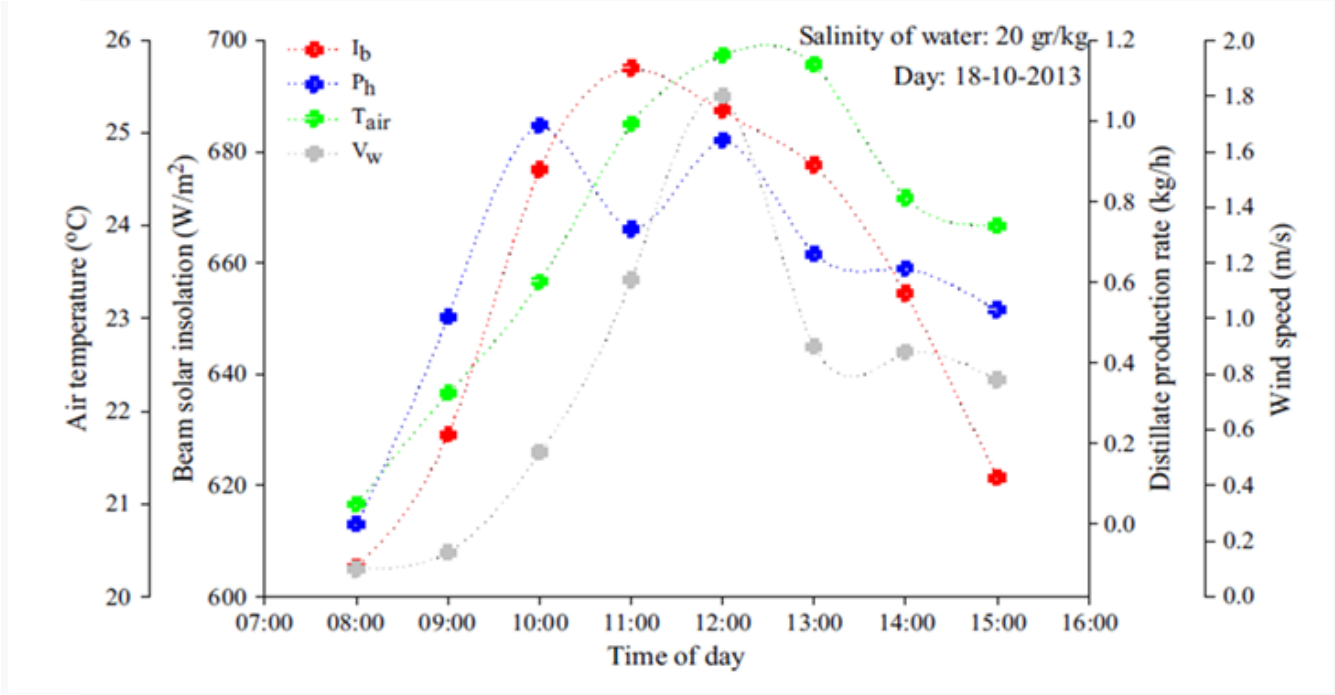

Figure (2.2): Variation of distillate production rate with weather data (day: 18-10-2013, the salinity of water: 20 g/kg) [1]

Rafid M. Hannun et al. (2018) [22] have been built a solar water desalination system using two parabolic dish models. They used two equivalent

basins of 1.13 and 2.545 square meters, respectively, which were covered by aluminum foil. The experiment was conducted in the city of Nasiriyah in southern Iraq in hree different months (march , april, jun). To improve absorption efficiency, the boiler is put in a focus location and painted black. It has two valves: one for the water inlet, which is sideways in the middle of the boiler, and the other is to regulate water entry so that the boiler is filled with water and the rate of evaporation is increased. The condenser is made up of three tubes, each is 50 cm long and 0.625 cm (1/4 inch) in diameter, fins are connected to increase the heat transmission area to the environment. It was found that increasing the basin area of the parabola dish while remaining in the same concentration area has led to an increase in evaporation efficiency and thus to an increase in water productivity which reached 2.5 and 5.25 liters for the first model and second model respectively. Where figures (2.5&2.6) shows the productivity of the first and second models, respectively, during the testing period

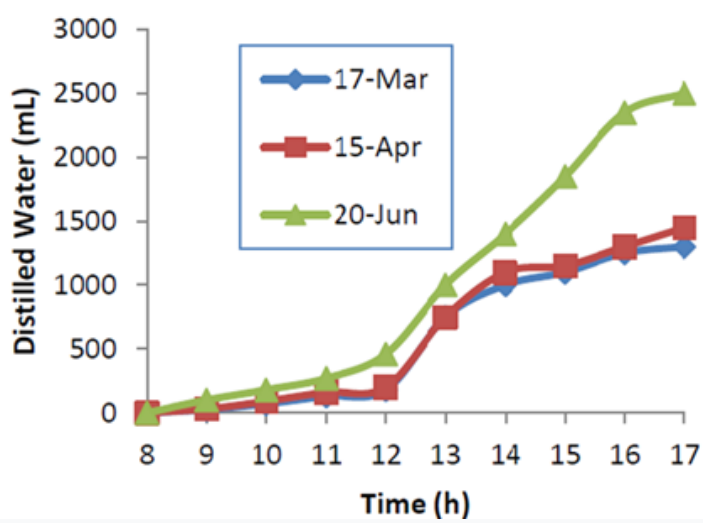

Figure (2.3). Production of distilled water (milliliters) at various times of the day (Rig 1)[22]

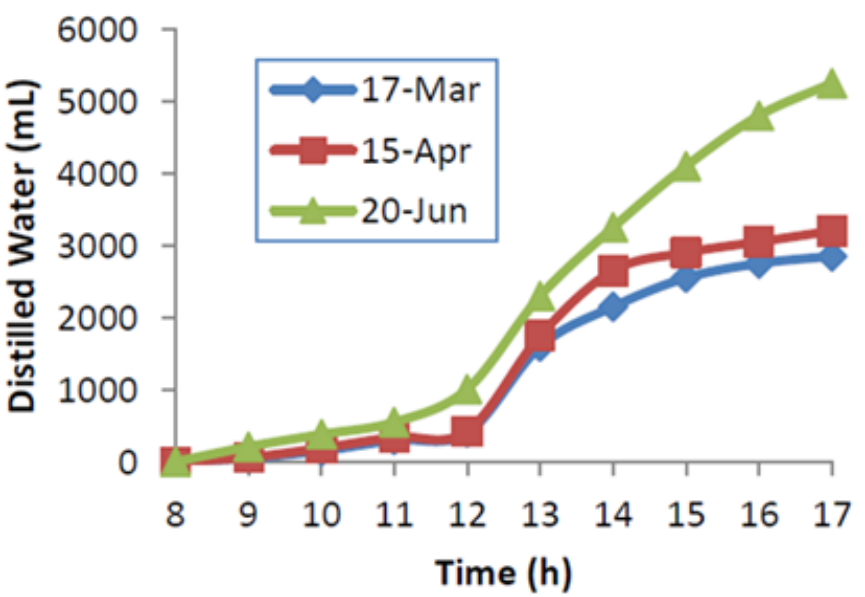

Figure (2.4). Production of distilled water (milliliters) at various times of the day (Rig 2)[22]

Z.M.Omara et al. (2013)[23]have built a solar distillation system using a 1 m diameter parabolic dish, covered with pieces of mirror strips of 0.004 m thickness. A specially boiler was constructed and put at the concentrator focus in this experiment. The size of the receiver (boiler) is designed to accept most of the concentrated sunlight while limiting radiation and convection losses. With a receiving surface of 0.046 cm^2, the boiler is formed like single slope solar still. The boiler measures 0.27 m in length, 0.16 m in width, 0.17 m in height from the backside, and 12 cm in height from the front side. At the top of the boiler, which inclines at 30° on horizontal, airtight clear glazing (glass cover) with a thickness of 0.003 m is fixed. The leftover steam flows via a coil condenser, where it condenses and is condensed by this glass cover. Furthermore, the glass cover may enable some direct sunlight to enter the boiler, enhancing the evaporation process.The results were compared with a conventional solar distiller where the productivity was 6.7 L/m^2 for the desalination system using an equivalent dish, and 3 $litter/m^2$ for the conventional

solar distiller. The results proved the effectiveness of the desalination system using the parabolic dish

Gustavo et al.(2016) [24] conducted a theoretical and practical evaluation of the performance of a condensed equivalent dish used for the purpose of desalinating brine. The oval dish with dimensions (68 cm height and 62 cm width), covered with a layer of chrome was used. Productivity was observed to decrease when the concentration of sea salt increased. However, when the solute concentration rises, the boiling temperature rises as well, a phenomenon attributable to water's aggregative qualities. Finally, the best return on investment comes from distilled water which has productivity of 4.95 L/m². This output is enough to meet the daily drinking water requirements of at least two people.

Hassanein Ghani Hamid et al.(2011) [25] studied the solar distillation system using a parabolic dish, where the dish has (d:1.5 m, depth: 0.17 m). and covered with a reflective layer of aluminum foil. The receiver was 0.22 m in diameter and 0.07 m deep, with an automatic solar guidance system used to increase productivity. The experiment was conducted in the holy city of Najaf in the months (March , and April). The results indicated the possibility of using a parabolic dish for water desalination purposes for domestic use. The productivity was ranged from 6.9 to 15.3 liters/day of freshwater.

Miqdam T.chaichan et al.(2015) [26] have used a system comprises of a dish assembly with a parabolic reflector that concentrates incoming solar energy on a container situated above the dish at a distance from the focal point. This parabolic dish has a diameter of 1.5 m and a depth of 0.23 m. To make the dish act as a reflector, the interior surface is coated with aluminum foil. To ensure that all the dish reflected rays are received, the receiver is situated at a distance from the focal point. The receiver is made of an aluminum container (d: 0.20 m, depth: 0.7 m). The receiver shadow cast on the collector's face can reduce the amount of solar energy reflected,

limiting the thickness of the receiver's insulation. To isolate the container from its rear, 1 cm thick glass wool is employed. A 100cm copper tube (d:0.96m) was rounded and plunged in paraffin wax (which served as the system's latent heat storage substance) to fill the container from the inside. A glass cover of 0.002 m thickness was used to cover the side facing the dish. Adding the Phase Change Materials (PCM) supplied the concentrating system to the distiller resulted in a 94.38 % increase in system water temperatures, a 157.8 % increase in system heating efficiency, and a 428.5 % increase in system productivity.

Miqdam T.chaichan et al.(2015) [27] used parabolic dish systems to focus the incoming solar radiation on a receiver situated above the dish at its focal point. This parabolic dish has a diameter of 1.50 m and a depth of 0.23 m and is covered with aluminum foil. A heat exchanger made of an aluminum container with a diameter of 20 cm and a depth of 7 cm was installed in front of the focal point. The test has been performed in Baghdad, Iraq, in the spring of 2013. Solar energy is stored in vast quantities during the day, and some heat is retrieved for later use. The temperature of the water is measured over a set period of time. Water as a storage material was tested in two scenarios: with and without a solar tracker. PCM was also used as thermal storage material, both with and without the use of a solar tracker. By using a focusing dish and adding PCM to the system, the system's working period was enhanced to around 5 hours. The system's concentrating efficiency, heating efficiency, and productivity have all grown by roughly 64.07 %, 112.87%, and 307.54%, respectively. When PCM was installed without the sun tracker, the system's operating duration increased to 3 hours. In addition, the system's concentrating efficiency improved by 50.47 %, while the system's heating efficiency improved by 41.63 %. Furthermore, the system's output rose by almost 180 %.

Mehmet et al. (2017)[28] manufactured and assembled a water desalination system based on solar energy using a parabolic plate condenser and a flat plate. The

results were compared to previous studies. The maximum production of 1038 ml / m^2 was obtained during the winter season and 1402 ml /m^2 during the summer. It was also found that Solar energy has contributed to reducing the salinity of water from 21,407 mg/liter to 10 mg/liter.

Ali Reza et al.(2019) [29] Studied the effect of nanofluids on the work of solar water desalination systems, 3.8 m diameter of the parabola dish that was used in the experiment. Oil nanofluids of Al2O3, Cu, and CuO, TiO2, and MWCNT. The feasibility of a desalination system using a conical cavity receiver was investigated. The working fluids in the solar collector were examined using oil nanofluids of Al2O3, Cu, and CuO, TiO2, and MWCNT at concentrations ranging from 0% to 5%. Thermal panels (photovoltaic) and dehumidifiers were used as part of the system. They are a closed-air open-water and heated water system comprised of the HDD system. It was found that the thermal efficiency improved as the nanofluid concentration increased, with Cu/oil nanofluid proving to be the best choice with a 3.84 %increase in thermal efficiency.The results showed that the highest quantity of freshwater production (17.3 L/hr), this productivity was at a concentration of 5% of the nanofluid, the flow of water into the air was 0.5, the speed of the water was 0.28 L/s.

Milad Bahrami et al.(2019) [30] studied the performance and effectiveness of the solar water desalination system, 2m diameter of the parabola dish that was used in the experiment. The absorbent material was Made of aluminum and insulated with glass wool. The results showed that the optical collector efficiency, absorbance reflectivity, plate aperture diameter, and absorber plate size have a great influence on the productivity of distilled water, initial brine temperature, salinity, and also quantity. Productivity was 20-23 liters in 7 hours, and the average solar radiation was 800-900 W / m^2 respectively.

Bechir choo chi et al.(2007) [31] studied the operation and performance of a solar water desalination system using a 1.8 m diameter parabolic dish covered with stainless steel pieces as a surface that reflects sunlight. The absorber is entirely insulated and placed at its focal point, which is formed like a cylindrical vase and has a receiving surface of 0.013 m^2. Except for the area lighted by sun rays reflected by the parabolic surface. The variations in the distilled water flow rate, the average temperature of the absorber enlightened face, the instantaneous global efficiency, and sun irradiation according to local time were also studied. The gap between theoretical and experimental data was minimal in terms of temperature, but it might reach a relative inaccuracy of 42 % for the distillate flow rate, the productivity was 6.22 liters/day.

K.Srithar et al.(2016) [32] Tested a parabolic dish solar distillation system consisting of 1.25 m in diameter and 0.5 m focus using a triple-basin solar concentrator (TBSS). A triple basin glass solar still, a parabolic dish concentrator, a cover cooling arrangement, and a photovoltaic panel make up the system. In order to maximize the heat transfer rate and position the energy storage materials, four triangular hollow fins are attached to the bottom, top, and middle basins. The system's performance was investigated using a traditional TBSS system, which integrates TBSS with cover cooling, TBSS with PDC, and TBSS with cover cooling and PDC. Each arrangement was also put to the test with fins that don't have any energy-storing substance, fins made of river sand, and fins made of charcoal as shown in Figure (2.7). where the researcher came to the conclusion of productivity of 16.94 liters / m^2. The researcher also recommended that coal and river sand to increase productivity by 34.28% and 25.7%, respectively. Figure (2.8) shows the variance of productivity with environmental factors

Figure (2.5). The triple basin desalination system[49]

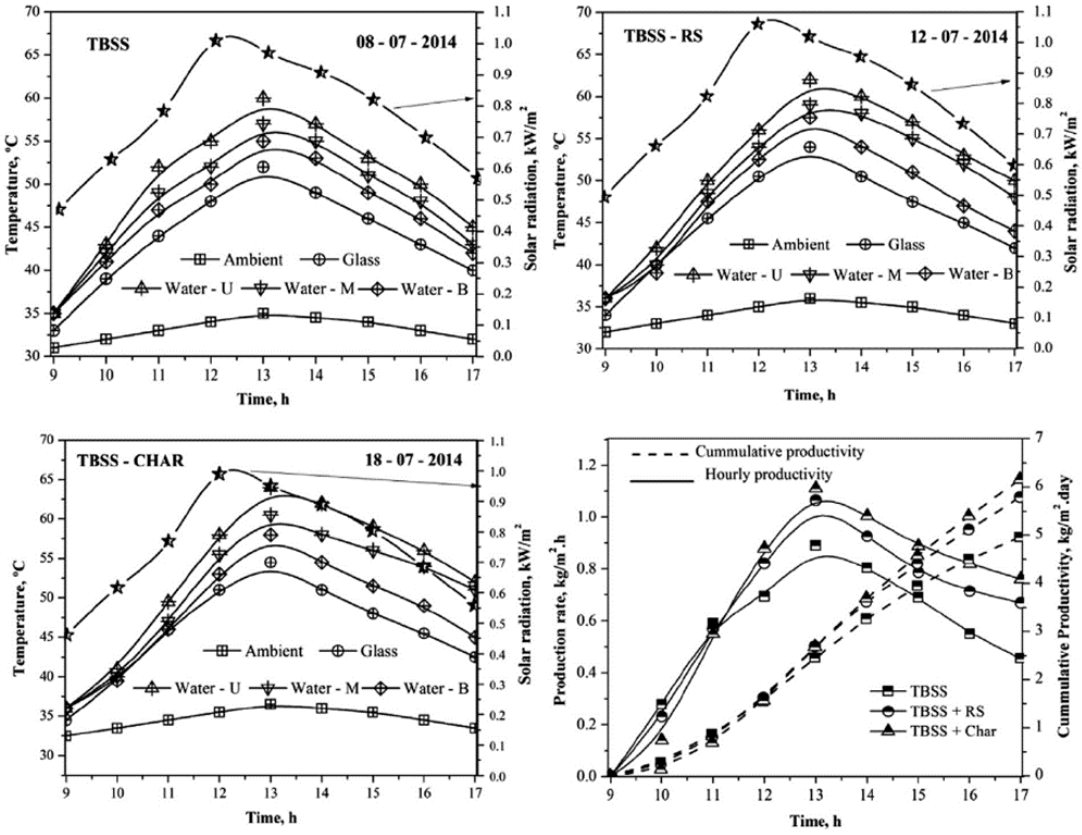

Figure (2.6). In TBSS, numerous parameters vary hourly [42]

Surendra Poonia et al . (2020)[33]used a solar thermal desalination apparatus with a parabolic concentration. With a surface area of 2.60 m. The device's performance was assessed by tracking daily distillate output in the hot desert climate of Jodhpur, India, over the winter and summer of 2019. The operating time of the system was9 hours per day, and a 6.5liter was obtained in the month of May, and this is the greatest productivity of the water distillation system, and it had solar radiation of 745 w / m², in December, 5.5 liters per day was obtained the greatest productivity in one hour was 0.85 liters, the maximum efficiency in May was 34.2% and in December 32.3%. The solar desalination device's distillate has been blended with saline water in a proper amount to make it drinkable. In reality, a solar desalination unit can produce 20 liters per day. of drinkable water (150–180 ppm TDS) from raw water with 300 ppm TDS in a single day. Because of the high productivity (76%) as well as the short recovery period for expenses, the CSP desalination system has been proven to be equivalently very cost-effective in economic analysis (1.45 years). The system's economic characteristics demonstrated its economic feasibility. As a result, this solar desalination equipment can successfully desalinate saline water in rural arid locations to meet the need for potable water according to WHO drinking water quality requirements.

Ali Babaeebazaz et al . (2021)[34]studied experimentally the performance of a small-scale two-stage solar PDC-MSF desalination unit. The influence of three distinct saline feedwater flow rates, as well as, negative pressure induced in one of the MSF unit's stages, was studied. The overall system's thermodynamic performance was then assessed. The maximum productivity that the system reached during five hours of continuous work was 3.22 liters.

Mohammed et al . (2021)[35] Using a parabolic dish, conducted an experiment on a solar-powered water desalination device. Cover a parabola plate (d:1.5m) with aluminum foil, an automatic steering system was used to track the sun.

The receiver is made of galvanized steel with a thickness of 0.5 mm and a basin size of 0.045 m^2. With measurements (length : 0.3 m, width: 0.15 m, high :0.2 m)from the backside, and 0.1 m tall from the front side, it is shaped as single slope solar still. To avoid harm from vapor pressure rise inside the tank, the single slope solar still was covered by the glass at 0.006 m. The daily productivity was 11.45 liters/day and the average working hours were 7 hours.

Amrit et al.(2021) [36] the effectiveness of integrating a solar water desalination unit based on a parabolic dish with a pre-heating system containing carbon pellets as energy storage materials was studied. Experiments were conducted in India using saline water. The maximum water temperature in the basin was 60.3 °C, which was increased To 69.4 ° C with the addition of the equivalent basin complex and activated carbon. When using activated carbon with hot water, the average absorption temperature of the desalination unit increased by 15%, 16.7% and 12.5%, respectively, when comparing the results with the conventional desalination unit. The productivity of the desalination unit was increased. The modified rate was 50.21%, where the productivity reached (3.081 liters / day) compared to the traditional unit (2.051 liters / day).

A.E.Kabeel et al . (2019) [37]conducted a pilot study in order to increase the productivity of freshwater for a single solar device. A solar dish with a diameter of 2m was used covered with cut-off reflectors made of 0.2 mm stainless steel plate coated with nickel in order to improve the reflectivity. The square aquarium on the sides was painted black with a side length of 1 m to increase solar energy absorption. The productivity of single solar dish was 8.8 kg/day, 5.54 kg/day, and in the case of double solar dishes was 13.48 kg/day, 7.5 kg/day at the two water depths of 10 and 20mm, respectively. Where Figure (2.9) compared the productivity of freshwater in different cases.

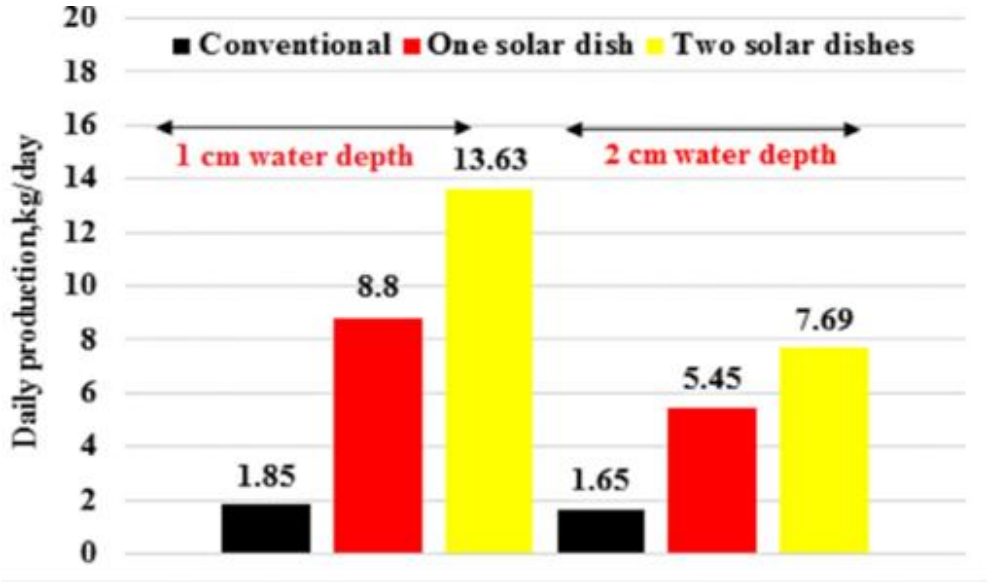

Figure (2.7). For various scenarios, a comparison of daily accumulated freshwater production is made[54]

F. M. Abed et al . (2016)[38] in order to improve, the multistage solar stills technology was combined with the solar collector. The dish's surface was stickled with an anodized metal sheet. The black-painted pot is positioned at the main point. The pot pipe is joined by two heat exchanger pipes. A timer-geared system controls the machinery that moves the dish so that it is normal in the solar direction. The dish and pot are sized to absorb energy and to raise the temperature of the liquid inside the pot. The water distillation system produced 4.95 liters per day.

Mohammed. Abd Al -Amir Khadim et al.(2021)[39] a new glass cover shape adopted of a vertical cylinder with spherical dome on the top. This design run under the climatic conditions of Najaf city in Iraq. A comparison done with traditional single slope still of the same basin area. Three cases of cylinder height taken 5 cm, 15 cm, and 20 cm. Two sets of experiments done, one in winter, and the other in summer. In each experimental day all climatic variables recorded by using a weather station, while another recording done for stills parts temperatures and hourly productivity. A yield amount of 5.8 l/m^2.day for 5 cm height, 6.7 l/m^2.day for 15 cm

height, 7.25 l/m2.day for 20 cm height, and 4 l/m^2.day for single slope solar still. Thermal efficiency measured was 18.8% for 5 cm height, 22% for 15 cm height, 23.3% for 20 cm height, and 15% for single slope solar still. Summer measurements may suggest that hemispherical solar still is more efficient than cylindrical solar still with hemispherical dome (CSSHD), but winter measurements show the opposite.

Hawraa Fadhel et al.(2021)[40]This study investigated the production of single slope solar still and the influence of combining with a parabolic trough collector. The effect of the different working fluid types on freshwater productivity, outlet working fluid temperature, heat gain, and thermal efficiency has been studied under the weather conditions of south city of Iraq/ Najaf (32°1' N / 44°1' E). The first type was water and the second type is nanofluid. The results of the comparison showed when using water as a working fluid flowing inside the receiving tube for different days; the highest temperatures were obtained at 12:00 pm, and the average productivity of distilled water was obtained in May and June 2021 were 4.5 and 6.733 kg/m^2/day respectively. While when using the nanofluid as a working fluid flowing inside the Parabolic Trough Collector (PTC) receiver tube, the outlet temperatures were rising for the same comparison days with an increase in the productivity of distilled water. Where the freshwater productivity during the day was 8.745328 kg /m^2 /day as, and it was 9.018119 kg/m^2/day during the other day. A productivity analysis was carried out for two different working fluid types (Water and nanofluid instead of water) as a fluid running inside the receiving tube of PTC. The freshwater produced from PTC (with nanofluid) was a 42.2% improvement in productivity compared with conventional PTC.

Arun et al. (2018) [41]the current research talks about the distillation of water by solar energy through the use of a parabolic solar collector of dimensions 2.5m x 1.75m, and a radiation absorber with a diameter of 25 mm and a length of 2.5m. The solar absorber was made of copper and covered with glass. Experiments were

conducted in February of 2016 in India. The equivalent collector sump was directed through the use of an automatic steering system consisting of a gear motor that is directed through a special program. Placing the sea water vessel at a height of 1.75 meters partially fills the receiving tube with the working fluid. The receiver tube is used to concentrate solar radiation. Salt precipitation and metals heat the sea water, which causes steam to develop. The steam is carried to the condenser, where it is cooled to pure water. The evaporation rate inside the receiver tube determines the flow rate from the sea water container to the receiver. salts and contaminants collecting in the collection tank on the south side of the receiver tube due to the phase change of sea water under gravity. A desalination system's yield is shown in Figure 12. The intake and output temperatures of the desalination system are recorded hourly in a sunny day process to examine the performance of the parabolic trough, as illustrated in Figure 13. The experiments were first carried out on the stainless steel receiving tube in the experiment setup. The usage of saline for the stainless steel receiver tube is heated to a maximum of 75 ° C, which is insufficient for the generation of steam due to the phase shift of salt water. In the desalination experiment, the stainless steel receiving tube performed poorly. receiver tube made of stainless steel in its place. The daily production rate of the desalination system was 2 liters / m², and the efficiency of the system was 12.74%.

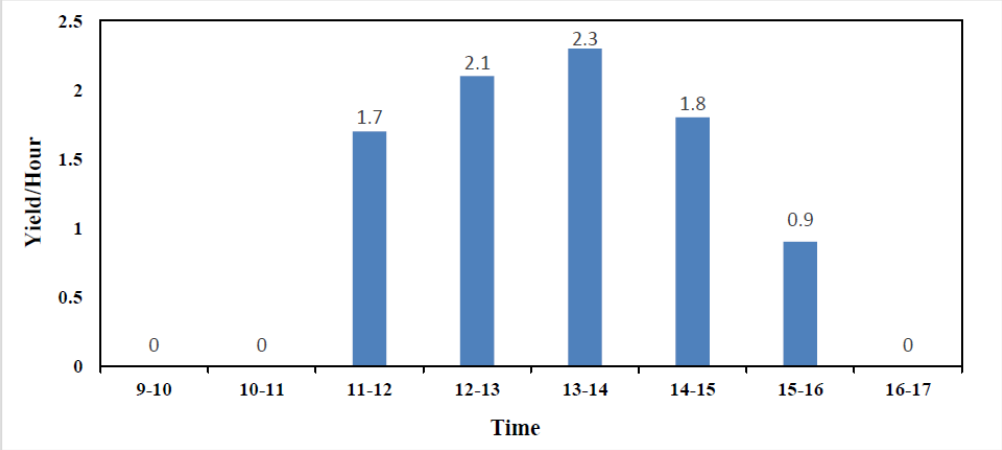

Figure (2.8).Productivity during the test period (hourly)[41]

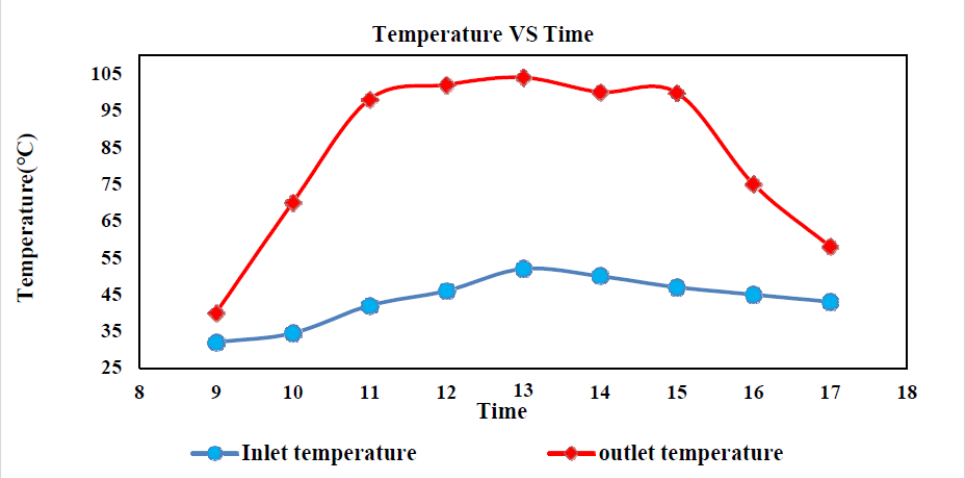

Figure (2.9).Inlet and outlet temperature of working fluid[41].

Mohamed Elashmawy (2017)[42]In the Kingdom of Saudi Arabia, a parabolic solar collector was used to study saline water distillation. The system consists of a tubular solar still (TSS) system with a rectangular tub filled with black color cloth saturated with raw water in the first experiment, a semi-cylindrical basin without wet cloth in the second experiment, and the TSS of the second experiment combined with a parabola Intensive Solar Tracking System in the third experiment (PCST-TSS) Table No. 3 shows the specifications of the distillation system in the three experiments that were conducted. When compared to traditional TSS, the results demonstrate that PCST-TSS has a lot of promise. For 0.059 m^2 TSS area (4.71, 3.6, and 3.53 L/m^2day), the yields were 0.28, 0.214, and 1.66 L/day (4.71, 3.6, and 3.53 L/m^2day) for the three tests, with daily efficiencies of 36.5 %, 30.5 %, and 28.5 %, respectively. The PCST-TSS yield was enhanced by 676 % while the cost per liter was reduced by 45.5 %(CPL).

TABLE3. Specifications of the three experiments

Item	Parameter	First experiment	Second experiment	Third experiment
Tube	Material	PMMA	PMMA	PMMA
	Length (meter)	0.54	0.54	0.54
	Weight (grams)	1098	1098	1098

	Diameters, ID × OD (meter)	0.10 × 0.11	0.10 × 0.11	0.10 × 0.11
Trough	Material Shape Dimensions Weight (gram)	Aluminum Rectangular 0.53 × 0.085 × 0.015 m 114	Aluminum Half cylindrical L-0.53 m × D- 263	Aluminum Half cylindrical L-0.53 m × D- 263
Absorbing material	Black cotton clothing (gram)	44	No	No
Concentrator (PCST)	Parabolic with manually tracking system	No	No	0.54 × 0.87

S. A. Kedar et al. (2021) [43] this experimental work discusses the desalination of groundwater by solar energy through the use of a parabolic solar basin. The hybrid solar water desalination system is divided into two parts: cutting and desalination. The initial component was a 1500mm volumetric vacuum tube assembly attached to ETC for cleansing water on one side and heat/steam on the other. Copper tubes are mostly used in ETC to improve heat transfer rates. The second component was a complicated exact equivalent capacitor that would be put beneath vacuum tubes to prevent solar radiation loss. Aluminum foil, commutator white paint, silver vinyl covers for chrome mirrors, and mylar are among the materials explored and employed above the compound equivalent capacitor. All experiments take place between the hours of 7 a.m. and 6 p.m. The productivity of the system during work was 3.4 liters / day. The figure(14) also shows the number of productivity of the system during working hours and in comparison with the intensity of solar radiation.

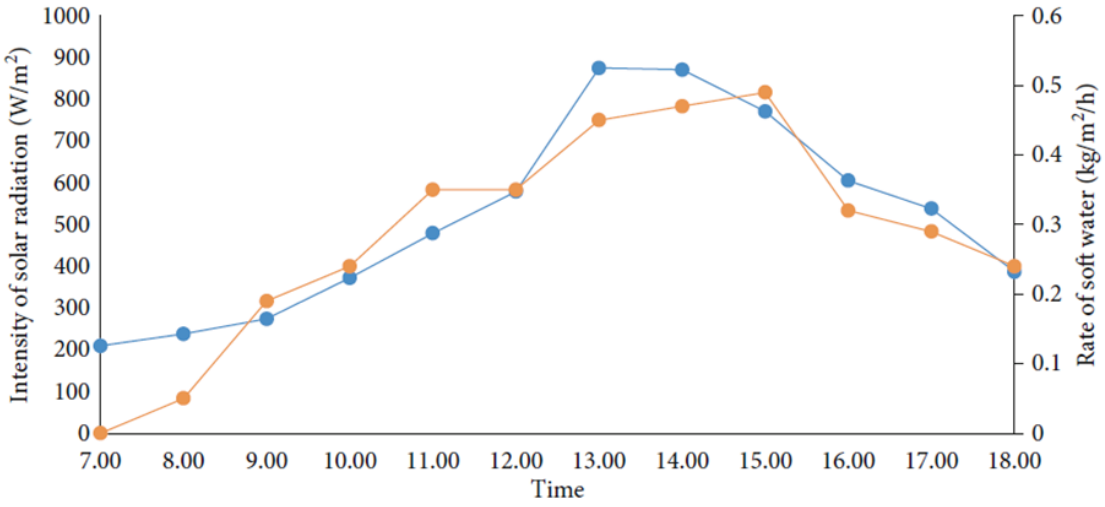

Figure (2.10). Productivity and intensity of solar radiation[43]

2.2 Nanomaterials and their use in solar water desalination

Dr. Bhupendra Gupta et al.(2016)[44] Studied increasing the productivity of the solar water desalination system using nanoparticles in two solar stills, each of 1 square meter, length of the front and rear walls was 21 cm and 63 cm, respectively, and a basin was painted black to increase absorbency. CuO nanoparticles were used with a concentration of 0.12% and at two different depths of 5 and 10 cm. The results indicated an increase in the thermal conductivity inside the basin as a result of mixing nanoparticles with water, as well as, the nanoparticles acted as energy storage materials. The distillation products using nanomaterials and at a depth of 5 cm were 3.443 liters / day compared to the productivity of the traditional solar desalination system, whose productivity reached 2.814 liters / day, and at a depth of 10 cm, the productivity of the modified system using nanoparticles was 3.058 liters / day compared to 2.351 liters / day for the conventional system, where the improvement rate at a depth of 5 cm was 22.4%, while at a depth of 10 cm 30%

Swellam W.Sharshir et al. (2018)[45] studied the productivity of the traditional solar water desalination and compared to the productivity of the modified solar water desalination system by using (graphite or CuO/nano). Where the

researcher made three models of solar still with the same dimensions to evaluate the performance of the solar water distillation system. The basins of the three models were painted black to reduce heat loss. The results showed that the efficiency of the solar desalination system in which graphite was used was 41.18%, while when using CuO it amounted to 32.35%, respectively, compared to the conventional system.

WenjingChen et al.(2019)[46] prepared a nano liquid mixed with brine for recovery to increase the heat efficiency of concentrated solar energy used in water desalination processes, multi-walled carbon nanotubes (MWCNTs) were used as a nanofluid. The absorbed solar radiation, as well as, the efficiency of the evaporation materials, increases with the increase in the concentration of magnetic nanomaterials and starts from 24.91% at 0% wt to 76.65% %.at 0.04 wt. It means that a higher productivity could be obtained in solar still with MWCNTs magnetic nanofluids.

S. Shanmugana al. (2020)[47] studied the effect of using nanomaterials on the performance of a solar distillation system. A mixture of nanoparticles (Cr_2O_3 -TiO_2) were used in the simulation model. The results showed that the increase in heat capacity in the still solar basin has increased with the increase in temperature. The average production of the desalination system during winter and summer was 5.39 and 7.89 liters / day, respectively.

2.3 Sumary of literature review

In this part of the chapter, we review a summary of water production by parabolic solar energy concentrators in terms of productivity, operating periods, area, geographical location, and the time period in which the experiments were conducted, as shown in Table (2.2).

Table (2.1): Summary of the productivity of some solar distillation systems

Ref.	Geographical location	Year	Month	Aperture area (m^2)	Experimental period	Productivity (L/day)	Productivity (L/h)
Shiva Gorjian[1]	Tehran	2013	October	3.141	09:00-16:00	5.12	0.731
Rafid M. Hannun[39]	Nasiriya	2018	June	2.54&1.135	09:00-17:00	5.25&2.5	0.656-0.3125
Z.M. Omara[40]	Kafrelsheikh	2012	July to September	0.78	09:00-17:00	6.7	0.8375
Gustavo Otero Prado[41]	Brazil	2016	September and October	1.325	09:00-16:00	4.95	0.707
Hassanein Ghani Hamid et al. [42]	Najaf	2010	March April	1.767	09:00-18:00	6.9 to 15.3	-----
Mehmet Emin Argun et al.[45]	Türkiye	2017	October	1	10:00-17:00	7.689	0.9611
Milad Bahrami et al. [47]	Iran	2018	June	1.767	8:30 - 17:30	20-23	----

Bechir choo chi et al. [48]	Tunisie	2007	----	2.544	9:00-18:00	6.22	0.691
Ref.	Geographical location	Year	Month	Aperture area (m^2)	Experimental period	Productivity per day(L/day)	Productivity (L/h)
K.Srithar et al. [49]	India	2016	-----	1.22	09:00-17:00	16.94	2.11
Surendra Poonia et al. (2020)[50]	India	2019	December	1.327	9:00–17:00	6.5	0.8125
Ali Babaeebazaz et al. (2021)[51]	Iran	2020	July	2.54	10:00-15:00	3.22	0.644
Mohammed et al. (2021)[52]	Iraq	2018	December	1.767	09:00-16:00	11.45	1.63
Present Work	Iraq	2022	March-April-Jun	1.96	09:00-15:00	10.17-16.11	1.695-2.685

2.6 Scope of The Present Work

From the literature reviewed, the following can be summarized:

1. Most of the techniques of water distillation using a solar parabolic dish depend on the integration of a parabolic dish solar with a solar still. In our study, a

simple heat exchanger that can be disassembled and easy to maintain and can be manufactured from materials available in the local markets, also used aluminum fins fixed to the inner surface For heat exchanger cover to increase heat transfer surface area. Also, a black thermal coating that bears high temperatures was used on the heat exchanger cover to increase absorption and reduce reflection from the heat exchanger cover, which positively affects the work of the heat exchanger.

2. The use of nanomaterials is still limited in water distillation techniques using a parabolic dish. In this study, a new and economical method was devised to use nanomaterials, where a nano-material (MWCT) was made inside the inner fins of the heat exchanger to help accelerate heat transfer through the fins. This research is considered the first to address the use of nano-filling in accelerating heat transfer.

In addition, the novelty in the use of nano-fill technology is one of the important factors that may help improve heat transfer, whether in the process of water distillation or other uses.

Chapter Three

Mathematical Model

CHAPTER THREE

MATHEMATICAL MODEL

3.1 INTRODUCTION

In this chapter, the theoretical analysis of a parabolic dish solar condenser will be studied. There are many factors that affect the performance of the center of parabolic dish such as diameter of the dish, the focal length, the aperture area, as well as, the edge angle.

To design a solar water distillation system with a parabolic dish concentrator, the following steps must be followed:

- Choosing the shape, type, and dimensions of the parabolic dish.
- Calculating the parameters of the parabolic dish such as aperture area, focal length, and edge angle.
- Determining the best reflective material to be used in the experiment to reflect the radiation falling on the parabolic dish to the heat exchanger (absorber).
- Choosing the type of material, shape and dimensions of the heat exchanger (absorber).

3.2 Geometrical analysis model of the parabolic dish

The geometry of the parabola is very important to ensure the correct performance of the parabola, as the error in the geometric calculation may lead to not taking full advantage of the reflected solar rays and thus not concentrating the heat in the focal length and thus reducing the efficiency.

To perform the correct geometric calculation of the parabolic dish, some parameters must be found such as the diameter of the parabola dish(d), the aperture area of the

parabolic dish(Aap,) focal length(f), focus ratio(CR), depth of the parabolic dish(h). Figure (3.1) shows the analysis used in the parabolic dish[48].

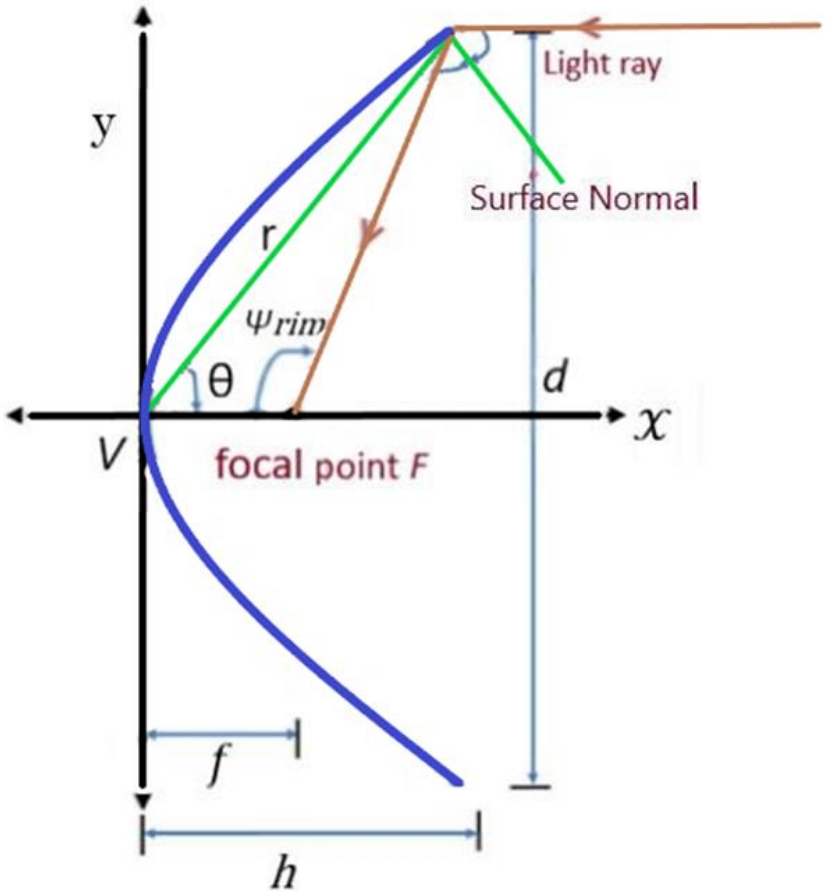

Fig. (3.1). Geometrical parameters of Parabolic Dish [48].

The surface area of a parabola can be calculated by using the equation(3.1)[37]:

$$S = \frac{8\pi}{3} f^2 \left[\left(1 + \left(\frac{d}{4f} \right)^2 \right)^{\frac{3}{2}} \right] - 1 \qquad (3.1)$$

Where (d) is the dish aperture diameter ,and (f) is the focal length for parabolic dish The aperture area of a parabola is calculated using the following mathematical relationship [49]:

$$A_a = \frac{\pi}{4} d^2 \qquad (3.2)$$

The depth of the parabolic dish (h) can be calculated by the relationship [24]:

$$h = \frac{d^2}{16\,f} \tag{3.3}$$

3.3 Model of optical analysis

Optical focus (C_{RO}) can be defined as the ratio between the amount of solar radiation absorbed by the heat exchanger (I_{abs}) to the amount of radiation falling on the aperture area of the parabolic dish(I_b)[50].

$$C_{RO} = \frac{I_{abs}}{I_b} \tag{3.4}$$

The geometric concentration is the ratio of the area of the aperture area(A_a) to the area of the absorber area(A_{abs}). The geometric concentration ratio controls the receiver's heat losses by influencing the selection of the absorbing area from the receiver area[50]

$$C_R = \frac{A_a}{A_{abs}} \tag{3.5}$$

The ratio between the amount of energy received by the receiver (absorber)(Q_{abs}) to the amount of energy received by the aperture area (Q_s)is called the optical efficiency($\eta_\circ$)[50-51].

$$\eta_\circ = \frac{Q_{abs}}{Q_S} \tag{3.6}$$

Where :

$$Q_s = I_b . A_a \tag{3.7}$$

There is another equation to extract the optical efficiency[51]:

$$\eta_\circ = \lambda \rho\, \tau\alpha \cos\theta \tag{3.8}$$

Where: λ is the un-shading coefficient or shape factor[*52*]

$$\lambda = \frac{A_a - A_t}{A_a} \quad (3.9)$$

Where:

A_a: aperture area.

A_t: area that is shaded by the receiver on the concentrator.

ρ: the reflectivity of the dish, τα is absorptance–transmittance produce[53]

γ : The receiver intercept factor which is the ratio of energy intercepted by the absorbed receiver surface to energy reflected by the concentration dish [54]:

$$\gamma = 1 - \exp[-820\left(0.7\frac{r}{f}\right)^2 (1 + \cos\psi)\ ] \quad (3.10)$$

For all the concentrates and receivers used in this research: γ≈1

θ: The angle of incidence of solar radiation, and because the parabola is always directed towards the sun, the value of this angle is zero, so equation (3-8) becomes:

$$\eta_o = \lambda\rho\,\tau\alpha \quad (3.11)$$

3.4 Model for thermal analysis

The useful heat absorbed (Q_{usufl}) is equal to the heat absorbed by the absorber (Q_{abs}) minus the heat loss(Q_l) Figure (3.2)[53]

$$Q_{usufl} = Q_{abs} - Q_l \quad (3.12)$$

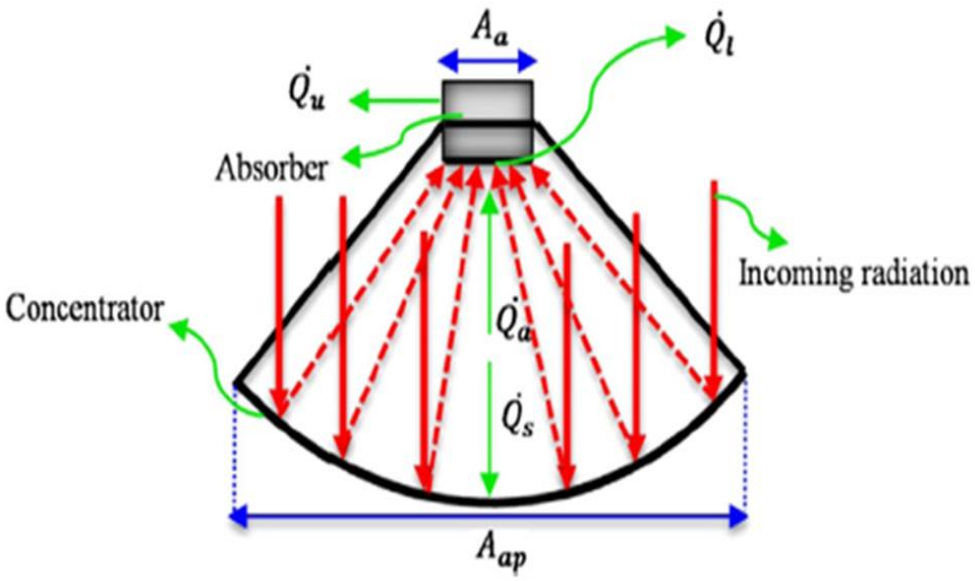

Figure (3.2): Schematic of the parabolic dish thermal powers[46].

The heat loss is equal to the heat lost by convection plus the heat lost by radiation, the conduction heat loss in this case is small and can be neglected, thus the total heat loss is as following[24]:

$$Q_{loss} = Q_{rad} + Q_{conv} \quad (3.13)$$

$$Q_{conv} = A_{abs} \times h_{air} (T_{abs} - T_{ambint}) \quad (3.14)$$

The heat convection coefficient between the absorber and ambient can be calculated by the following equation[55,56]

$$h_{air} = 2.8 + 3 \cdot 5\ V_{air} \quad (3.15)$$

The heat loss by radiation can be calculated by using the following equation [48]:

$$Q_{rad} = \varepsilon_{abs}\ \sigma A_{abs} (T_{abs}^4 - T_{ambint}^4) \quad (3.16)$$

The efficiency of the collector can be calculated by dividing the useful energy absorbed by the liquid inside the absorber by the energy falling on the aperture area of the parabola plate as following[51]:

$$\eta_c = \frac{Q_{useful}}{Q_s} \quad (3.17)$$

Overall thermal efficiency (η_u) was calculated by the following equation [28]

$$\eta_u = \frac{m_w \cdot CP_W \cdot \Delta T_f}{I_{b\,av} \cdot \mathrm{Aa} \cdot \Delta \mathrm{t}} \quad (3.18)$$

Where:

m_w = mass of water (kg).

CP_w: specific heat of water, it may be estimated at any temperature in between range (273.2 – 600 K) by the following equation [38].

ΔT_f = the temperature difference between the highest water temperature and the temperature of the ambient air.

$I_{b\,av}$ = The average beam solar intensity during the period (W/m^2).

Aa = is the reflector aperture area of the solar cooker (m^2).

Δt = time to reach the highest temperature(s).

$$C_{p_w} = 1.7850 \times 10^{-7} T^3 - 1.9149 \times 10^{-4} T^2 + 6.7953 \times 10^{-2} T - 3.7559 \quad (3.19)$$

Where

$$T = \frac{Tw_1 + Tw_2}{2} \quad (3.20)$$

3.5 Calculation's procedure

- Calculating the dimensions of a parabola dish (dish diameter, dish depth, focal length, aperture area)
- Calculating the dimensions of the solar radiation receiver (absorbed)
- Calculating of the optical properties (solar radiation intensity, geometric concentration ratio, and optical efficiency) of the water desalination system.
- Calculating of the thermal properties of the solar water desalination system (heat loss, heat absorbed by the receiver (absorber), heat on the aperture area of the parabolic dish, efficiency of the complex of the parabolic dish complex and the total thermal efficiency.

Chapter Four

Experimental Work

CHAPTER FOUR

EXPERIMENTAL WORK

4.1 INTRODUCTION

Experiments were carried out in the Iraqi city of Diwaniyah, located in the middle Euphrates region, between latitudes 31.17 and 32.24 north and longitudes 44.24 and 45.49 east, during the months (March, April, May) of the year 2022. As shown in Figure (4.1).

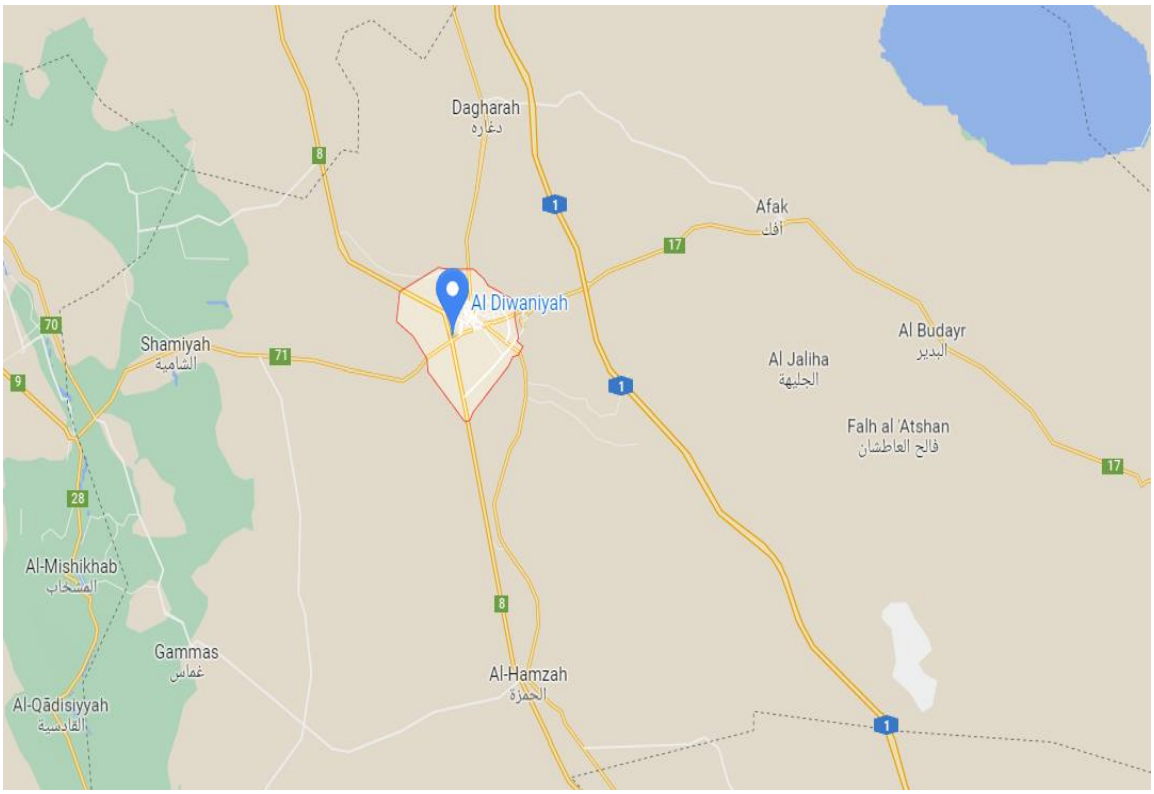

Figure (4.1).Location of experimental test

4.2 Materials and methods

The solar distillation system that is manufactured is consistes of a parabolic dish, solar tracking system, a tank for storing salty water and another tank for storing

the distilled water, two models of a heat exchanger (absorber), and a heat exchanger to condense the generated steam. Figure (4.2) is a schematic diagram showing the parts of the solar distillation system, as well as Figure (4.3) is a photograph showing the parts of the solar distillation system.

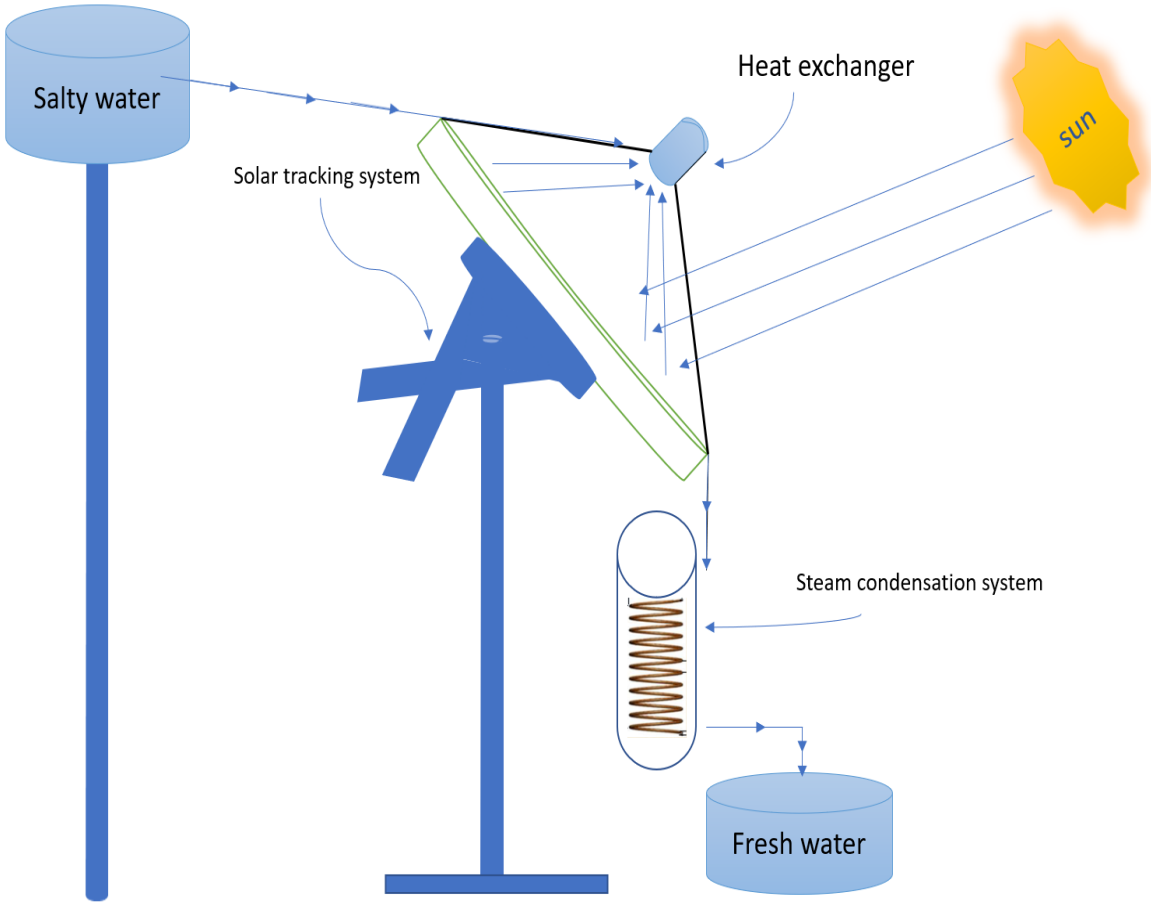

Figure(4.2): Schematic diagram of the parts of the experiment

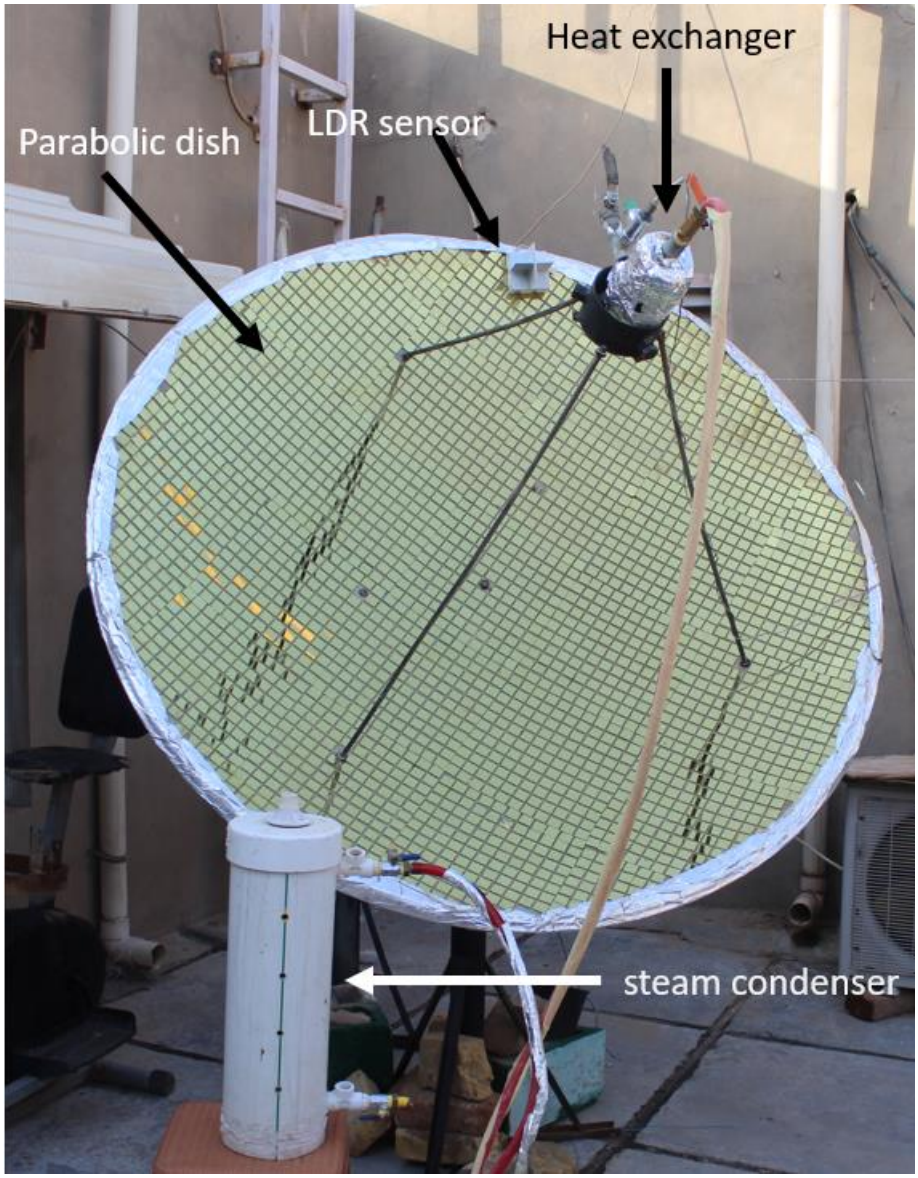

Figure (4.3): picture of distillation system

4.2.1 Parabolic Dish collector (PDC)

A parabolic dish was used as a solar concentrator. Its diameter (d: 158 cm), its depth is 20 cm, and a focal length of 78 cm. The parabolic dish is originally a recycled satellite receiving antenna, which is made of aluminum metal Figure (4.4) shows the parabolic dish.

Figure (4.4): Photograph of a parabolic dish (antenna)

4.2.2 Reflective material

The choice of the reflective material is one of the most important factors that control the efficiency of the parabolic dish, the higher the reflectivity of the material, the higher the efficiency of the parabola. As the amount of reflected solar radiation increase, the absorbance efficiency of the heat exchanger (absorber) of solar radiation will also increase, and thus the temperature inside the heat exchanger will rise. In the current study, glass mirrors were used as a reflective material, as glass mirrors are characterized by their high reflectivity, and mirrors with dimensions (2X2) cm and 0.1 cm thickness were used. As the mirrors used are available in the local markets, as well , as resistant to the harsh weather conditions that characterize Iraq.Figure (4.5) shows of the glass mirrors, which are installed on the parabolic dish plate.

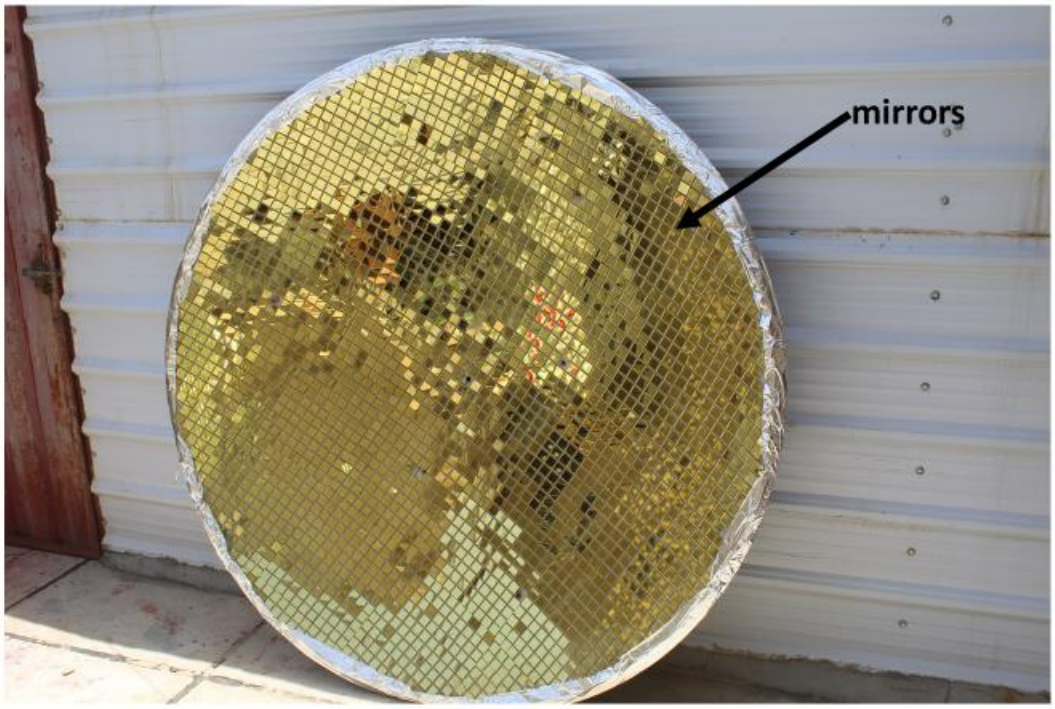

Figure (4.5): Parabolic dish after covering its surface with glass mirrors

4.2.3 Absorber

Two heat exchangers (absorber) are used in the present experiment. The first one is a cylindrical steam generator made of metal (CK45 alloy). Its outer diameter of 7.6 cm, length of 16.6 cm, and thick wall of 0.2 cm. The heat exchanger (absorber) was insulated with a thick layer of glass wool, 2.5 cm thick. The heat exchanger (absorber) contains a bypass valve for the ingress of salt water, and a sensor is installed inside it to measure the temperature of the water entering it. On the top of the heat exchanger, a manually controlled valve is installed to let the steam out into the condenser. A small hole is also made in the heat exchanger to install the temperature sensor, which measures the temperature of the water inside the heat exchanger. Figure (4.6) shows the steam generator before and after thermal insulation.

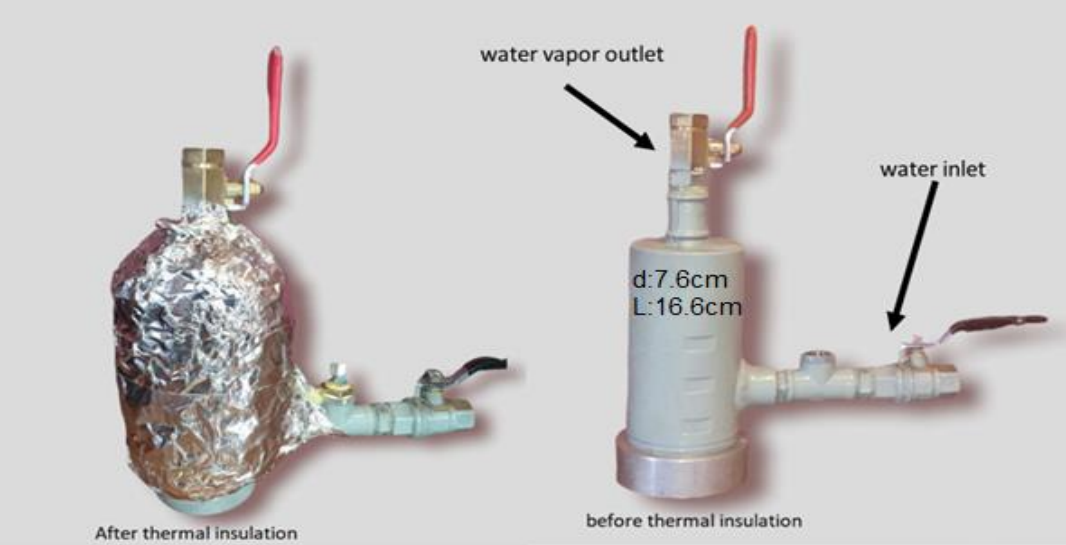

Figure(4.6): Heat exchanger (absorber) before and after thermal insulation.

The heat exchanger cover (absorber) was made of aluminum metal, with an outer diameter of 9 cm and an inner diameter of 7.6 cm, a height of 2.5 cm, and a depth of 1.5 cm from the inside. It contains five holes, threaded from the inside, with a diameter of 0.988 cm and a depth of 0.7 cm as shown in table(4.1). Five fins were made of aluminum metal, with a diameter of 0.988 for each one, serrated on one side, and a length of 10.786 cm. These fins are installed inside the holes in the heat exchanger cover (absorber). A small hole was made in the absorber cover with a diameter of 0.2 cm and a depth of 1.5 cm using a lathe machine to measure the surface temperature. Figure(4.7) shows the heat exchanger cover (absorber) and the inner fins. The outer surface of the heat exchanger cover (absorber) is painted with high temperature resistant black paint (up to1093°C) to increase the absorbing efficiency and to reduce reflectivity.

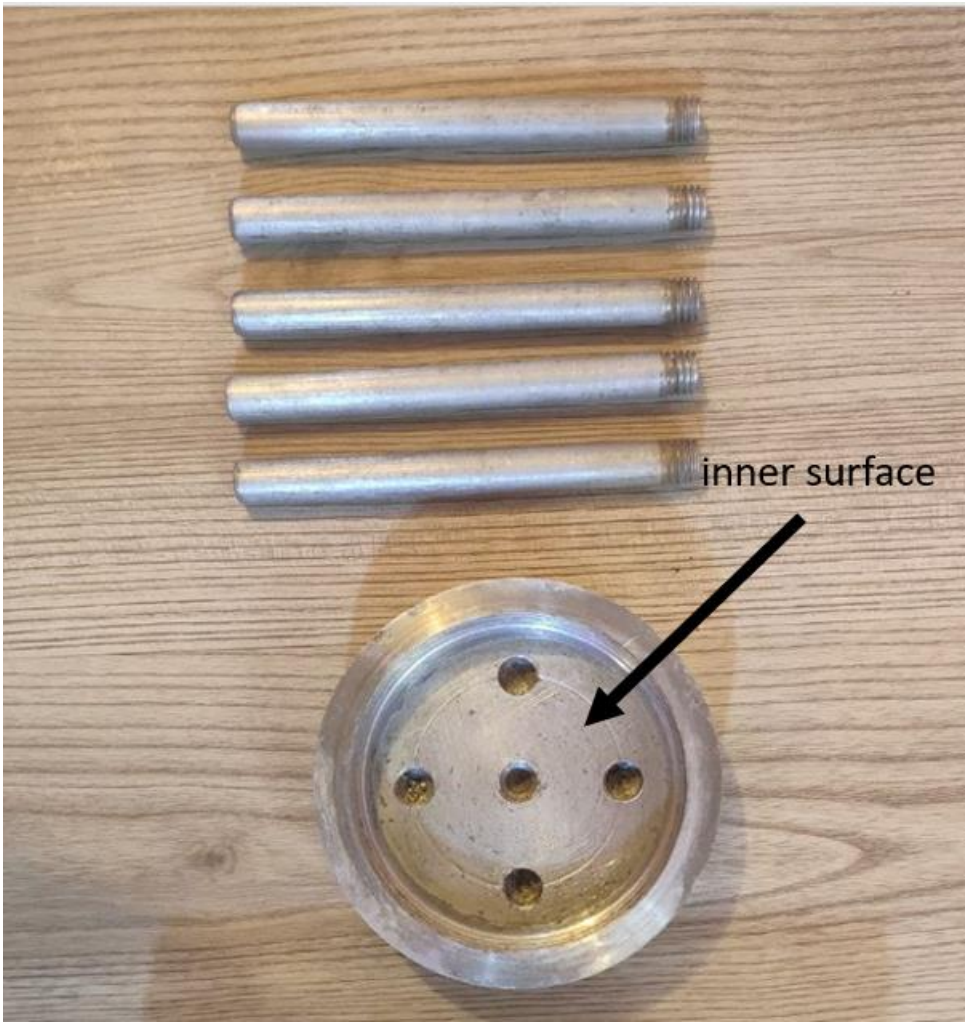

Figure (4.7): Steam generator cover with fins.

The second heat exchanger was also made of CK45 alloy with the same dimensions of the first heat exchanger with a difference that each fin is including a hole with a diameter of 0.3 cm, made by using a lathe machine. These holes are filled with Multi-Walled Carbon Nanotube (MWCT), the holes are filled carefully to ensure that the geometry of the nanomaterial did not deform, and vibration is used when filling to ensure that the material was properly distributed inside the holes. Figure (4.8) shows the inner fins which are perforated, as well as, Figure (4.9-4.11), which explains the process of filling the nano-material. After completing the filling process, the open ends of the fins are welded using aluminum welding, where a type (high cellulose sodium) welding powder is used with an aluminum welding wire.

The welding wire is immersed in the powder to help melting the aluminum (to reduce the melting point of the wire) which in turn will decrease the welding temperature. This step of process welding will prevent the deformation which resulted from the excessive heat of the fin during welding. Figure (4.12) shows the final shape of the heat exchanger (absorber) cover. To ensure that the MWNCT did not affected by welding process, a cut of one unused fin were carried out.

Figure (4.8): Inner holes for the fins of the heat exchanger (absorber)

Figure (4.9): The process of filling nanomaterial into the inner holes of the fin

Figure (4.10): The process of welding the fins after filling them with nanomaterial

Figure (4.11): The final shape of the fin after filling it with nano-material and welding it

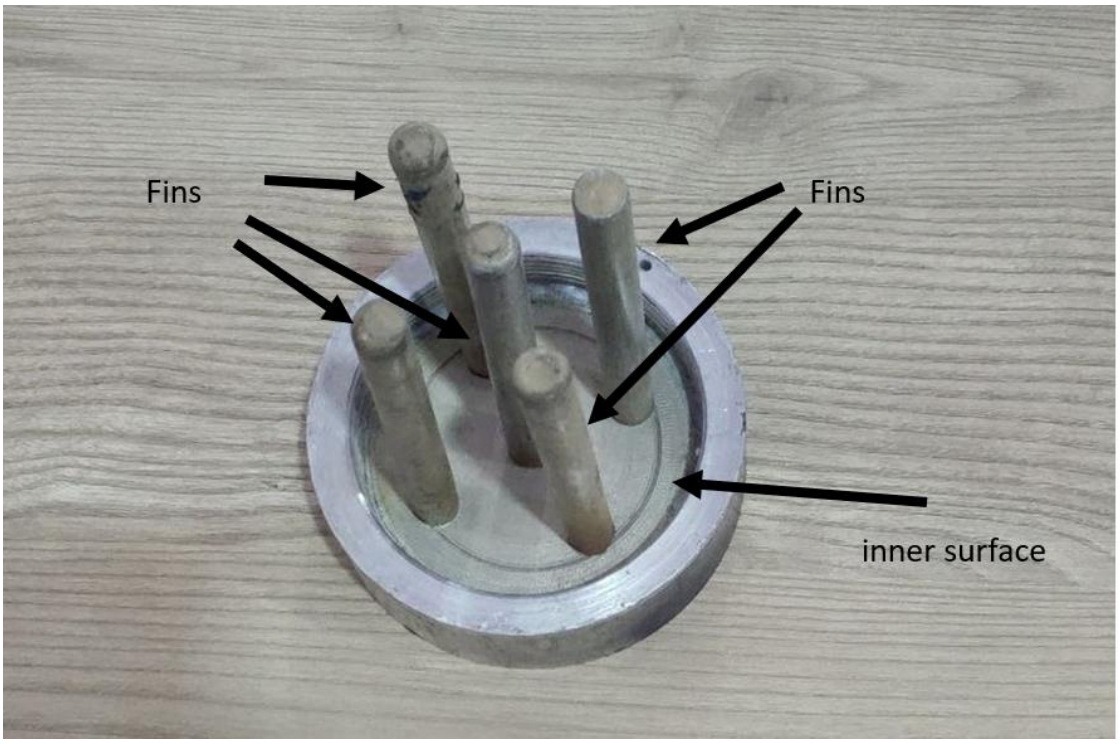

Figure(4.12): Heat exchanger cover (absorber) final shape

4.2.4 Multi Walled Carbon Nanotubes (MWCT)

In this experiment, multi-walled carbon nanotubes are used as a filling inside the inner fins of the heat exchanger, as this material has a very high thermal conductivity of 3500 W/m.K. Where (6.5 g)of this substance was used in this experiment with a rate of 1.3 gm in each fin, it was filled with high accuracy and using a vibration device to ensure the proper spread of nanoparticles inside each fin, table (4.1) shows the properties of this nano-material . Figure (4.13) shows the nanomaterial that was used.

Table 4.1: Characteristics of multiwalled carbon nanoparticles(MWCT)

Appearance	Inner diameter	Outer diameter	Tube length	Apparent density	purity	Electric Conductivity	Thermal Conductivity
Black Powder	3-6(nm)	5-15 (nm)	10-30 (µm)	0.10 g/cm3	>95%	8-10 S/cm	3500W/m.K

Figure (4.13): Carbon nanoparticles used in the experiment

4.2.5 Frame and Support Structure

Because this test uses materials available in the local markets as well as to recycle consumables, the base of the parabolic dish was made from the base of the antenna. It is modified to move in two directions (vertical and horizontal) in order to facilitate the process of sun fatigue. Figure (4.13) illustrates the base of the antenna. Installing a parabola plate and guiding system.

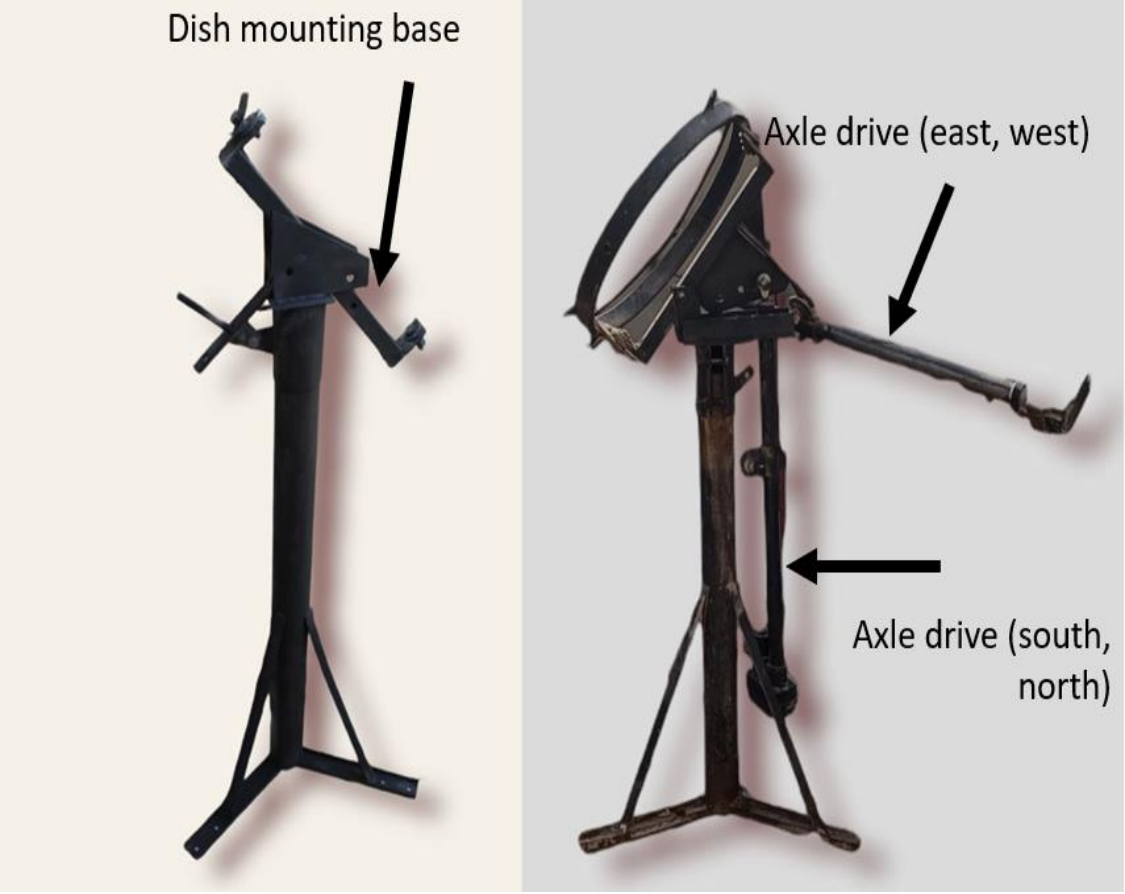

Figure (4.14): Frame and Support Structure

4.2.6 Solar Tracking system

A dual-axis tracking system is used which consisting of two DC motors as shown in the figure (4.14), a pull of 1200 Newton / 120 kg, and a maximum thrust load of 1500 Newton / 150 kg, the voltage of each was 12 volts, the maximum loaof current was 6 A, and the operation temperature is ranged from -20℃ to 65℃.

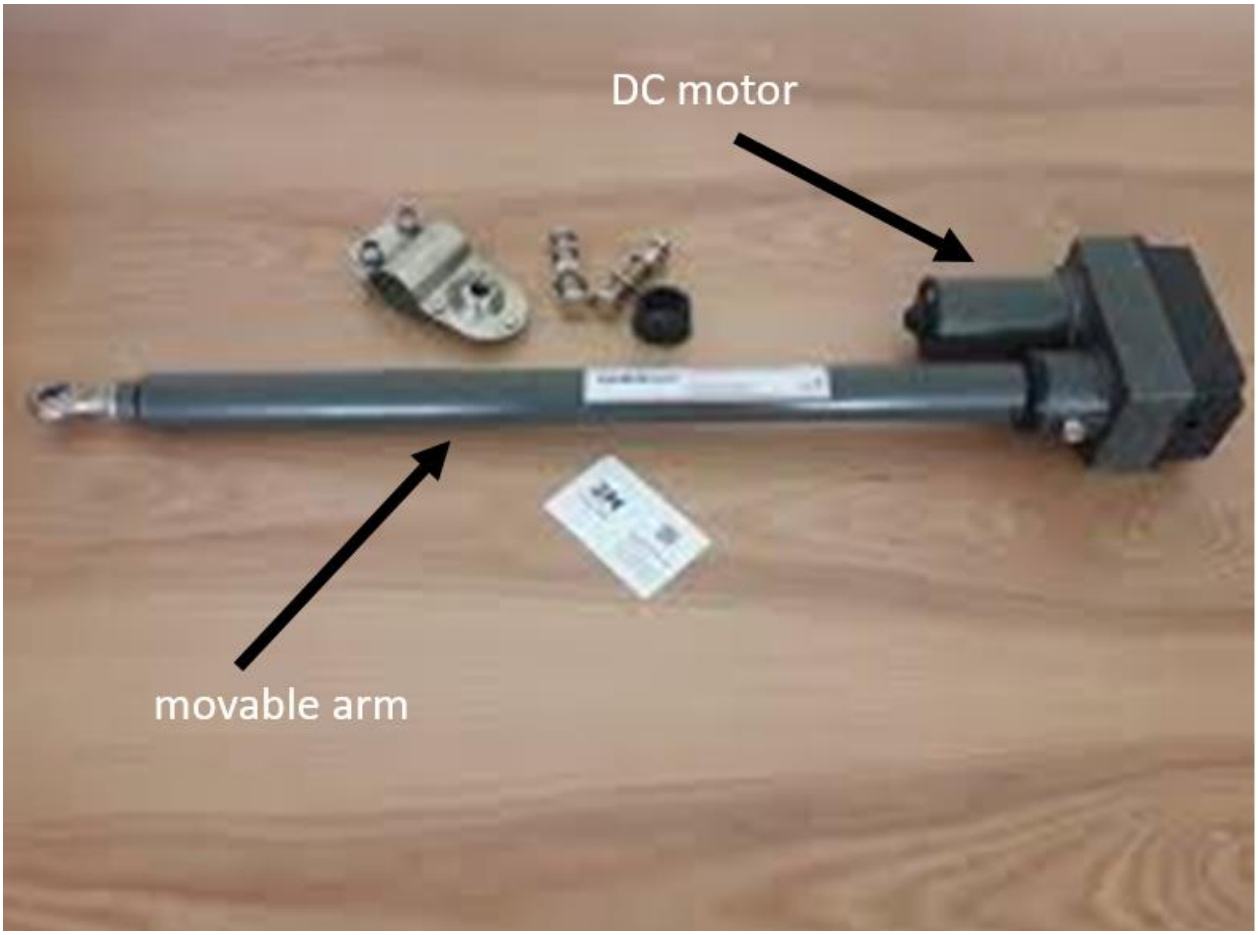

Figure (4.15): DC motor

The solar tracking system is controlled by a control panel consisting of an electronic circuit that is programmed using Arduino. Where this electronic circuit senses sunlight and follows it through the LDR sensor, where four sensors were used, two of which sense the light in the right and left direction, and the other in the direction of up and down, as shown in Figure (4.15&4.16).

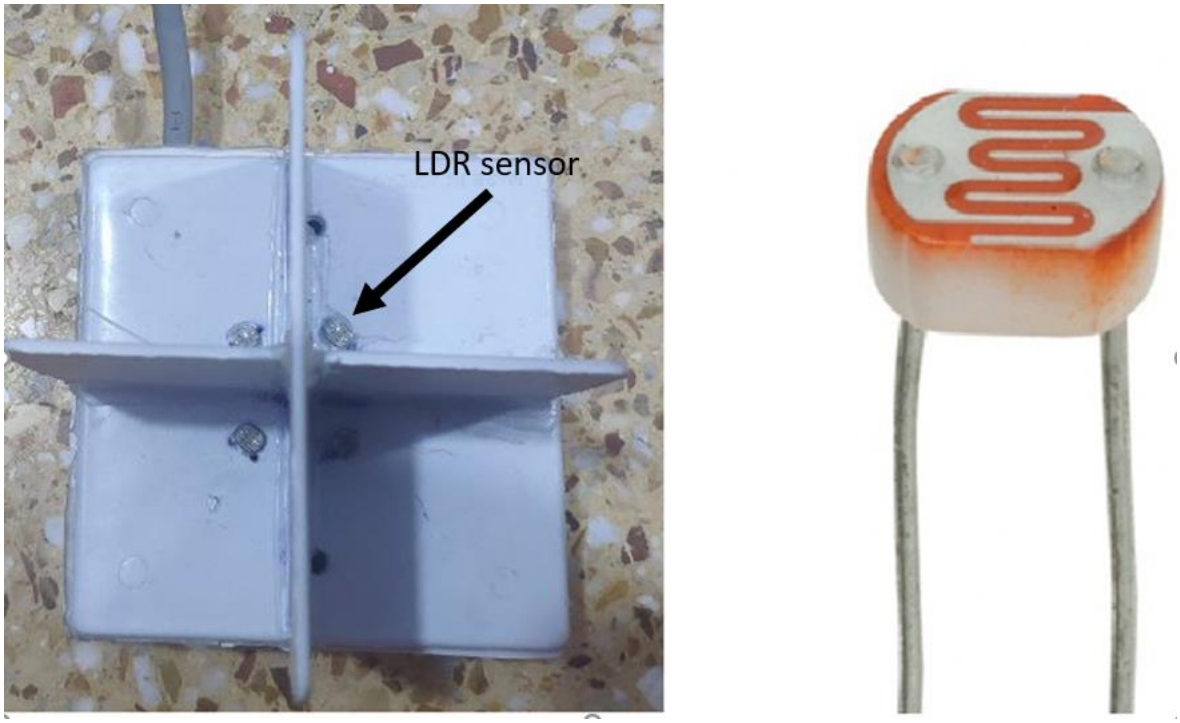

Figure (4.16):LDR sensor.

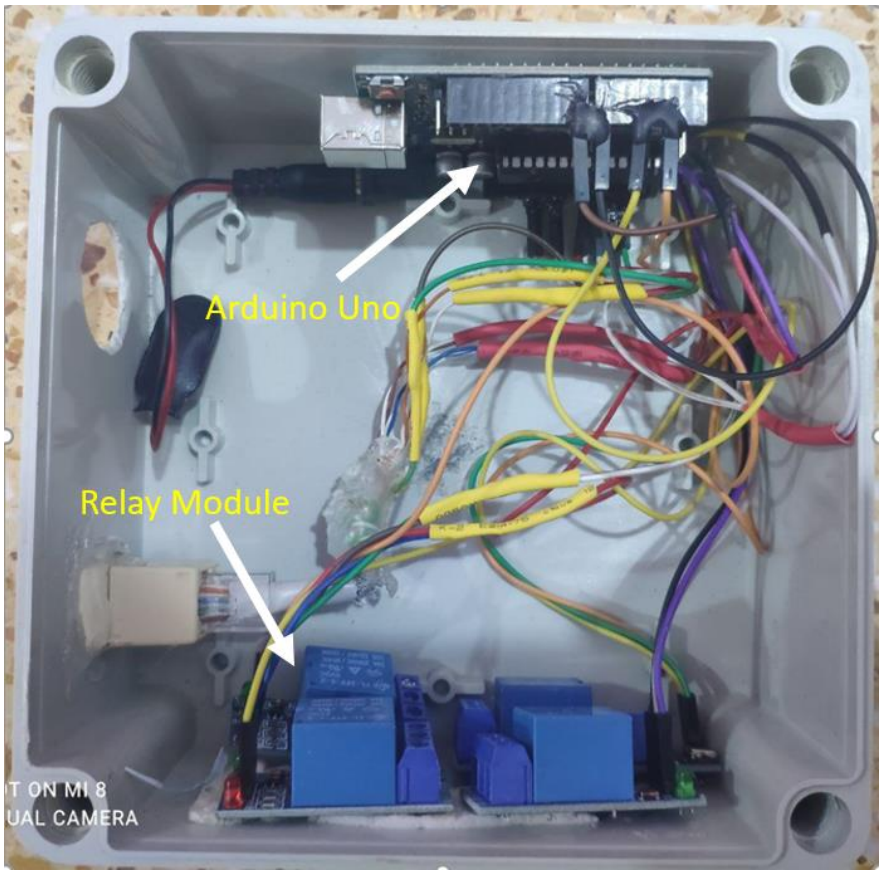

Figure (4.17): The electronic circuit of the solar tracking system.

4.2.7 Steam condensing system

The traditional shell and screw tube heat exchanger is used to condense the steam generated from the brine heating process inside the absorber.This type of heat exchanger consists of an outer vessel made of polyvinyl chloride (PVC), 14.5 cm in diameter, 0.025 cm thick, and a total length of 50 cm. A spiral tube is installed inside it, made of copper, with a number of coils of 11 laps, and the diameter of one lap is 11 cm, and the distance between one lap and another is 3 cm. The total length of the spiral coil is 38 cm, as shown in Figure(4.17).

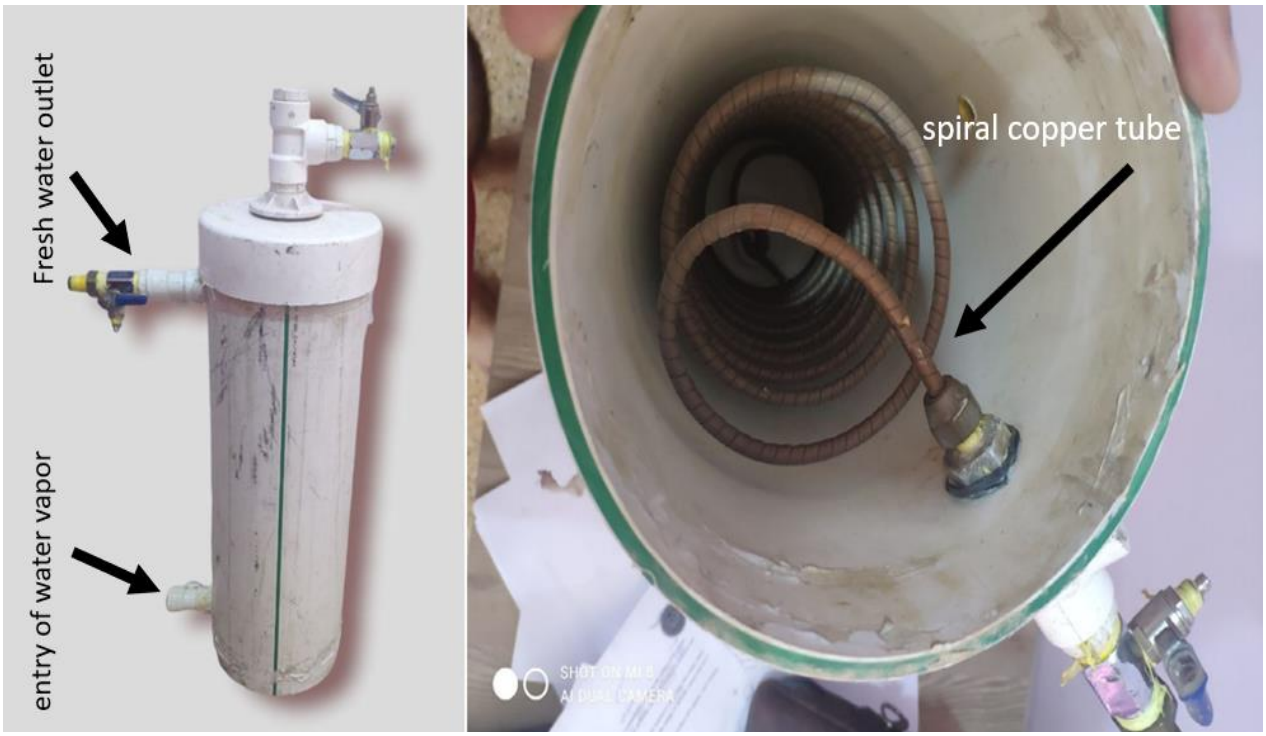

Figure 4.18: a steam condensing system.

Table (4.1) shows the dimensions of the solar distillation system that was manufactured.

Table 4.2: Summary of the dimensions of the solar parabolic dish distillation system.

Parameter	Value	Unit
Parabolic dish diameter	1.58	m
Aperture area of the parabola	1.96	m^2
focal length	0.78	m
Heat exchanger length (absorber)	0.166	m
The diameter of the heat exchanger	0.076	m
Heat exchanger wall thickness	0.002	m
Thickness of the thermal insulation layer (glass wool)	0.025	m
Outside diameter of the heat exchanger cover	0.09	m
Inside diameter of the heat exchanger cover	0.076	m
Heat exchanger cover height	0.025	m
Inside heat exchanger cover depth	0.015	m
Shell diameter (outrer)	0.15	m
Shell thickness	0.025	m
Shell height	0.5	m
Coil tube diameter	0.11	m
Pitch between the rings	0.03	m
Number of coil ring	11	-

4.3 Measurement Devices

To investigate collector efficiency, we must collect primary data that provides an impression of the system based on the measuring tools. The temperature of the water entering the receiver, the temperature of the distilled water exiting the receiver, and the ambient temperature are the primary recorded data. The quantity of direct solar irradiance reaching the dish, wind speed, the amount of water flowing into the receiver, the temperature of the receiver base exposed to concentration, and the productivity of the system's distillation are all measured.

4.3.1 Data Logger

An eight-output data logger (TC-08) is used to measure the temperature of (water, heat exchanger cover, outer surface after insulation). Where it can measure temperatures from(-250℃ to +1370 ℃), which is characterized by high accuracy.

It also has the ability to store the information obtained by linking it to the pico log program. Figure (4.18) shows the data logger.

Figure 4.19: Picolog data logger with eight-output.

4.3.2 Thermocouple

To measure the temperature of the water, the temperature of the steam generator cover (absorber), the temperature of the outer surface of the heat exchanger after being isolated, six temperature sensors of type K (4.19) connected to a data logger are used. The temperature sensors are distributed as follows:

- Two sensors for measuring the temperature of the heat exchanger cover (absorber), Small holes are made inside the heat exchanger cover to install the thermocouple .
- A sensor to measure the temperature of the water entering the heat exchanger(absorber), and another sensor implanted at the top of the heat exchanger from the inside to measure the temperature of the steam inside the heat exchanger
- Two sensors are placed on the surface of the external heat exchanger after being insulated with glass wool.

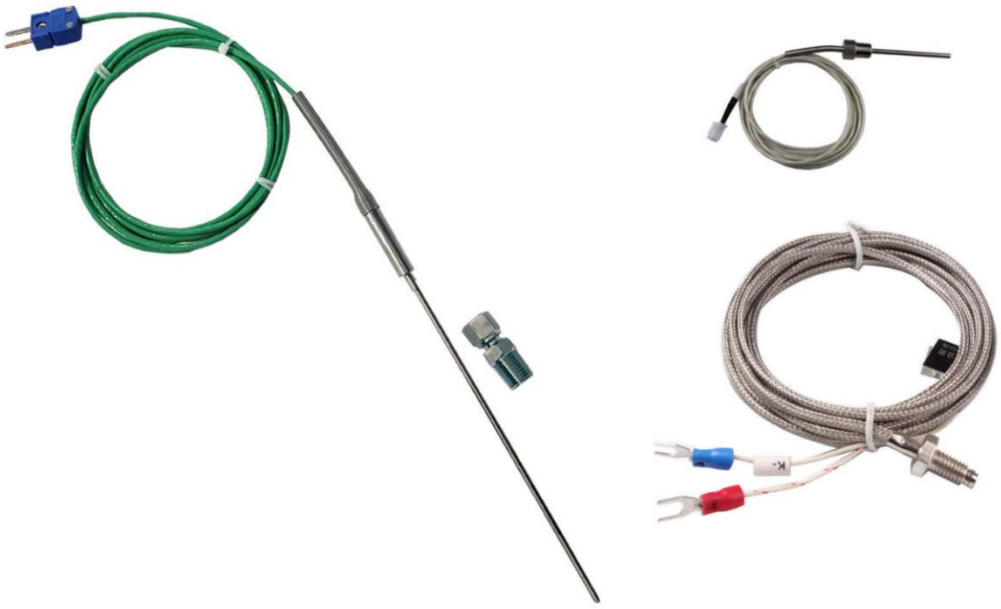

Figure 4.20: Temperature sensors

4.3.3 Measurement of the intensity of solar radiation

To calculate the intensity of solar radiation falling on the parabolic dish, (Solar Transmission & Power meter SP2065) was used, which has a measurement range from 0 to 1999 w / m², and Figure (4.20) shows the solar radiation intensity measurement device.

Figure 4.21: Solar Transmission & Power meter SP2065

4.3.4 Measuring ambient temperature and wind speed

To measure the ambient temperature around the steam generator (absorber), and the wind speed (Anemometer Plus AR836) is used. Wind speed range from 0 to 45m/s, and temperature measuring range from 0℃ to 60℃. Figure (4.21) shows a device for measuring temperature and wind speed

Figure 4.22: Anemometer Plus AR836

4.3.5 Error analysis

The accuracy of various measuring instruments used in the experiments is presented in Table 2.

No.	Instrument	Accuracy	Range	% error
1	Data Logger TC-08	±0.5 °C	-250°C to +1370 °C	±0.2%
2	Thermocouple (K Type)	± 2.2°C	-200°C to 1260°C	±0.75%
3	Anemometer Plus AR836	1m/s	0-45 m/s	±3%
4	Anemometer Plus AR836	±2°C	0°C to 60°C	±3%
5	Power meter SP2065		0 to 1999 w / m²	

4.4 Thermal camera test

To find out the effect of using nano-filling in the inner fins of the heat exchanger, a thermal camera test was conducted for two samples of different fins, one of them with a nano-stuffing. They were placed in a container of hot water at a constant temperature (60°C) and the camera was turned on. The heat transfer in the fin with the nanofiber is faster than in the other sample.. This is the biggest evidence that the nano-filling made a channel that accelerates the heat transfer from the surface of the heat exchanger to the inside of the water in it. As shown in figure (4.22) where

the fin on the right is the nano-filled fin, and the one on the left is the normal fin used in the first model.

Figure 4.23: Thermal camera result

4.5 Experimental procedure

In this work, experiments were conducted on different days with two models of the heat exchanger, the first model (finned heat exchanger),while the second model (finned heat exchanger filled with nanomaterial), the following point summarize the work:

1. The test begins with the installation of all parts of the solar water distillation system, the installation of measuring devices and the examination of electrical connections, and connections of sensors.
2. Preparing the heat exchanger with water from the salt water storage tank by opening the inlet valve and closing it after it is filled with water. The entry of water into the heat exchanger is manually controlled by the valve ,the same is

the case with the steam generated in the heat exchanger whose exit is manually controlled.

3. Operating the solar tracking system, measuring devices and starting to take readings.
4. After the water changes to steam inside the heat exchanger, the steam exit valve is opened to condense inside the condensing heat exchanger.
5. The yield of distilled water is measured using a graduated laboratory beaker.
6. Experiments were conducted for the days 17/3/2022 & 24/4/2022 & 3/5/2022 & 13/5/2022 using the first internal fin heat exchanger, and on 18/3/2022 & 25/4/2022 & 6/5/2022 & 14/5/2022 the experiments were conducted Using a finned heat exchanger with a nano-filling.

Chapter Five

Results and Discussion

CHAPTER FIVE

Results and Discussion

INTRODUCTION

In this chapter, the results of the distillation system using the solar concentration resulted from the parabolic dish will be discussed, and the effect of environmental conditions such as ambient temperature, wind speed, and solar radiation intensity on the system's performance will be discussed. As well as, the results of using nano-filling in the heat exchanger (absorber) and its effect on the efficiency and productivity of the system will be discussed. The experiments were conducted in Al-Diwaniyah city in the months (March, April, and May) of the year 2022.

5.1 Sources of Solar heat with fins

5.1.1 Water Productivity

In this section of the chapter, the productivity of the solar distillation system using the first model of the heat exchanger (Fins without nano filling) is discussed.

The productivity of the solar distillation system using the heat exchanger (the first model) which is conducted as the first run on17/3/2022, where the heat exchanger was charged (absorbed) with brakish water and the experiment extended from 9:00 to 15:00 is shown in Figure (5.1). In the first hour of operating the solar distillation system, the productivity is 0.89 liter, and the intensity of averge solar radiation is 651W/m^2 and the ambient temperature is 19.4℃. With the passage of time, the intensity of solar radiation began to increase until it reached to maximum value between 12:00 and 13:00, where it reached 823W/m^2 and the ambient temperature is at 23.6℃. Productivity reached its maximum between 12:00 and 13:00

and amounted to 1.85 liters. The total productivity was 7.94 liters at an average solar radiation intensity of 736.38W/m^2, and an average ambient temperature of 22.7℃.

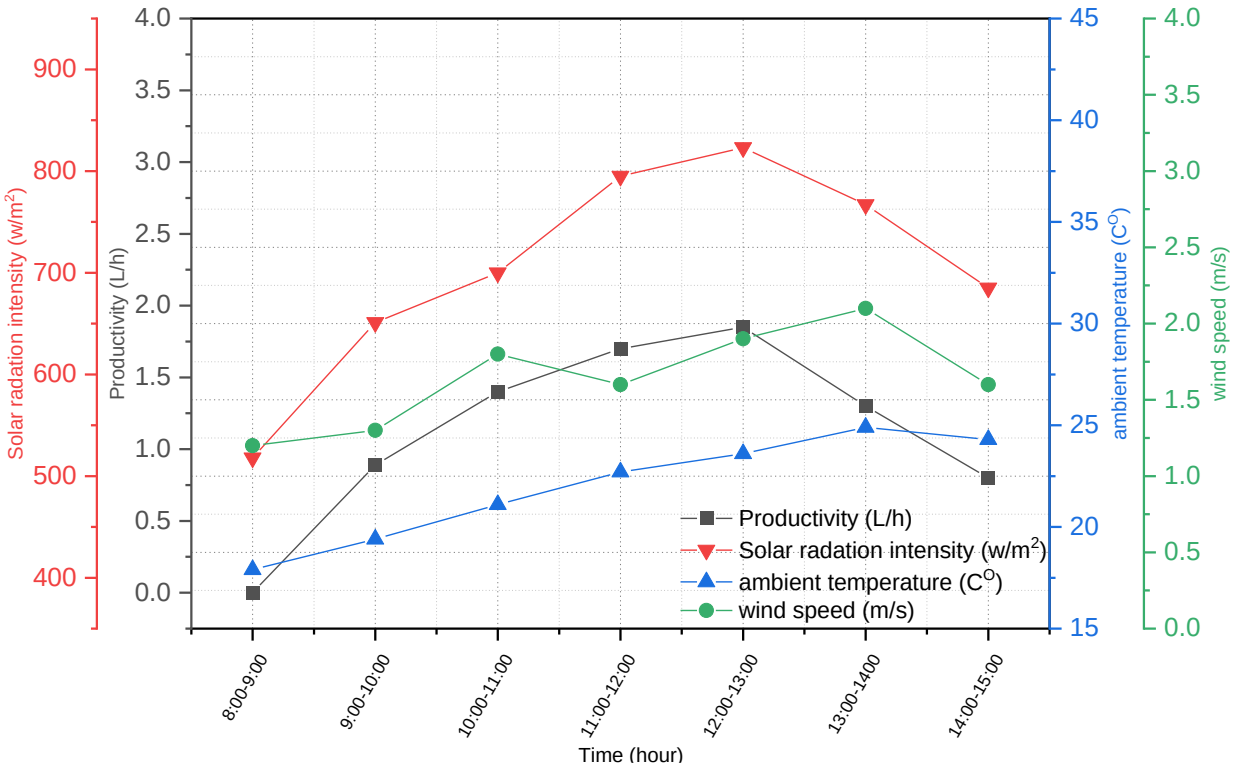

Figure(5.1): Variation of the productivity of the solar distillation system with the environmental conditions for a day (17/3/2022).

On 04/24/2022, second run experiment was conducted using the first model of the heat exchanger (absorber), as Figure (5.2) its clearly shown that the variation in productivity with environmental conditions. In the first hour of the experiment, the productivity was 1 liter at the intensity of solar radiation 695 W / m^2. The greatest productivity was obtained between 12:00 and 13:00 and it was 1.92 liters and the intensity of average solar radiation was 875 W/m^2, the averge ambient temperature was 27.3℃, and the averge wind speed was 0.9 m/s. The total productivity of this experiment was 8.61 liters at an average solar radiation of 770.16W/m^2, the ambient temperature of 25.7℃. It can be noted that the second experiment gave greater

productivity than the first experiment due to the increase in the intensity of solar radiation.

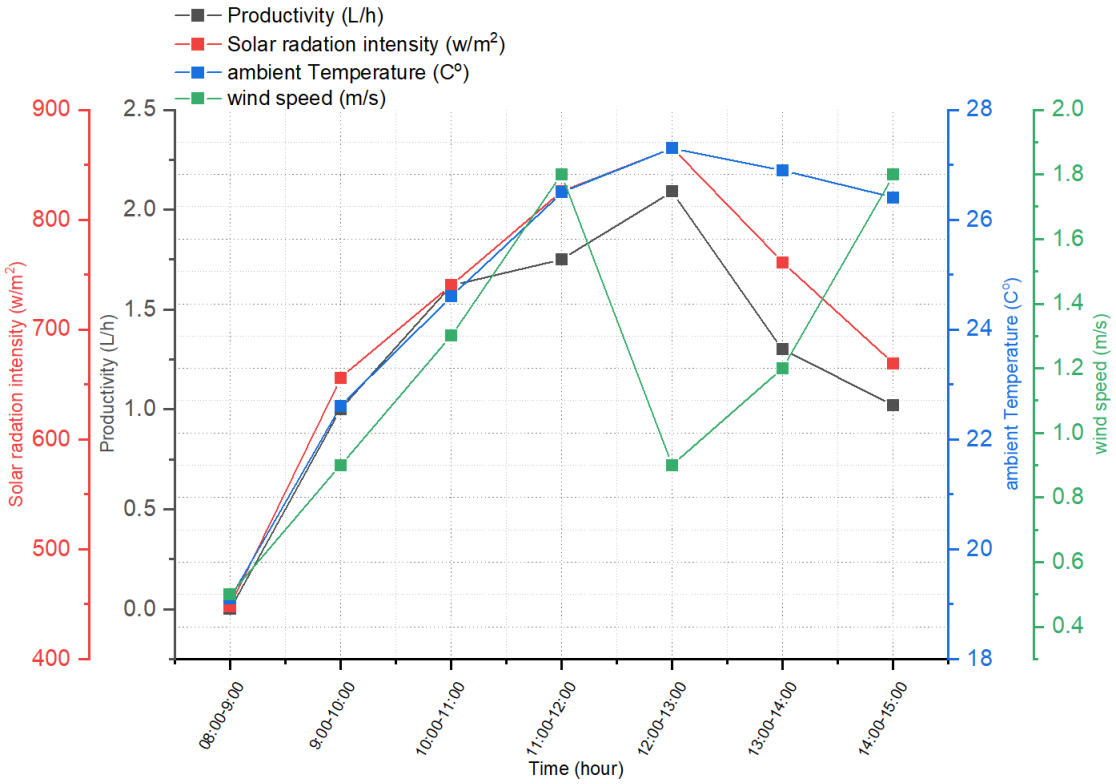

Figure(5.2): Variation of the productivity of the solar distillation system with the environmental conditions for a day (24/4/2022).

On 3/5/2022 another experiment was conducted, where the productivity of the distillation system was 9.6 liters. Figure (5.3) shows the variation in productivity with environmental conditions, and it should be noted that the maximum production limit was Between the hours of 12:00 and 13:00, the productivity reached 2.1 liters, and then the intensity of solar radiation was 886 W /m^2. One of the indicators of the practical readings in the third experiment give greater productivity than the first and second experiment, and this is clear from the fact that the value of solar radiation increased.

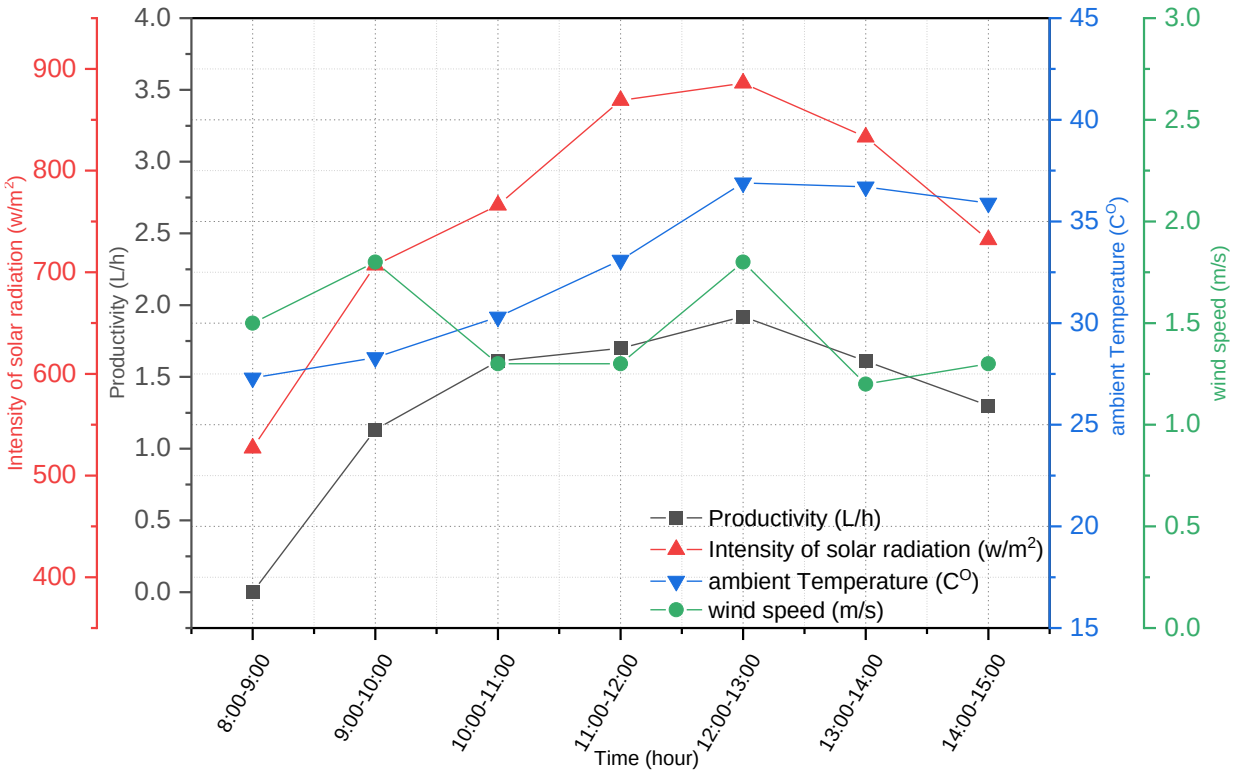

Figure(5. 3): Variation of the productivity of the solar distillation system with the environmental conditions for a day (3/5/2022).

Figure (5.4) shows the results of distillation for the day 13/5/2022 and their variation with the environmental conditions. The average solar radiation for that day was 817.83 W/m^2, and the average temperature was 35.6°C. Experiments of this day resulted in a total productivity of 10.17 liters of the first model. The maximum productivity of 2 liters was obtained between 12:00 and 13:00, the intensity of solar radiation was 911 W/m^2 and the temperature was 36.8 °C. Table (5.1) shows the productivity of the distillation system for days for the experiments that were conducted using the first model. The productivity of the distillation system in the fourth experiment was higher than the other experiments due to the high intensity of solar radiation in this experiment.

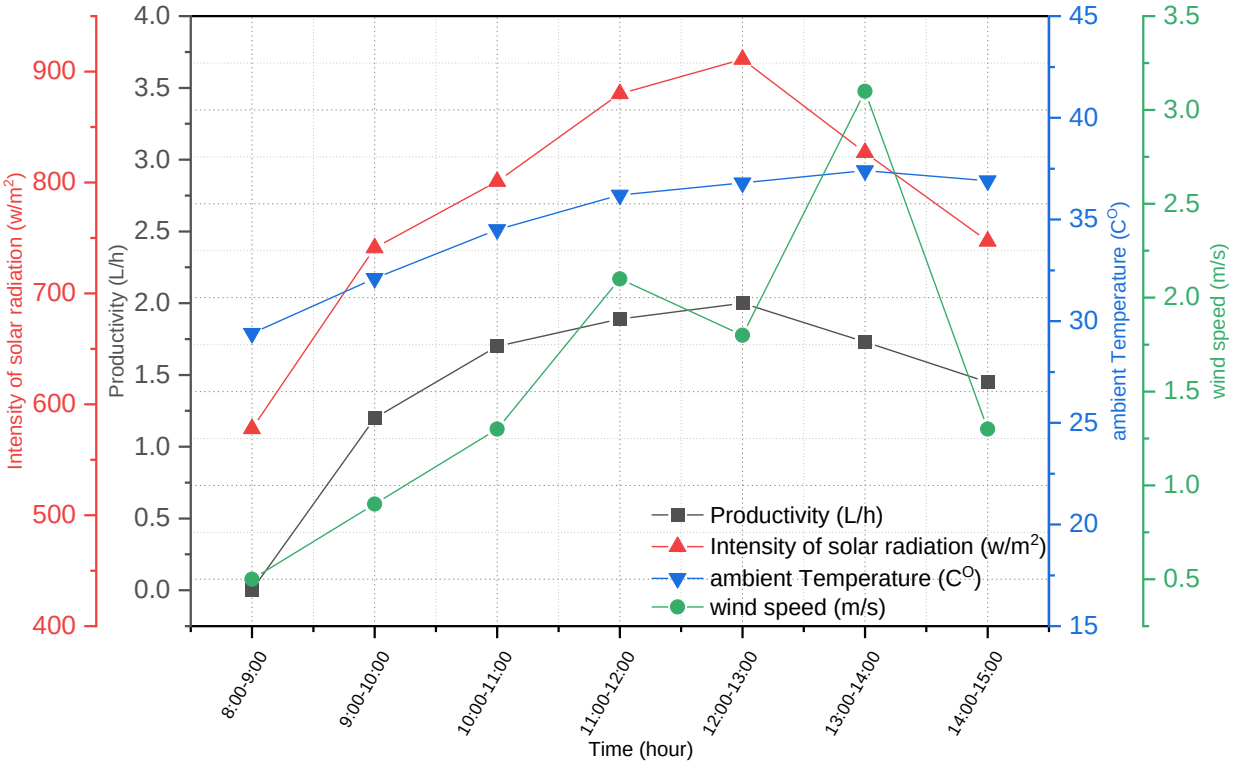

Figure(5.4): Variation of the productivity of the solar distillation system with the environmental conditions for a day (13/5/2022).

From Table (5.1), it can be observed the increase in water productivity with the increase in the intensity of solar radiation. In addition, it indicates the increase in water productivity on the amount of thermal energy flow and its transformation into water through the water-contact surface inside the metal container, as well as through its transmission through the five fins.

Table (5.1) Variation of the productivity of the distillation system during the days of experiments

Time	Productivity(L/h)			
	17/3/2022	24/4/2022	3/5/2022	14/5/2022
09:00-10:00	0.89	1	1.132	1.2
10:00-11:00	1.4	1.62	1.67	1.7
11:00-12:00	1.7	1.75	1.8	1.89
12:00-13:00	1.85	1.92	2	2.2
13:00-14:00	1.3	1.3	1.61	1.73
14:00-15:00	0.8	1.02	1.3	1.45
Sum	7.94	8.61	9.612	10.17

5.1.2 Temperature of working fluid

In order to understand what happens inside the heat exchanger (absorber) during the evaporation process, we will look at the temperature of the water during evaporation.

Figure (5.5) shows the gradual rise in the temperature of the water inside the heat exchanger (absorber) when the water distillation system started at 9:00 . On 17/3/2022, the water needed 43 minutes to reach the temperature of 115 ° C, and then the radiation intensity was Solar 651 W/m^2. While on 24/4/2022, it took 36 minutes for the water to completely convert the water charge into steam, and the intensity of solar radiation was 695W/m^2, and the ambient temperature was 22.6℃. On the days 3/5/2022 & 13/5/2022, the water charge inside the heat exchanger (absorbed) turned into steam after 33 minutes, when the intensity of solar radiation was 707&741W/m^2 respectively. Where it is noted that the intensity of solar radiation greatly affects the temperature of the water inside the heat exchanger (absorbed), the higher the intensity of the solar radiation, the greater the heat content associated with the

reflected from the parabolic dish. The use of the five fins helped the acceleration process in the transfer of heat falling on the surface and its delivery to the water. Heat transfer by the fins is of two types, thermal conduction through the cross-sectional area of the fin metal, as well as thermal conduction across the circumference of the fin through the side area.

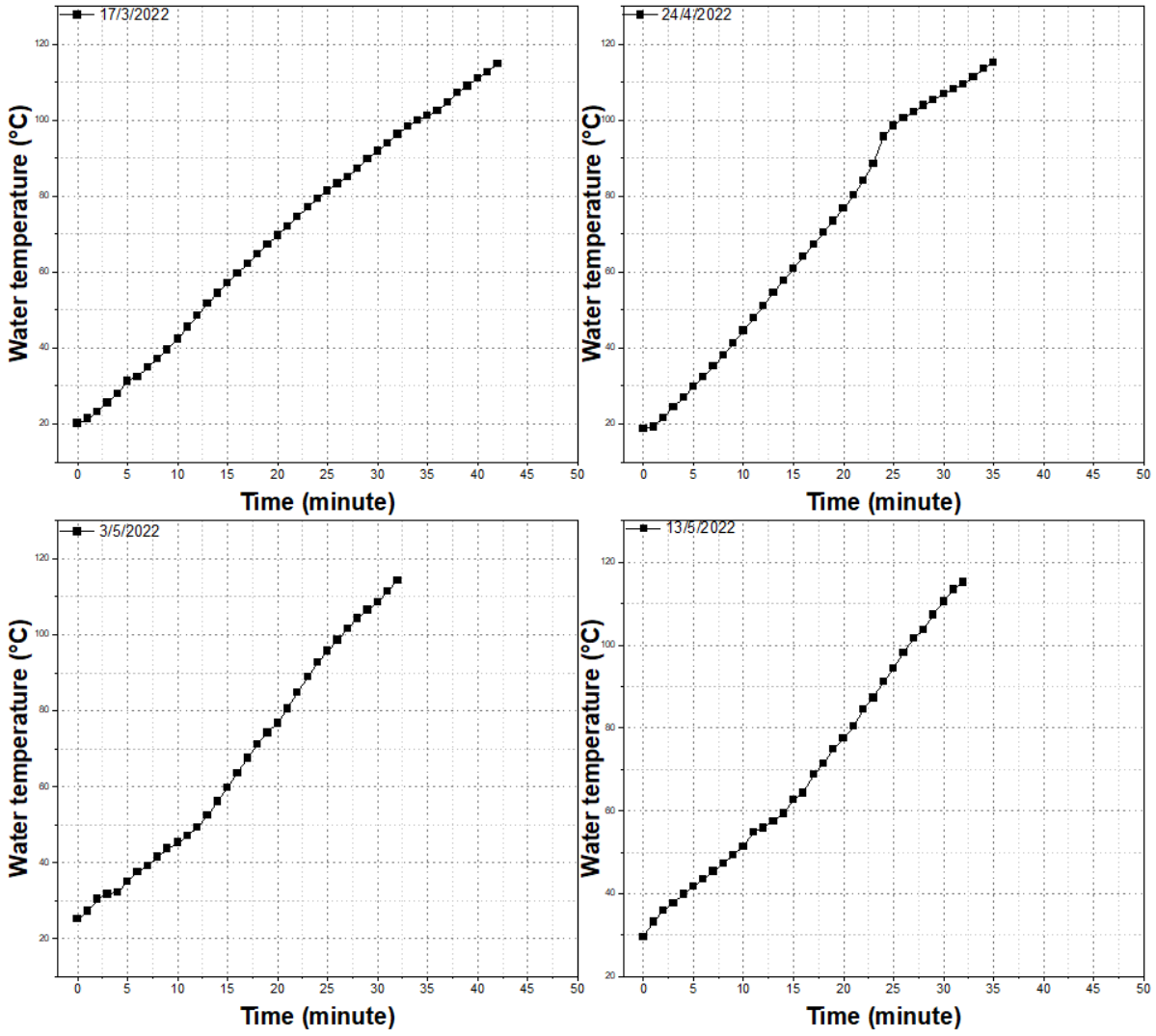

Figure (5.5): Variation of water temperatures inside the heat exchanger (absorber) at the start of the experiment at 9:00

5.1.3 Surface Temperature of Heat Exchanger absorber

Figure (5.6) shows the temperature of the heat exchanger cover (absorber) during the different days of experiments when starting the solar water distillation system at 9:00.

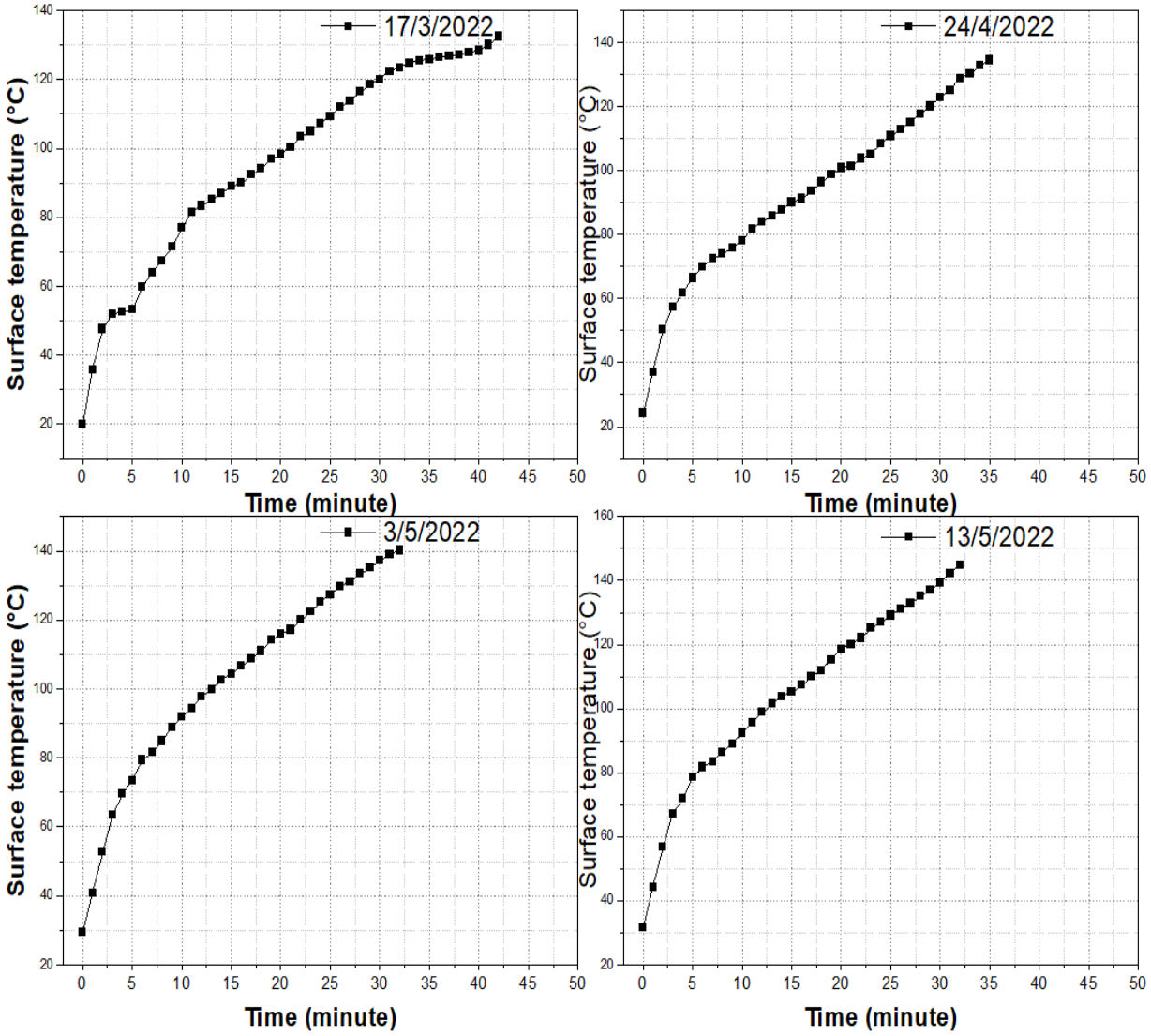

Figure(5.6): Variation in the temperature of the heat exchanger cover when the system starts operating at 9:00

On 3/17/2022, it is noted that the temperature started to rise gradually until it reached its maximum value after 43 minutes when the intensity of solar radiation was 651W/m^2, the ambient temperature was 19.4°C, and the wind speed was 1.3 m/s.

On 24/4/2022, the heat exchanger cover (absorber) took less time to reach its maximum value, which was 134.5℃, and the water temperature inside the heat exchanger (absorber) was 115.2℃. At this hour, the intensity of solar radiation was 695W/m^2, the ambient temperature was 22.6℃, and the wind speed is 0.9 m/s. On 3/5/2022 the heat exchanger cover (absorber) temperature reached 140.2℃ after 33 minutes, where all the water charge inside the heat exchanger (absorber) turned into steam, and then the intensity of solar radiation was 707W/m^2, ambient temperature 28.3℃, wind speed 1.8 m/s.

On 13/5/2022 the heat exchanger cover (absorption) also took 33 minutes to reach a temperature of 144.9℃, as all the water charge inside the heat exchanger turned into steam. The intensity of solar radiation was 741W/m^2, ambient temperature 32.1℃, and a wind speed of 0.9 m/s.

The new design of the heat exchanger and the location of the concentrated solar radiation fall on it ensures the transmission of the largest amount of heat energy through the surface connected to the water, despite the presence of heat losses.

5.2 Sources of Solar heat with fins Filling/Nanomaterial

In this part of the chapter, the productivity of the solar distillation system using a parabolic solar dish with nanoparticle filling inside each fins will be discussed.

5.2.1 Water Productivity

On 18/3/2022, the experiment extended from 9:00 to 15:00 is shown in Figure (5.7). The productivity of the first hour was 1.66 liters, the intensity of solar radiation was 659W/m^2, and the ambient temperature was 21.7 ℃. It is worth noting that the use of the nano-material has increased the evaporation speed inside the heat exchanger (absorber) increased and thus the productivity increased. The maximum productivity obtained on this day between 12:00 and 13:00 was 2.8 liters, with an intensity of solar radiation 825 W/m^2, and the ambient temperature was 25.7 ° C. The

total production rate for this day was 12.48 liters, with average solar radiation of 741.16 W/m^2, an average ambient temperature of 24.66℃, and an average wind speed of 1.08m/s.

The nano-filling was a channel for accelerating the transfer of energy from the hot outer surface to the water in contact with the five fins, successful welding processes ensured that the nanomaterial was prevented from leaking and mixing with the steam.

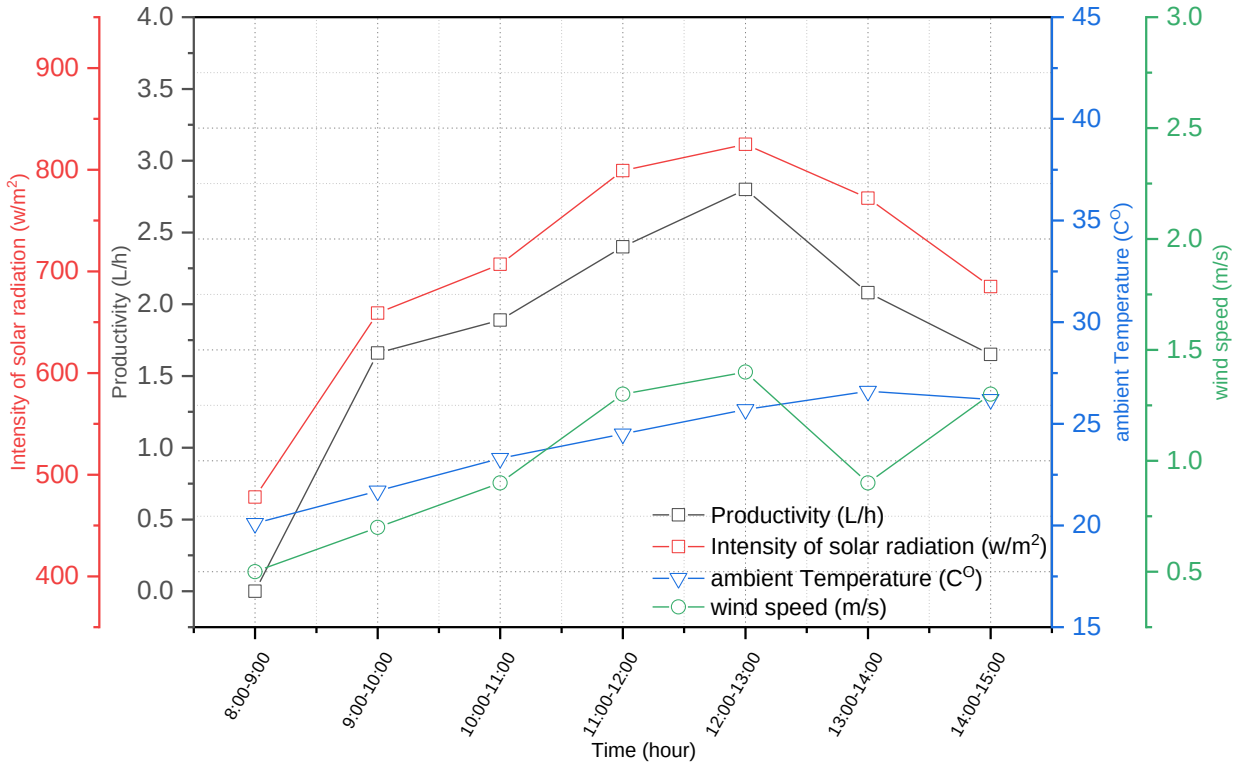

Figure(5.7): Variation of the productivity of the solar distillation system with the environmental conditions for a day (18/3/2022).

On 25/4/2022, the daily production of the solar distillation system was 13.886 liters at an average solar radiation intensity of 773.66W/m^2, an average temperature of 27.13℃, and an average wind speed of 1.5 m/s. The maximum productivity obtained between 12:00 and 13:00 was 3.17 liters, with an average solar radiation intensity of 880W/m^2. Figure (5.8) shows the variation of productivity with environmental conditions. Compared with the results of the experiment on the first

day using the nano-filling, the effect of increasing solar radiation on increasing water production was very clear

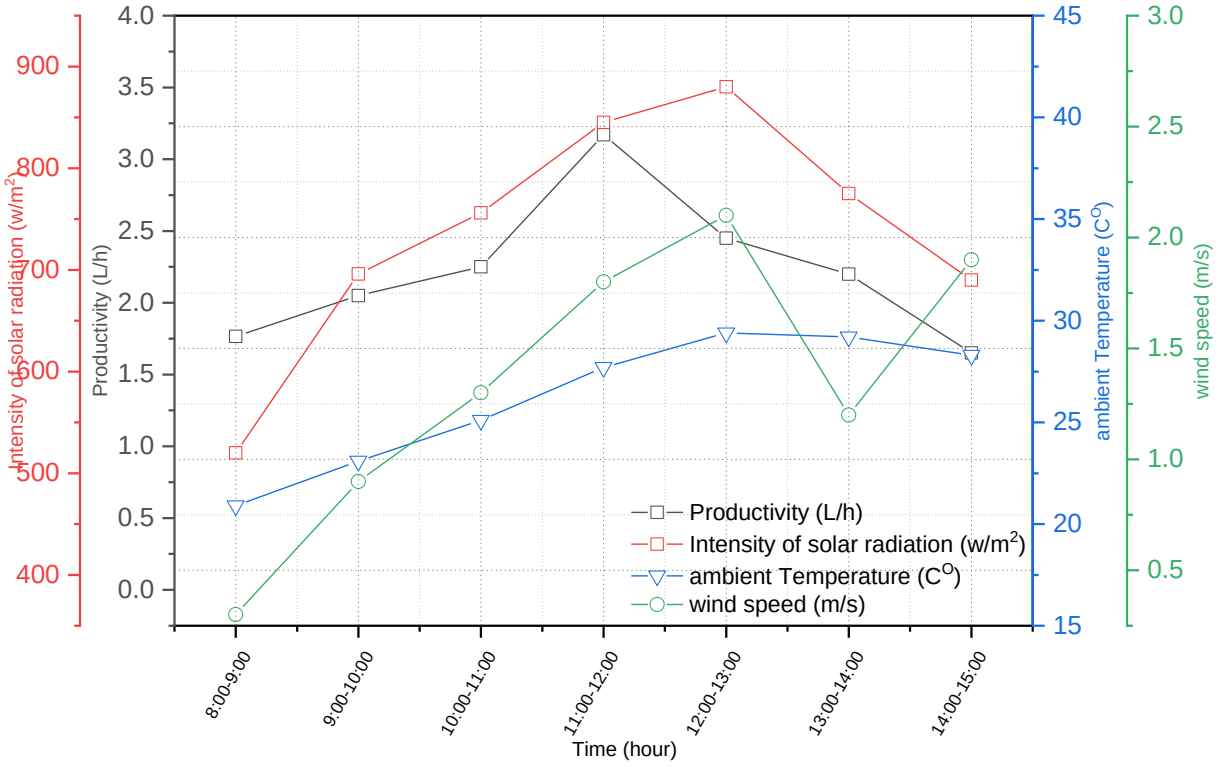

Figure(5.8): Variation of the productivity of the solar distillation system with the environmental conditions for a day (25/4/2022).

Figure (5.9) shows the variation of the products of the distillation system for the day 6/5/2022 with the environmental conditions. The distillate products when using the second model of the heat exchanger (absorbed) on this day amounted to 14.56 liters and at an average solar radiation intensity of 803.83 W/m^2, the average temperature 34.4℃. The productivity of the first hour of work of the solar water distillation system was 1.8 liters, the intensity of solar radiation was 711W/m^2, and the ambient temperature was 28.5℃. It is very clear that the productivity increased by increasing the solar radiation as a result of the passage of the largest amount of solar energy through the nanopath

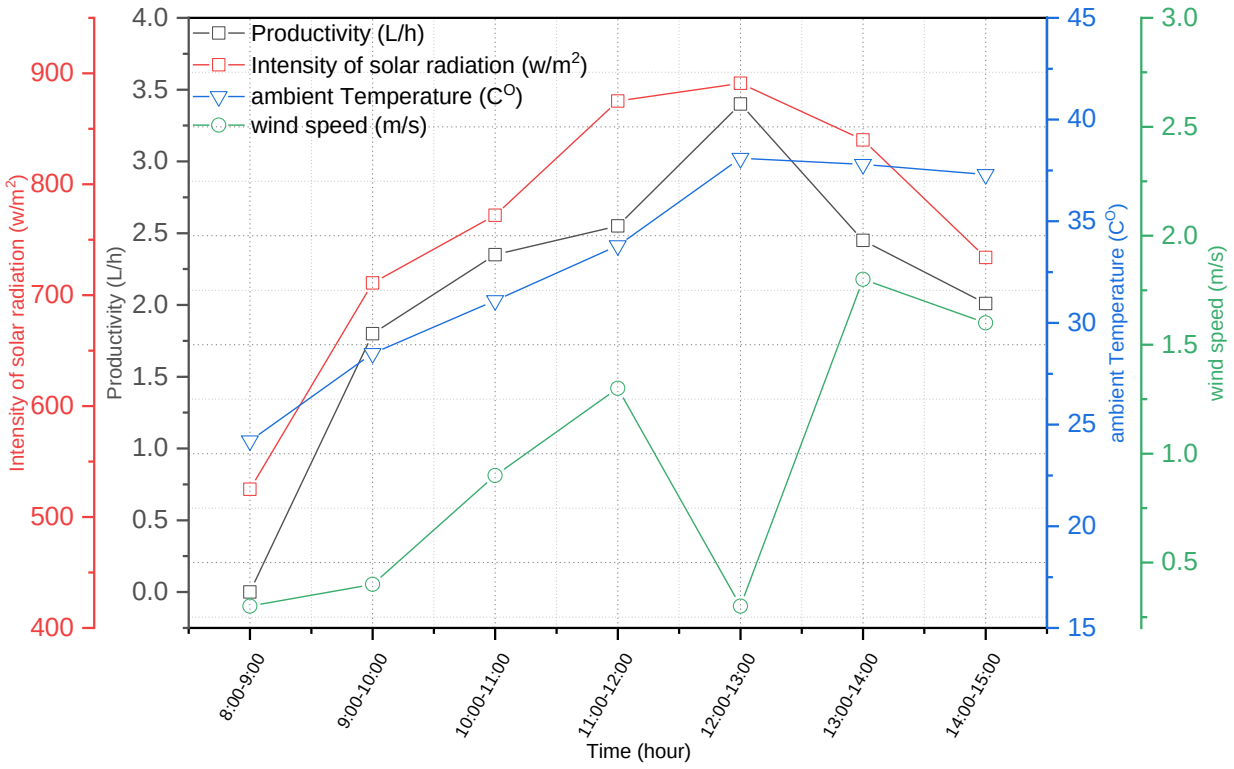

Figure(5.9): Variation of the productivity of the solar distillation system with the environmental conditions for a day (6/5/2022).

On May 14, 2022, an experiment was conducted using the second model of the heat exchanger (absorber), where the experiment lasted from 09:00 to 15:00. The intensity of solar radiation in the first hour of conducting the experiment was 738W/m^2, ambient temperature 30.9℃, and then the productivity of the solar distillation system reached 2 liters. The greatest productivity of the solar distillation system of 3.49 liters was obtained between 12:00 and 13:00 at an intensity of solar radiation of 913 W/m^2. The total productivity of the system on this day was 16.11 liters and the average solar radiation was 820.33 W/m^2. Figure (5.10) shows the variation of productivity with atmospheric parameters. It is worth noting that the average temperature for this day is 36.2℃, and the average wind speed is 2.4 m/s. The practical data for the fourth day of using nano-fillers gave the largest amount of productivity compared to previous research, which indicates that the use of nano-fillings has a significant impact on increasing productivity.

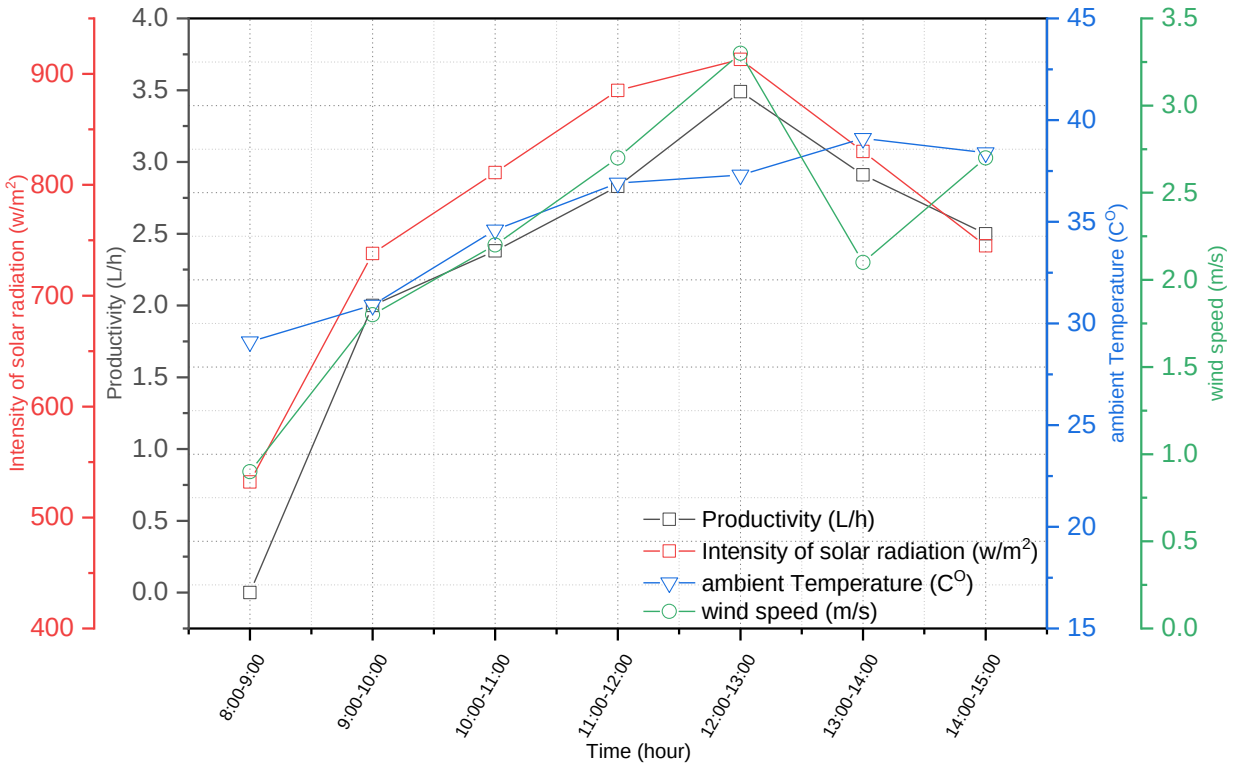

Figure(5.10): Variation of the productivity of the solar distillation system with the environmental conditions for a day (14/5/2022).

From Table (5.2), it can be seen that the productivity of the solar distillation system increased due to the use of nano-filling, where the nano-channels contributed to increasing the heat flow from the hot surface to the water in contact with the nano-filled fins.

Table (5.2) shows the productivity of the solar distillation system for the different days of experiments and using the heat exchanger (absorber) with nano-filling

Time	Productivity(L/h)			
	18/3/2022	25/4/2022	6/5/2022	14/5/2022
09:00-10:00	1.66	1.766	1.8	2
10:00-11:00	1.89	2.05	2.35	2.38
11:00-12:00	2.4	2.25	2.55	2.83

12:00-13:00	2.8	3.17	3.4	3.49
13:00-14:00	2.08	2.45	2.45	2.91
14:00-15:00	1.65	2.2	2.25	2.5
Sum(L/day)	12.48	13.886	14.8	16.11

5.2.2 Temperature of working fluid

Figure (5.11) shows the high temperature of the water inside the heat exchanger. In the first experiment that was conducted on 3/18/2022, the average intensity of solar radiation was 659W/m^2 when the experiment started at 9:00, the average ambient temperature was 21.7℃, and the average wind speed was 0.7m/s. The temperature of the water inside the heat exchanger began to rise gradually until all the water charges inside the heat exchanger changed to steam, and this process took 26 minutes. The water temperature before operating the distillation system was 19.8 ℃.

On 25/4/2022, the average intensity of solar radiation was 696W/m^2, the average ambient temperature was 23.1℃, and the average wind speed was 0.9 m/s. All the water charges inside the heat exchanger turned into steam after 24 minutes of starting the experiment, and the temperature of the water was 20.4℃ before the experiment started. The average intensity of the solar radiation was 711W/m^2, the ambient temperature was 28.5℃, and the average wind speed was 0.4 m/s on 5/6/2022. Where it is noted that the water charge inside the heat exchanger all turned into steam after 23 minutes. While it took 22 minutes to change to steam on 05/14/2022, where the average intensity of solar radiation was 738W/m^2, the average ambient temperature was 30.9℃ and the average wind speed of 1.8 m/s. The acceleration in the working fluid temperature with time can be observed with packings or nanochannels, which have a great advantage over this process.

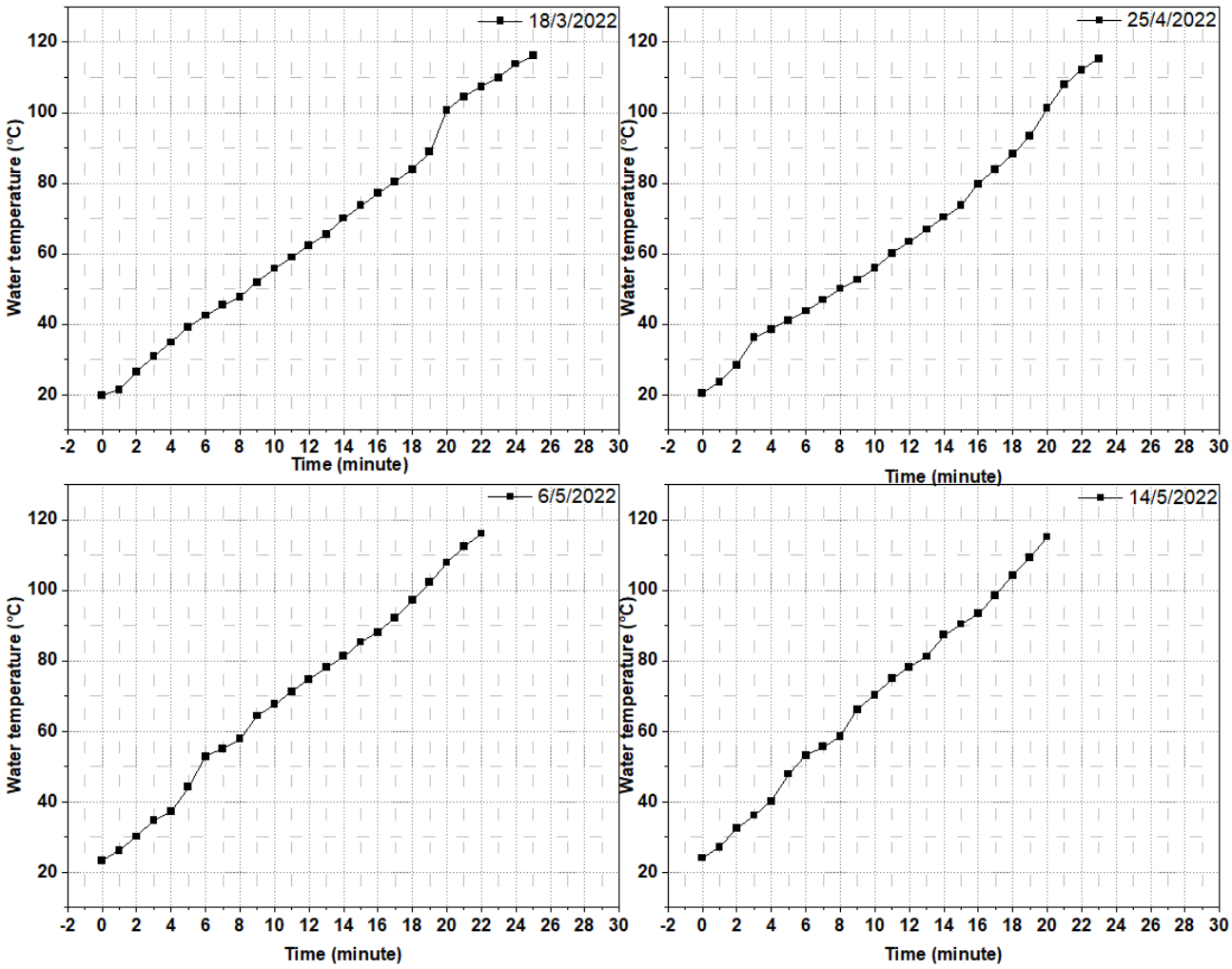

Figure(5.11): Variation of water temperature inside the heat exchanger

5.2.3 Surface Temperature of Heat Exchanger absorber

The temperature of the heat exchanger cover rises when it begins (starting run) to absorb the reflected rays from the parabolic dish, as the heat exchanger cover is made of aluminum, which has a thermal conductivity of (237W/m.K). The temperature of the heat exchanger cover (absorber) begins to rise gradually until all the water charge inside the heat exchanger turns into steam. This section of the chapter will discuss the temperature of the heat exchanger cap (absorber) when starting the system at 9:00 solar distillation for each experiment.

On 3/18/2022, the temperature of the heat exchanger cover reached 120.1 ℃, at this temperature all the water charge turned into steam, and the average solar radiation intensity between 9:00 and 10:00 was 659 W/m^2, ambient temperature 21.7℃, and wind speed of 0.7 m/s. On 25/4/2022, the surface temperature of the heat exchanger (absorber) was 135.4℃, the average ambient temperature in this experiment was 23.1℃, average wind speed of 0.9 m/s, and the average intensity of solar radiation 696 W/m^2. The heat exchanger took 25 minutes to convert all the water charge into steam.

On 6/5/2022, the temperature of the heat exchanger cover was 144.1 ℃, the average ambient temperature was 28.5 ℃, the average wind speed was 0.4 m/s, and the average intensity of solar radiation was 711W/m^2. In the last experiment, which was conducted on 14/5/2022, the temperature of the cover reached 149.3 ℃, and the average intensity of solar radiation was 738W/m^2, wind speed of 1.8 m/s, and ambient temperature of 30.9 ℃. Figure (5.12) shows the temperature of the heat exchanger cover for the different days of experiments. Thermal energy is transmitted through the nano-filling materials faster compared to its transfer through the metal materials for each of the five fins, because the thermal conductivity coefficient of the nano-material reaches 4000 W/m.℃ compared to aluminum metal, which is 273 W/m.℃.

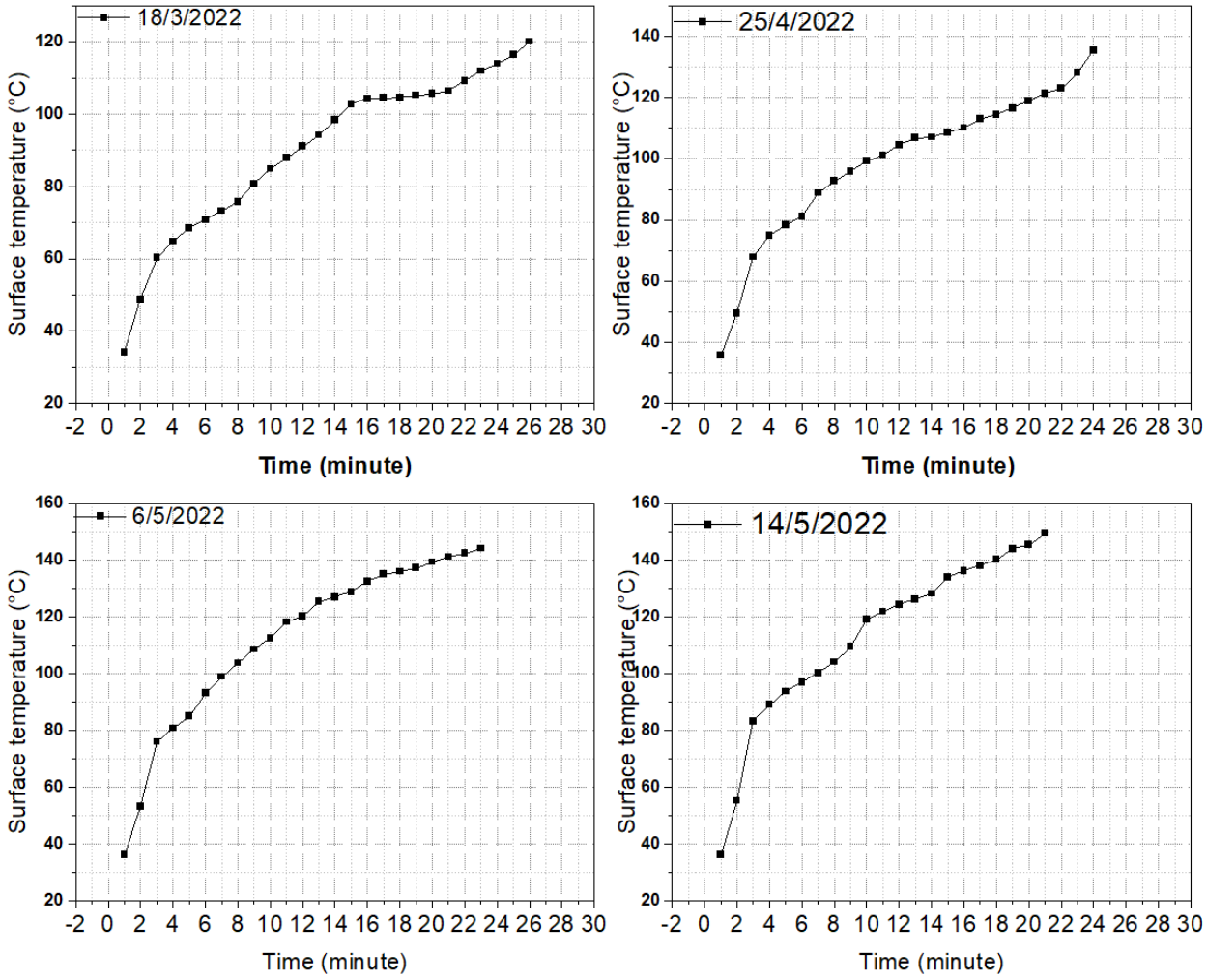

Figure(5.12): Variation in the temperature of the heat exchanger cover when starting the system

5.3 Effect of Using Nanomaterial on Thermal Performance of Heat Exchanger

5.3.1 Water Productivity

The use of nano-filling is considered an innovative method to increase heat transfer. The nano-material that was used (Multi-Walled Carbon Nanotubes) is characterized by its high thermal conductivity(3500 W/m.K). Results showed the use of nano-filling in the second model of the heat exchanger (absorber) resulted in a significant increase in productivity. When comparing the results obtained from both

models on 3/17/2022 and 3/18/2022, the improvement rate in productivity reached to 57.17%.

Figure (5.13) shows the variation of the distillate products for the days 17/3/2022 and 18/3/2022, where the first model was used in the first experiment, and on the second day, the second model of the heat exchanger was used in which the nano-filling was used. In the first model, the productivity was 7.94 liters and the average solar radiation was 736.38 W/m^2, while in the experiment that was used in the second model, the productivity was 12.48 liters and average solar radiation intensity of 741.16 W/m^2

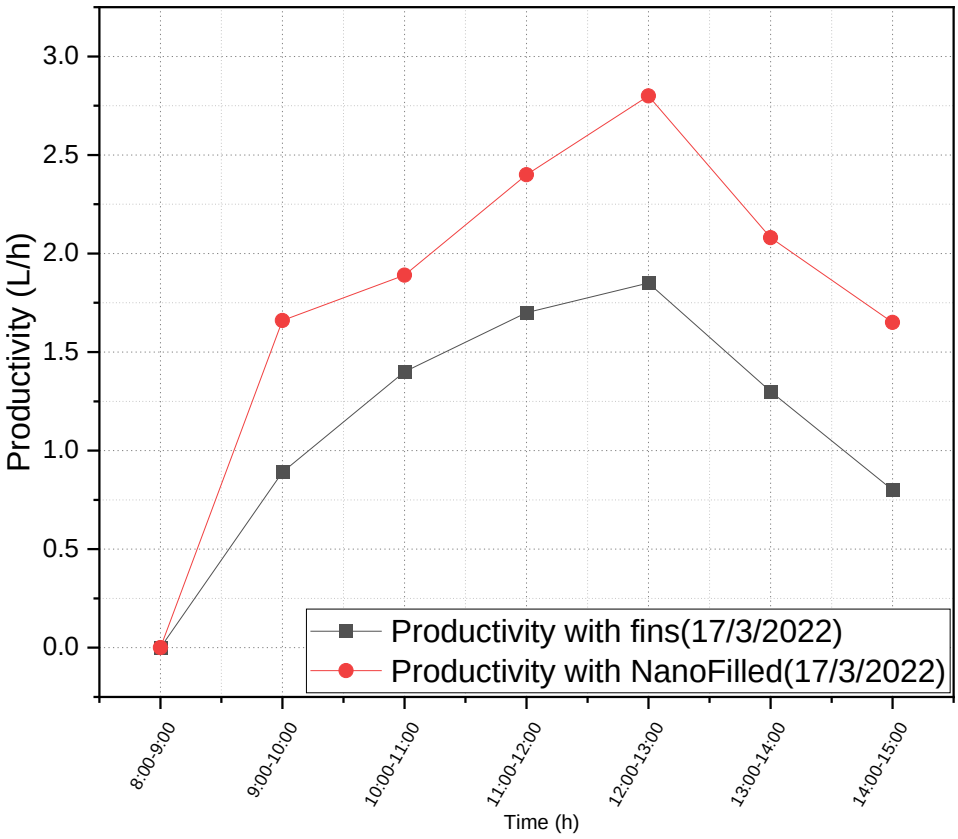

Figure(5.13): Comparison between the outputs of the distillation system using both models of the heat exchanger for the days of 17/3/2022 & 18/3/2022

Where the nano-material (MWCT) contributed to speed of heat transfer from the heat exchanger cover to the water inside the heat exchanger, and this contributed to shortening the time required for evaporation to occur. At the beginning of the operation of the distillation system in the first model, the water charge took more than 40 minutes to evaporate, while when using the nano-filling, the water charge evaporated completely after 23 minutes.

In the experiments that were conducted on 4/24/2022 and 4/25/2022, the productivity increased by 58.1% when using nano-filling. When using the first model on 4/24/2022, the amount of production was 8.78 liters with an average intensity of 770.16 W/m^2 solar radiation. On 25/4/2022, the total productivity of the solar distillation system was 13.886 liters, with an average solar radiation intensity of 773.66 W/m^2. Figure (5.14) shows the variation in the production outputs of both models on 24/3/2022 and 25/4/2022.

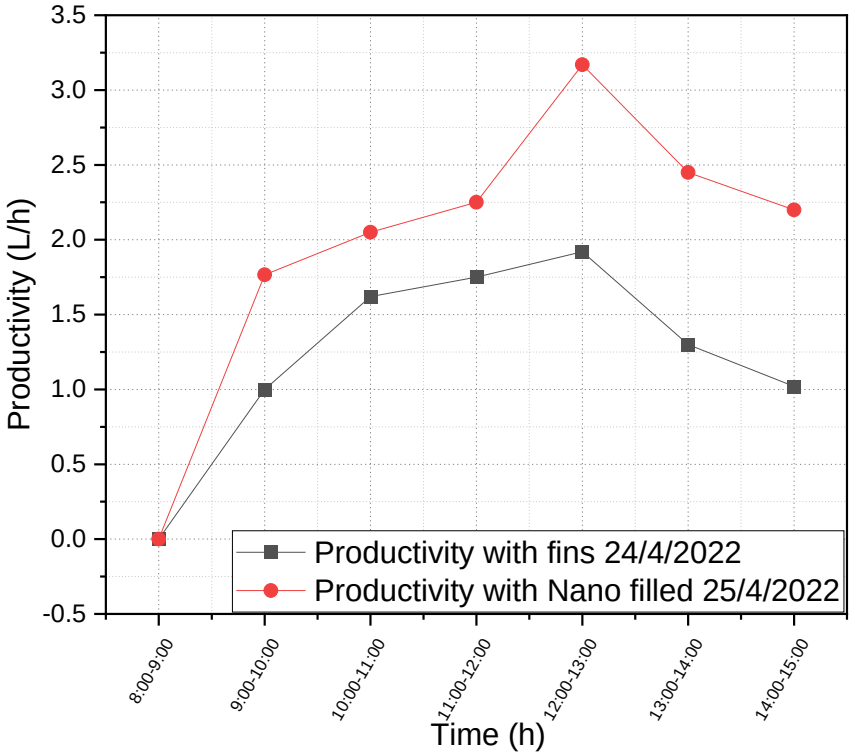

Figure(5.14): Comparison between the outputs of the distillation system using both models of the heat exchanger for the days of 24/4/2022 & 25/4/2022

At the peak of the intensity of solar radiation, the productivity in the second model increased by 51.6%, and then the intensity of solar radiation was 865 W/m^2. Where the productivity between 12:00 and 13:00 was 3.17 liters on 25/4/2022, while the productivity at the same hour on 24/4/2022 was 2.09 liters.

Figure (5.15) shows the difference between the productivity of the distillation system for the days 3/5/2022 and 6/5/2022. On 3/5/2022 the first model of the heat exchanger was used, while on the other day the second model was used in which the nano-filling was used.

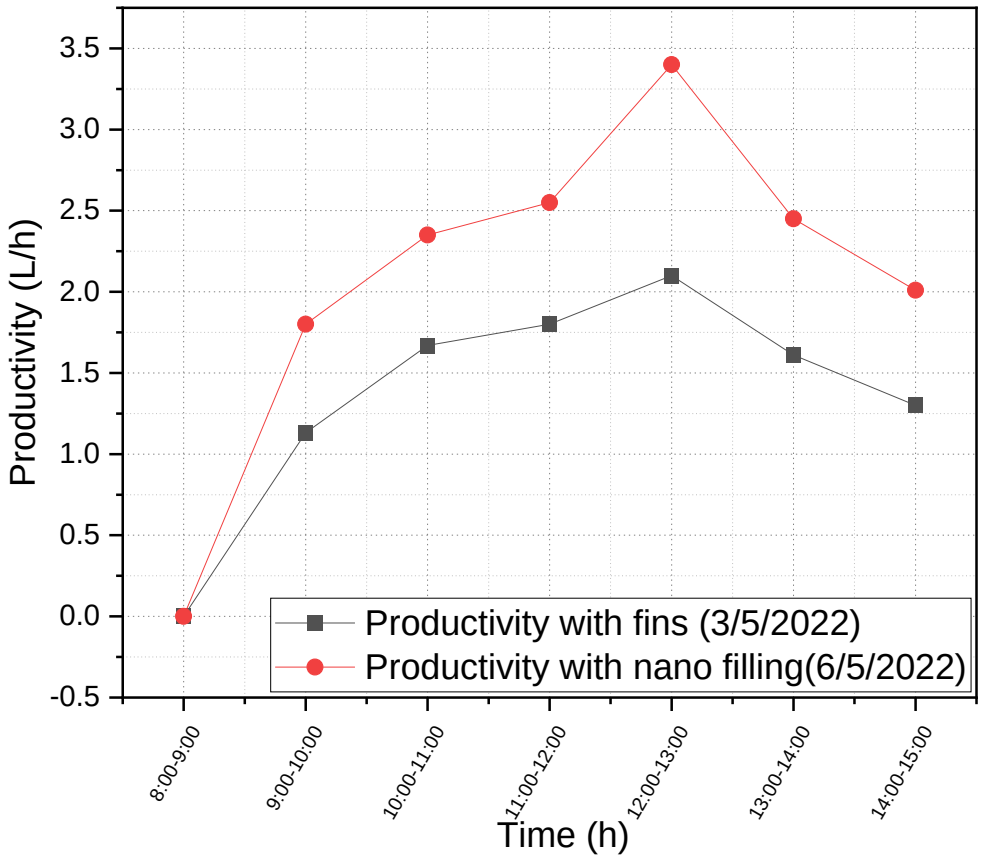

Figure(5.15): Comparison between the outputs of the distillation system using both models of the heat exchanger for the days of 3/5/2022 & 6/5/2022

The improvement rate was 57.06% when using the nano-padding in the heat exchanger (absorber) on 6/5/2022, the productivity of the solar distillation system was 14.56 liters and at an average solar radiation intensity of 803.83 W/m^2, while

using the first model on day 3/5/2022, the productivity was 9.27 liters, with an average solar radiation intensity of 798.8 W/m^2.

In the last productivity comparison that was made, the improvement rate in the productivity of the distillation system using a parabolic solar dish was 58.4%. Where the first experiment was conducted using the first model of the heat exchanger (absorber), the total productivity was 10.17 liters and the average solar radiation intensity of 817.83 W/m^2, while the productivity on May 14, 2022, was 16.11 liters with an average solar radiation intensity of 820.33 W/ m^2

The productivity increased significantly when using the nano-filling on May 14, 2022, where the maximum value of production reached 3.49 liters was between 12:00 and 13:00 when the intensity of solar radiation was 913W/m^2. The productivity of the first model at the same time on 13/5/2022 was 2.2 liters at a solar radiation of 911 W/m^2, where the rate of improvement in productivity at this hour was 58.6%. Figure (5.16) shows the variation of Distillation products during the days 13-14/5/2022.

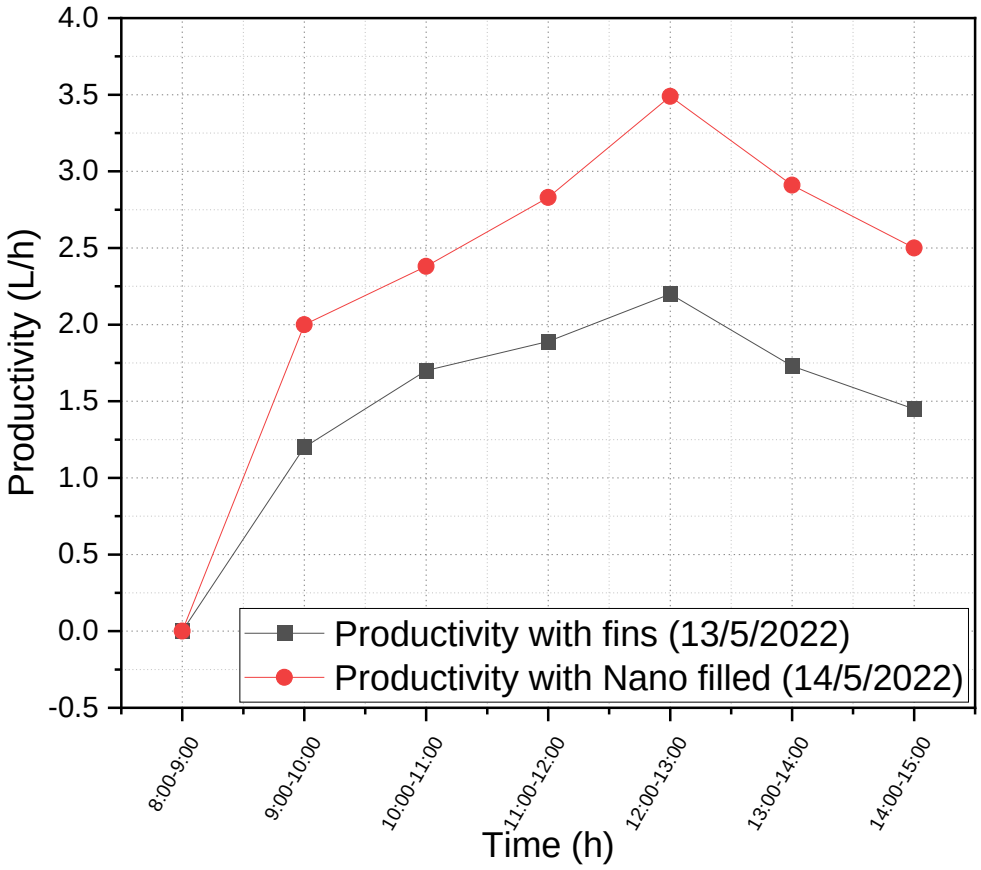

Figure(5.16): Comparison between the outputs of the distillation system using both models of the heat exchanger for the days of 13/5/2022 & 14/5/2022

From the examination of the results obtained during the experiments, it can be concluded that the productivity was significantly affected by the use of nano-filling inside the internal fins of the heat exchanger (absorbent), as it contributed to an increase in productivity with an average rate of 56.98%. This increase can be attributed to the nanomaterial (MWCT) due to its high conductivity which in turn contributes to increase the heat transfer from the surface of the heat exchanger cover to the water inside it.

5.3.2 Temperature of working fluid

The use of nanoparticles (MWCT) contributed to increasing the heat transfer from the surface of the heat exchanger cover (absorber) to the inside of the exchanger through the fins filled with nanoparticles. As the increase in enthalpy shortens the

time required for the transformation of water inside the heat exchanger. Figures (5.17&5.18&5.19&5.20) show a comparison between the water temperatures inside the heat exchanger when the solar distillation system is operating for the different days of experiments.

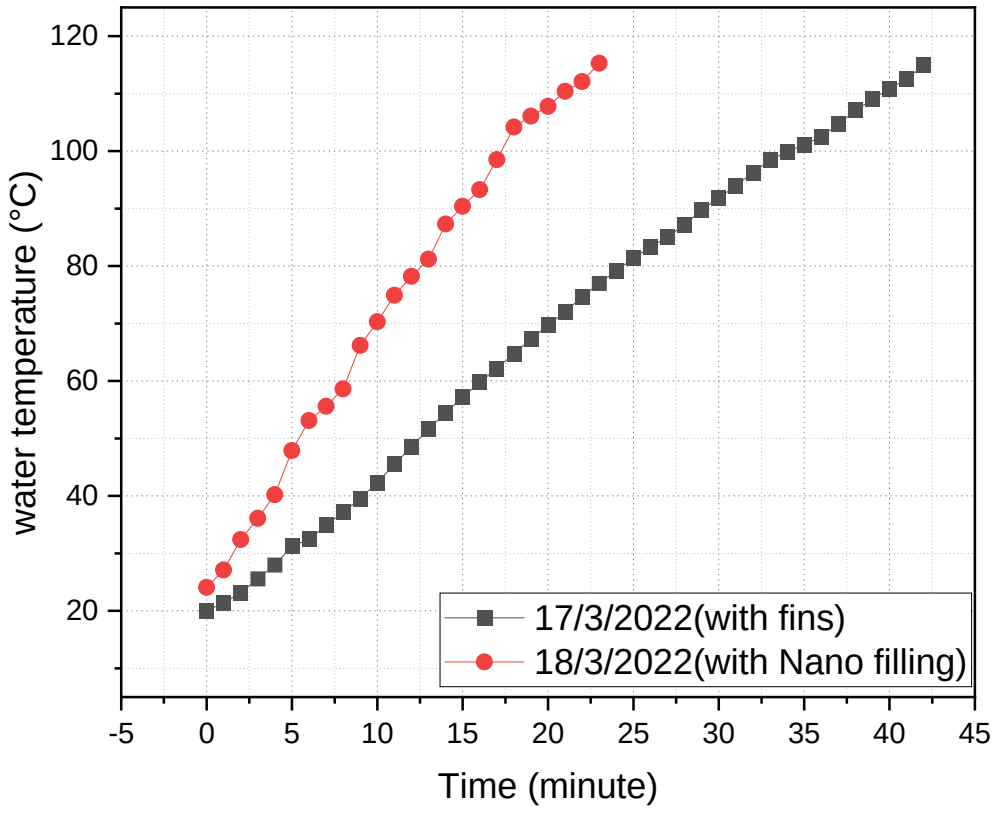

Figure(5.17): Comparison of the water temperature inside the heat exchanger when the system starts operating between 17/3/2022 and 18/3/2022

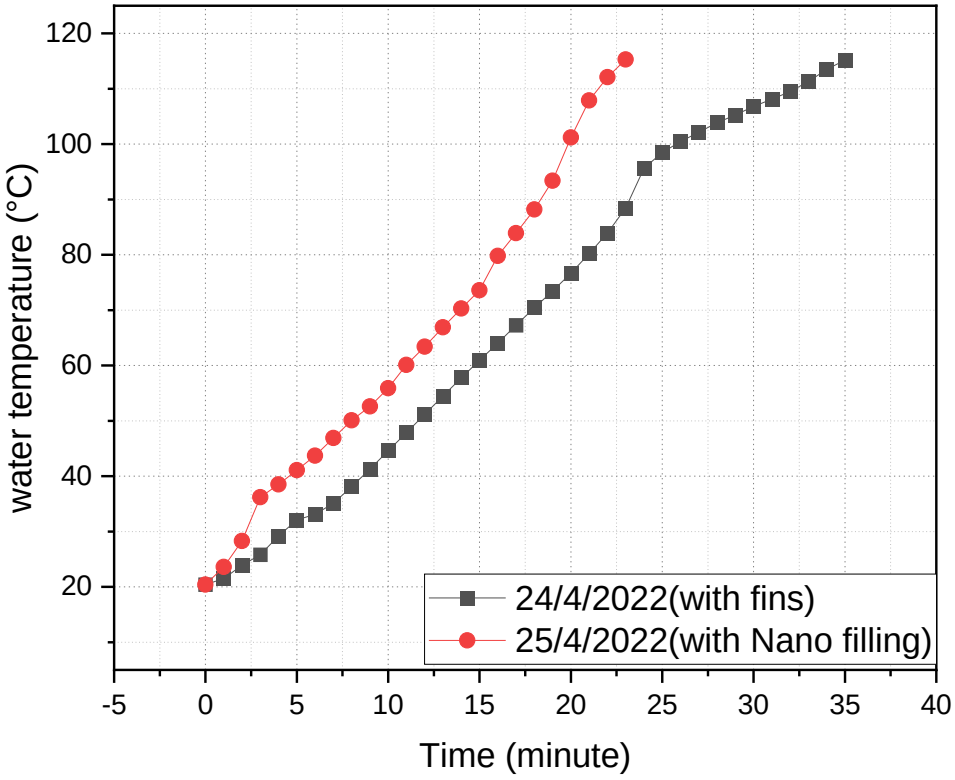

Figure(5.18): Comparison of the water temperature inside the heat exchanger when the system starts operating between 24/4/2022 and 25/4/2022

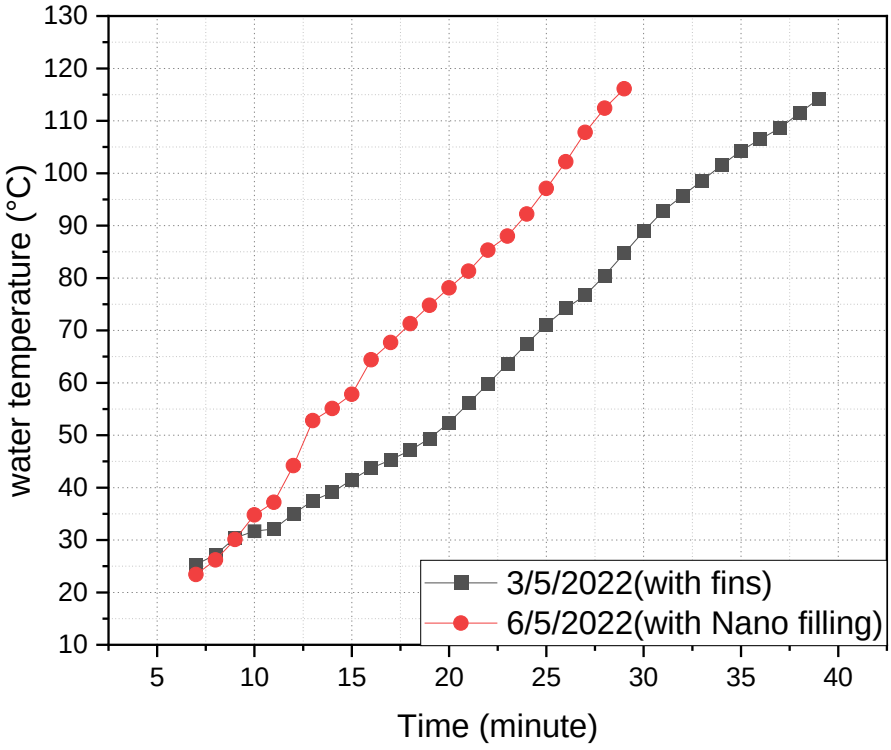

Fig (5.19): Comparison of the water temperature inside the heat exchanger when the system starts operating between 3/5/2022 and 6/5/2022

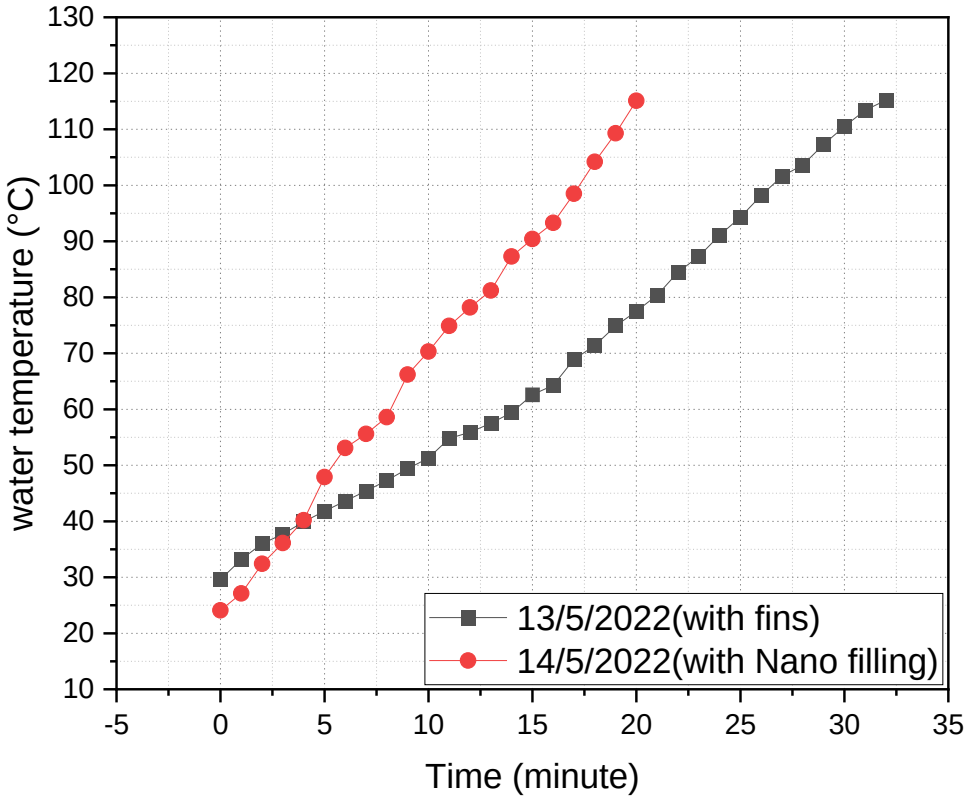

Figure(5.20): Comparison of the water temperature inside the heat exchanger when the system starts operating between 13/5/2022 and 14/5/2022

When comparing the water temperature inside the heat exchanger when operating the solar distillation system for the days 3/17/2022 and 3/18/2022 and as shown in Figure (5.17), we note that the water temperature rose faster on 3/18/2022, where it was used Nano-filled heat exchanger In this experiment, the water temperature reached its maximum when 24 minutes passed, compared to the first model, which took 43 minutes to reach the same temperature. will most importantly use the nanomaterial by reducing the time between the two experiments by 41.18%.

Figure (5.18) shows the temperature of the water inside the heat exchanger at the start of the first operation at 9:00 on 24/4/2022 and 25/4/2022, where the first model of the heat exchanger was used on 24/4/2022 and on 25/ 4/2022 The heat exchanger with nano-filling was used. It is noted that the water temperature inside the heat exchanger with nano-filling rose faster than the heat exchanger, as it needed

a shorter time to reach the same temperature. In the comparison shown in Figure (5.19), it is noted that the water temperature also rose faster in the nano-filled heat exchanger. The water temperature also increased inside the nano-filled heat exchanger in the experiments that were conducted on two consecutive days and at the same time on 13-14/5/2022. And the high water temperature in the nano-filled model shows that the nano-material (Mwct) enhanced the heat transfer from the surface of the heat exchanger cover (absorbent) to the water inside it.

5.3.3 Surface Temperature of Heat Exchanger absorber

Figure (5.21 & 5.22 & 523 & 5.24) shows the comparison between the surface temperature of the heat exchanger cover for both models when starting at 9:00 of the solar water distillation system for all experiments

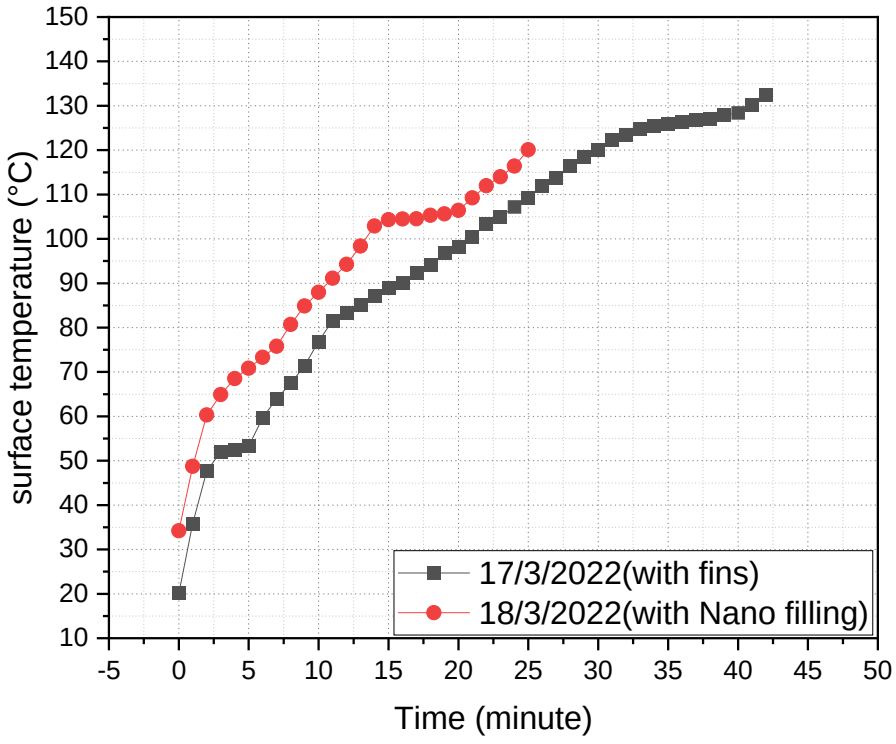

Figure(5.21): Comparison of the temperatures of the heat exchanger cover during the start of operation of the solar distillation system between 17/3/2022 and 18/3/2022

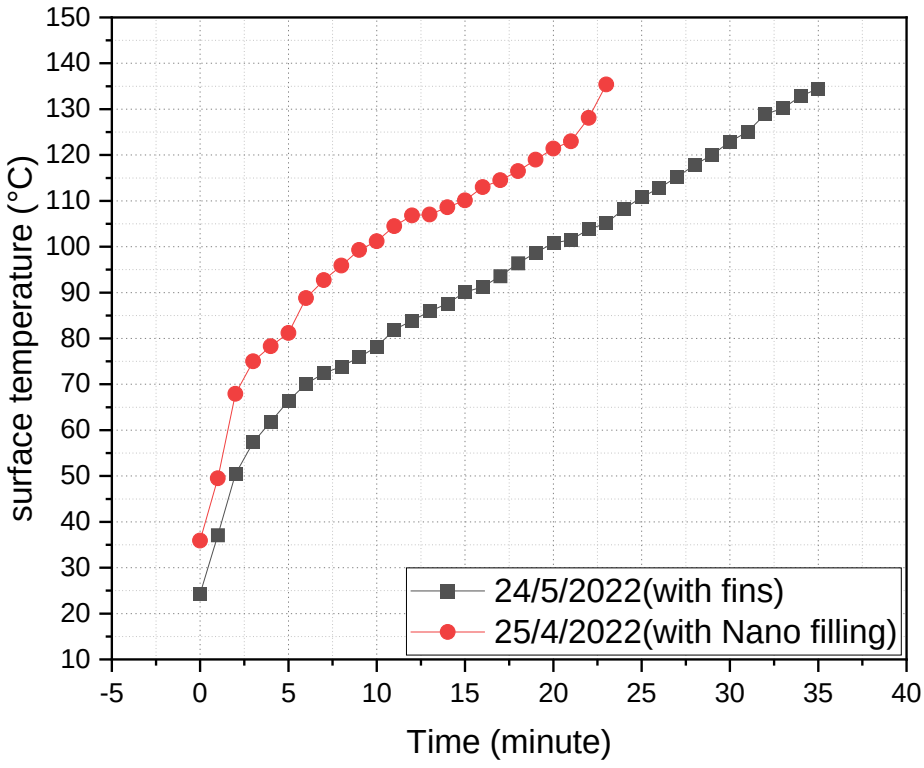

Figure(5.22): Comparison of the temperatures of the heat exchanger cover during the start of operation of the solar distillation system between 24/4/2022 and 25/4/2022

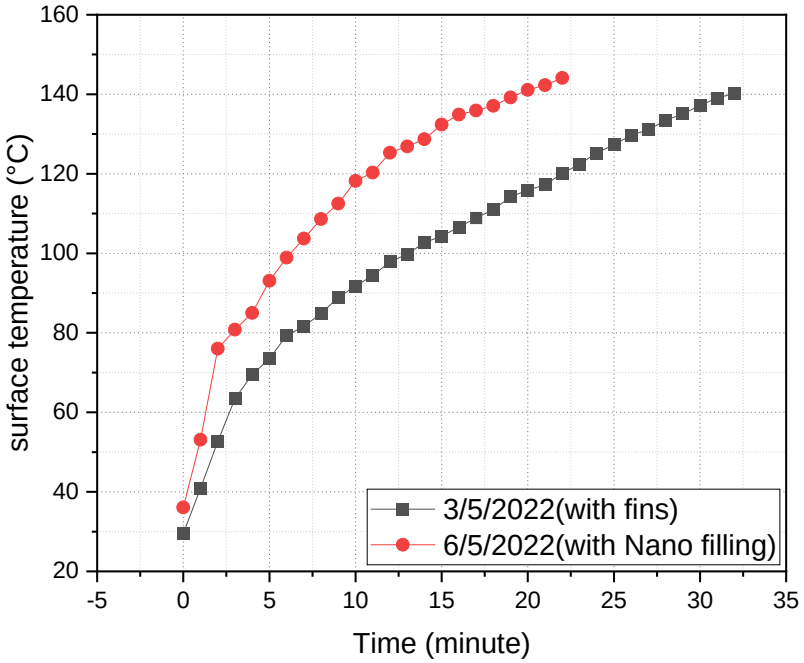

Figure(5.23): Comparison of the temperatures of the heat exchanger cover during the start of operation of the solar distillation system between 3/5/2022 and 6/5/2022

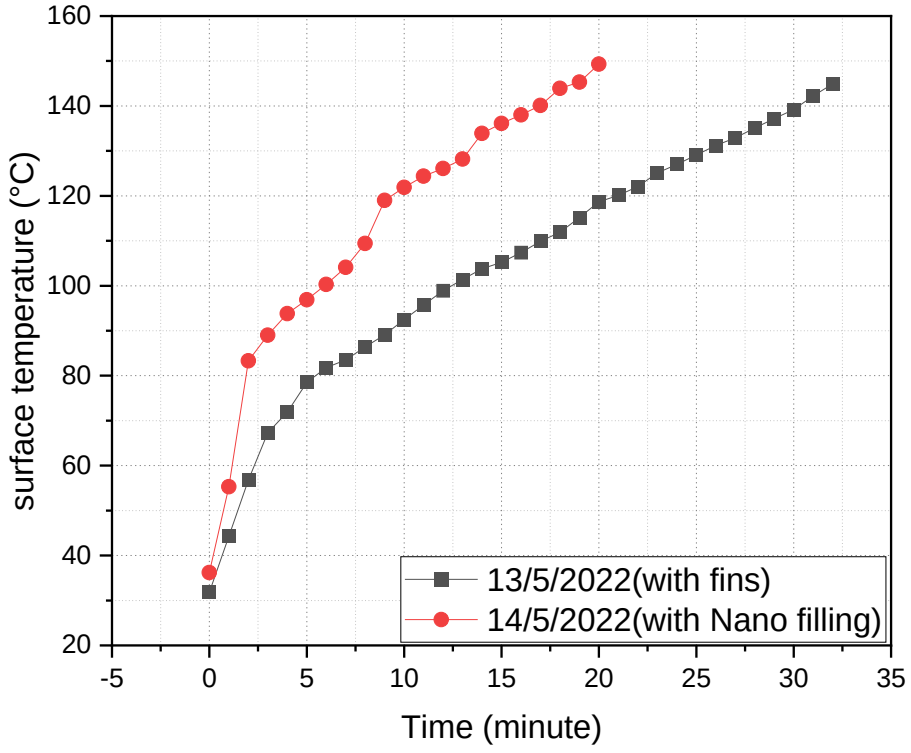

Figure(5.24): Comparison of the temperatures of the heat exchanger cover during the start of operation of the solar distillation system between 13/5/2022 and 14/5/2022.

It is noticed from the above figures that the surface temperature of the heat exchanger cover rises faster in the heat exchanger with nano-filling and this is due to the increase in the speed of heat transfer from the surface of the cover to the water inside the exchanger.

When comparing the surface temperature at the beginning of the operation between the days of 17/3/2022 and 18/3/2022, note that the surface temperature became 120.1℃ in the experiment that was conducted on March 18, 2022, in the heat exchanger with nano-filling, where the water charge shifted Inside the heat exchanger, it turned into steam, while on the other day, the surface temperature of the heat exchanger cover became 132.5 ℃ after 43 minutes, and at this temperature, the water charge turned into steam. On 4/25/2022, the surface of the heat exchanger took 24 minutes to reach a temperature of 135.4 ℃, as at this temperature all the

water charge inside the heat exchanger turned into steam, while on 24/4/2022 the temperature became 134.5 ℃after 36 minutes of switching off. operating the system.

While the surface temperature of the nano-filled heat exchanger cap became 144.1 ℃ after 23 minutes passed on 5/6/2022, and it also became 140.2℃ on 3/5/2022 after 33 minutes. On May 14, 2022, the surface temperature became 149.3 ℃after the passage of 21 minutes, while on May 13, 2022 the temperature became 144.9℃ after the passage of 33 minutes.

5.4 Heat losses from the heat exchanger

The value of the heat loss from the heat exchanger in all the experiments that were conducted is relatively small compared to the amount of energy that the heat exchanger is exposed to or absorbed by the parabolic dish, and this is due to the use of glass wool material with a thick layer (2.5 cm) around the heat exchanger. The heat exchanger is divided into two types of heat loss, the first is heat loss by convection, and the other is heat loss by radiation. Figures (5.25) shows the average heat loss from the heat exchanger during the experiments conducted using the first model of the heat exchanger (fins without nano-filling. Figure (5.26) shows the average heat loss for the days of the experiments that were carried out using the second heat exchanger (fins with nano-filling).

It is noted that one of the factors affecting heat loss is the ambient temperature around the heat exchanger, wind speed, when speed increases Wind increases heat loss due to the high coefficient of heat transfer by convection, and the ambient temperature also contributes to an increase in heat loss from the heat exchanger.

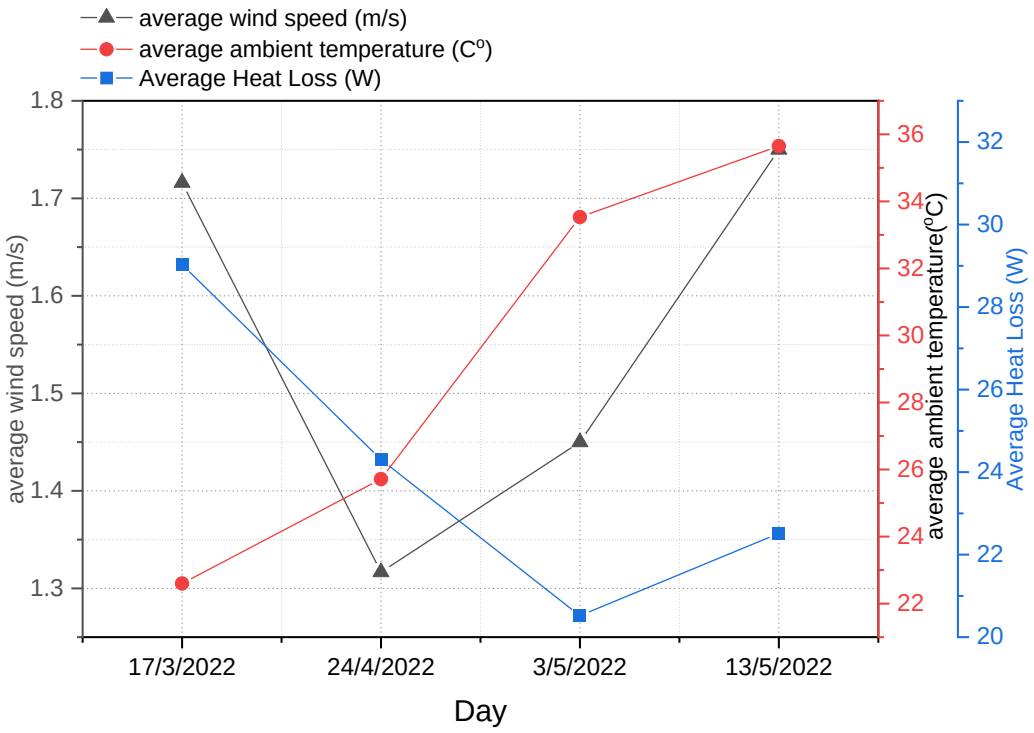

Figure(5.25): The average heat loss for the experiments carried out using the first model of the heat exchanger

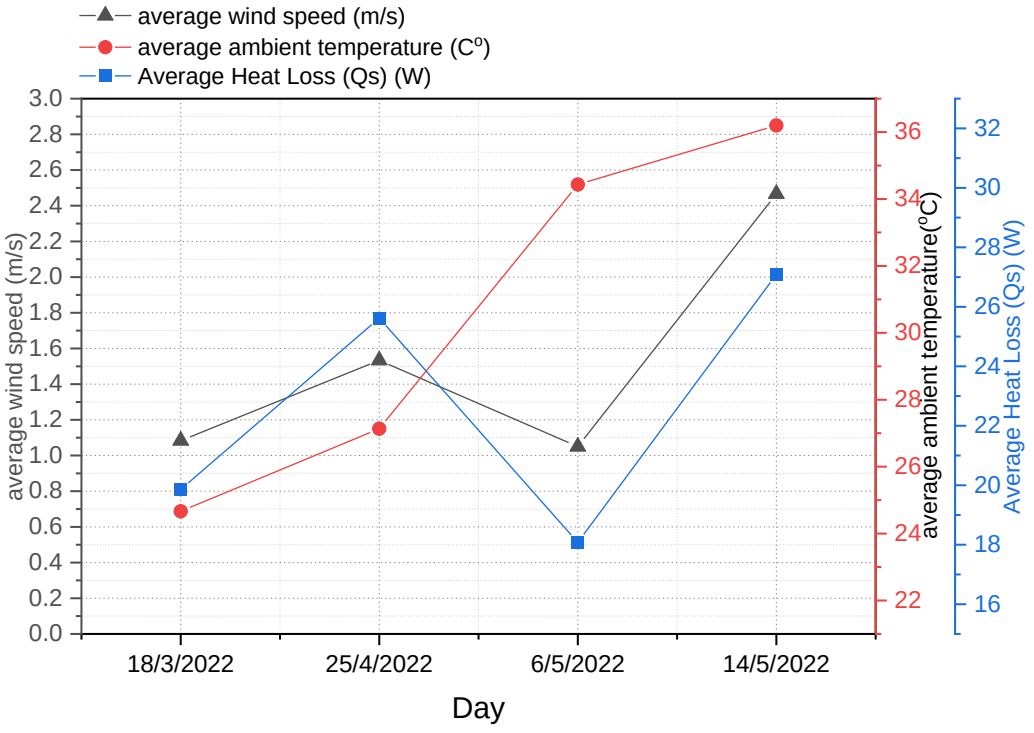

Figure(5.26): The average heat loss for the experiments carried out using the second model of the heat exchanger.

Figures (5.27 to 5.34) show the variation of heat loss with the environmental conditions for the days in which the experiments were conducted

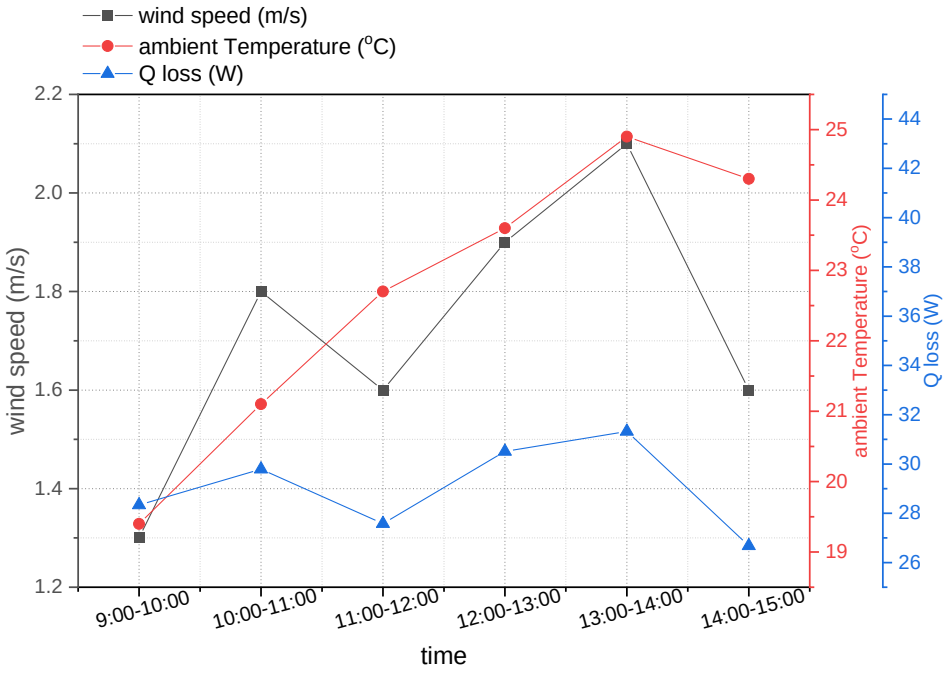

Figure (5.27): Variation of heat loss with environmental conditions for the day 17-3-2022

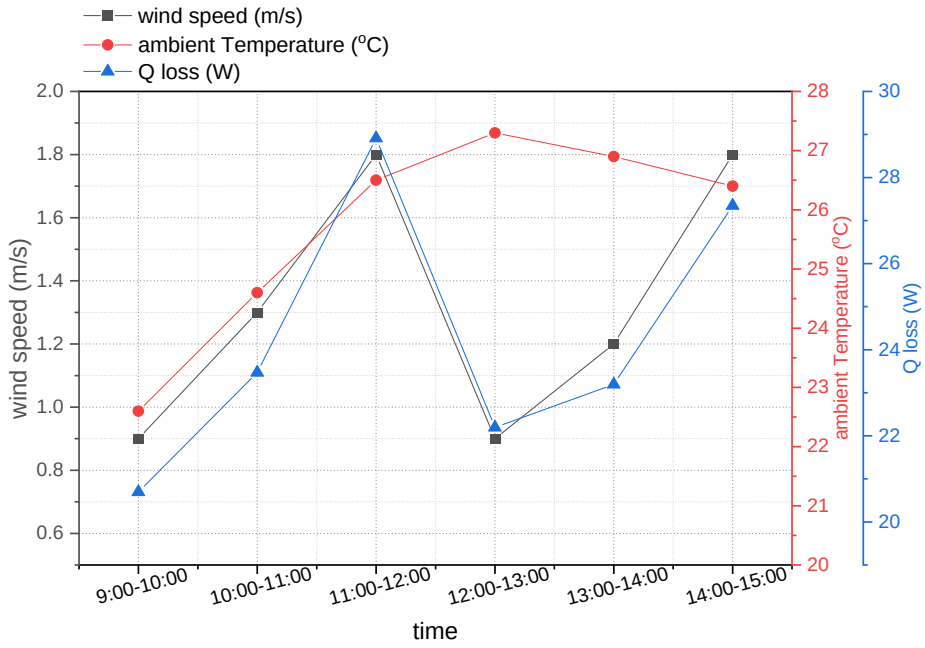

Figure (5.28): Variation of heat loss with environmental conditions for the day 24-4-2022

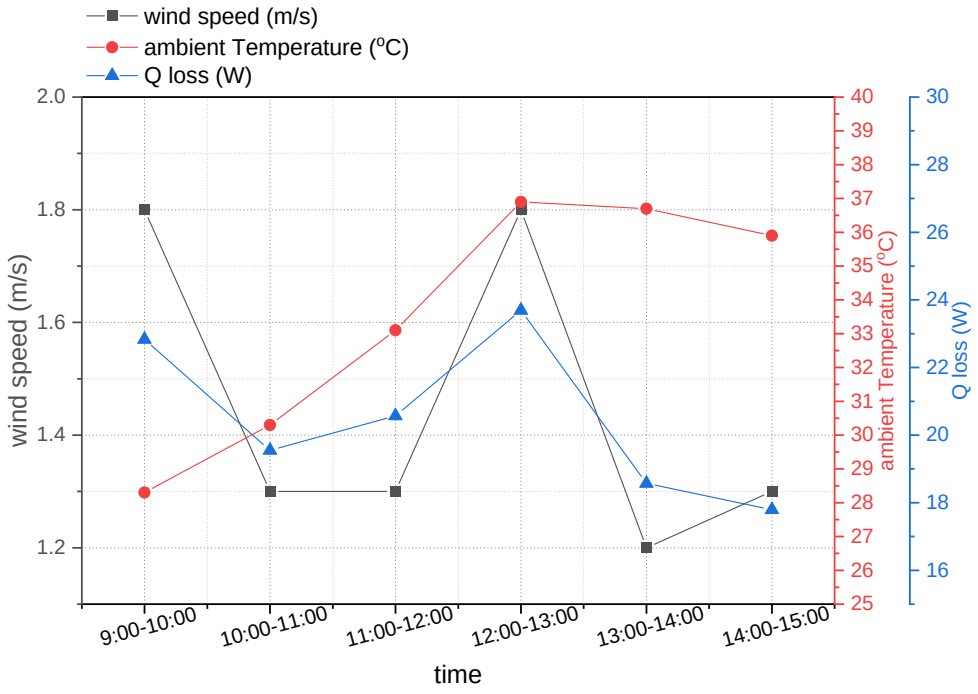

Figure (5.29): Variation of heat loss with environmental conditions for the day 3-5-2022

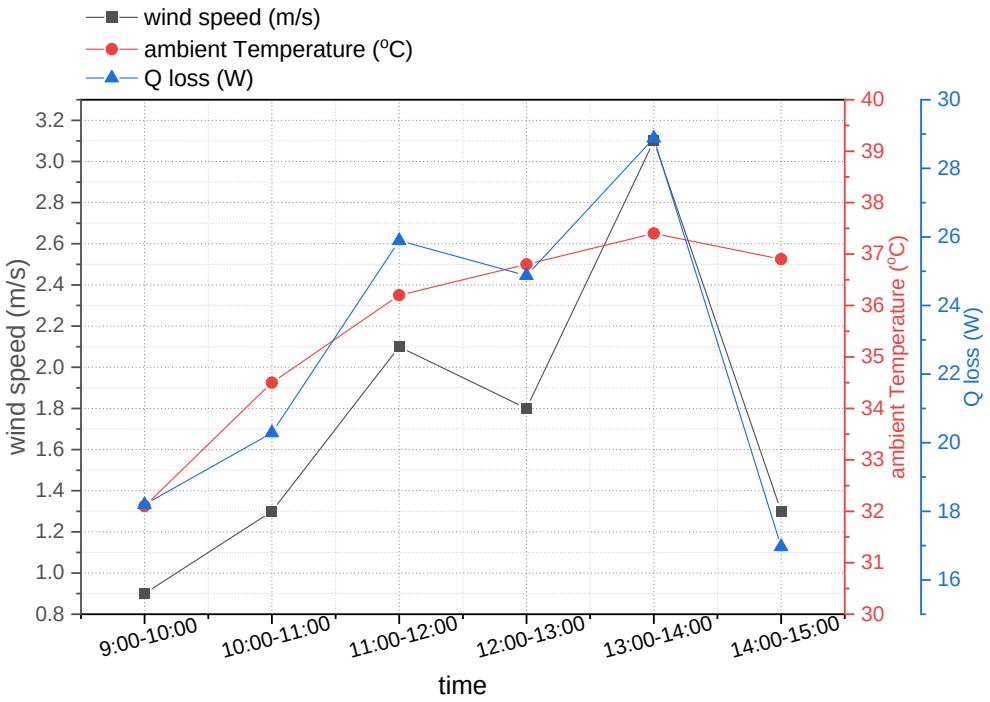

Figure (5.30): Variation of heat loss with environmental conditions for the day 13-5-2022

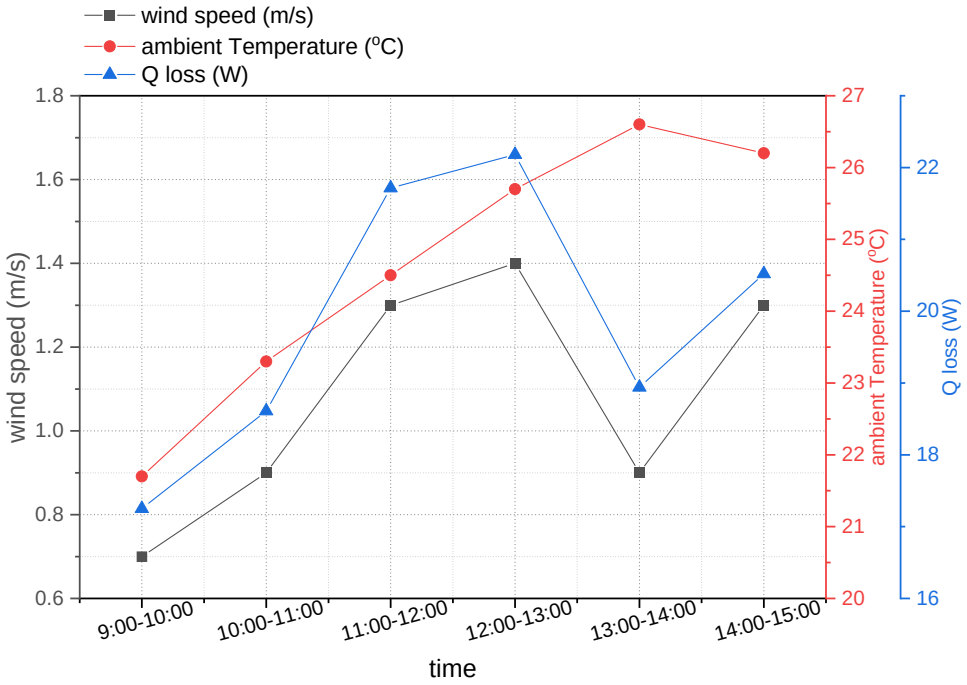

Figure (5.31): Variation of heat loss with environmental conditions for the day 18-3-2022

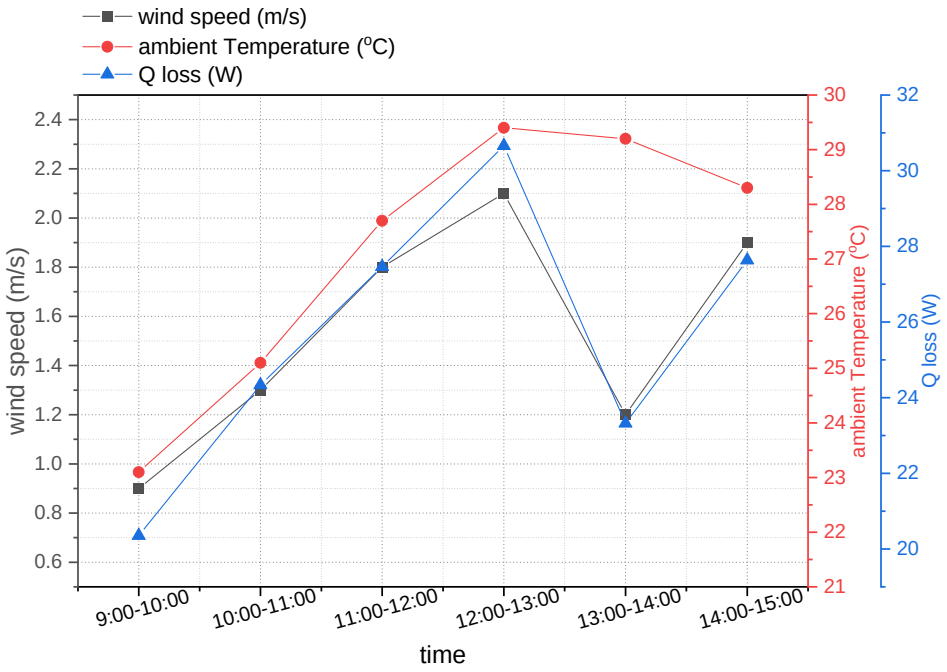

Figure (5.32): Variation of heat loss with environmental conditions for the day 25-4-2022

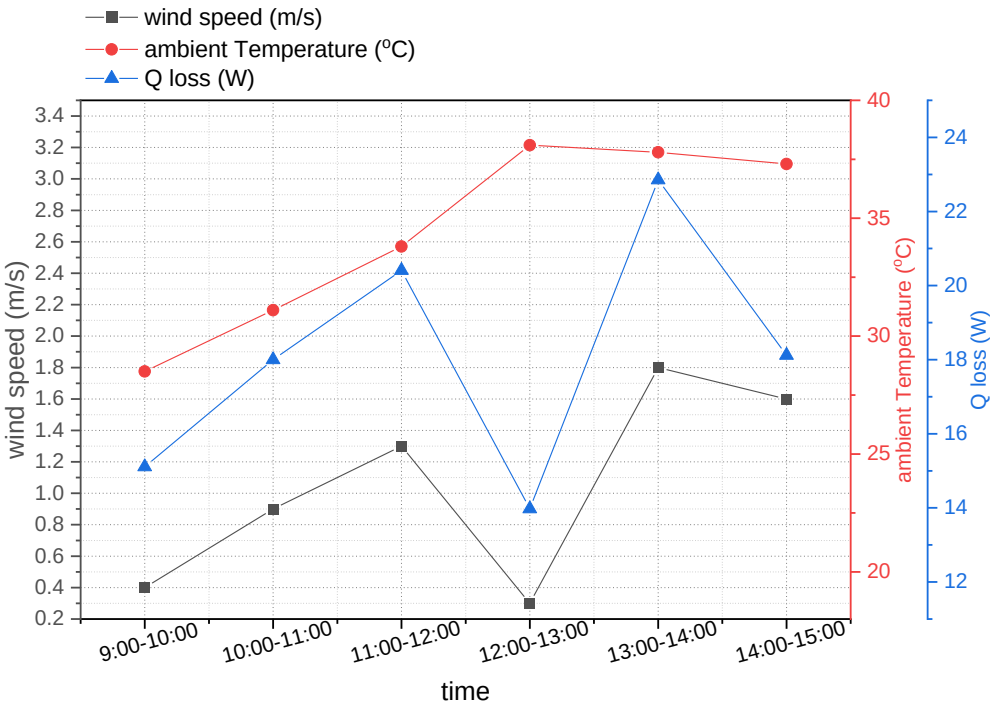

Figure (5.33): Variation of heat loss with environmental conditions for the day 6-5-2022

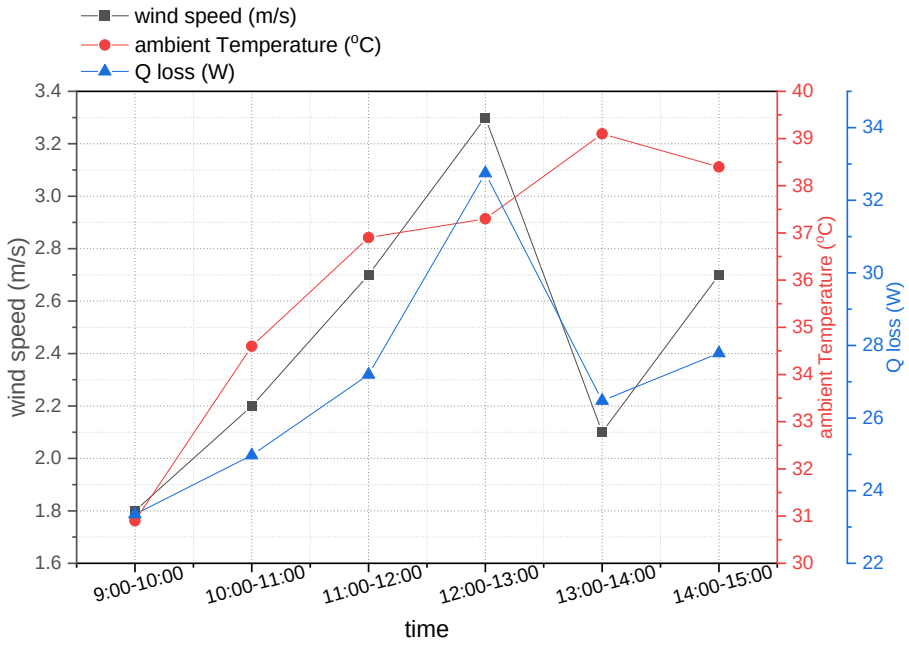

Figure (5.34): Variation of heat loss with environmental conditions for the day 14-5-2022

From the above, it can be said that the influence of environmental factors (wind speed, ambient temperature) does not have a high or effective effect on the performance of the heat exchanger, and this is due to the good thermal insulation of the heat exchanger.

Chapter Six

Conclusion and Recommendati

CHAPTER SIX

CONCLUSIONS AND RECOMMENDATIONS

INTRODUCTION

The experiments were conducted in Al-Diwaniyah, Iraq (32N, 45E) during March, April, and May of the year 2022. The current study aims to study water distillation by a parabolic dish solar energy center, and study the effect of using nanomaterials on the thermal performance of the solar distillation system. Where a solar distillation system was designed consisting of a solar parabolic dish, a solar guiding system, a heat exchanger (absorber), and steam condenser. The results showed that the use of nanomaterials (MWCT) contributed significantly to improving the productivity of the solar distillation system, and the conclusions can be summarized as follows:

1. The most important parameters affecting the productivity of the solar distillation system are the diameter of the parabolic dish, the type of reflective material, the accuracy of the solar tracking, in addition to the environmental conditions such as the intensity of solar radiation. When the average intensity of solar radiation was 741.14W/m^2 on 3/17/2022, the productivity of the solar distillation system was 7.94 liters/day, while the productivity was 10.17 liters/day on 13/5/2022 due to the rise in the average intensity of solar radiation to 820.3W/m^2.
2. The results showed that wind speed and ambient temperature do not have an effective effect on the performance of the solar distillation system, as the

thermal insulation of the heat exchanger (absorber) contributed to reducing the impact of these parameters on the performance of the system.

3. The maximum productivity that was reached for the solar distillation system using the first (absorbed) heat exchanger was 10.17 liters at an average solar radiation of 817.83 W/m^2, and an average ambient temperature of 35.65℃
4. The maximum productivity of the distillation system using the second heat exchanger (absorbent) with nano-filling was 16.11 liters at an average solar radiation of 820.33 W/m^2, and at an average ambient temperature of 36.2℃
5. The use of nano-filling contributed to an increase in the productivity of the solar distillation system by 57.69%.
6. The use of nano-filling contributed to reducing the time required for water evaporation inside the heat exchanger, especially when starting to operate the solar distillation system. An example of this in the first experiment that was conducted at the start of the system at 9:00 on 17/3/2022, the time required to convert water into steam inside the heat exchanger (fins without nano-filling) was 45 minutes, while at the same time in the experiment that was conducted in 18/3/2022 The time required for water to turn into steam is 28 minutes..
7. When comparing the results obtained with the rest of the experiments using the same type of solar concentrator (parabolic dish), it is considered acceptable, as Shava Gorjian et al. [31] The productivity was 5.12 liters / day, and when Bechir choo chi et al. [41] the productivity was 6.22 liters / day.

6.2 Recommendations

1. The use of materials with high reflectivity to increase the efficiency of the solar distillation system, as well as of light weight to reduce the load on the solar tracking system.
2. Manufacture of the heat exchanger cover (absorber) from copper metal manufactured specifically for food purposes because of its high conductivity compared to the aluminum used in our experiment, which contributes to an increase in heat transfer.
3. Increasing the diameter of the solar parabolic dish, as well as increasing the dimensions of the heat exchanger, which will positively affect the productivity of the solar distillation system.
4. Finding a new method for distributing the nano-material (Mwct) inside the heat exchanger housing (absorber)

REFERENCE:

[1] Gorjian, S., Ghobadian, B., Hashjin, T. T., & Banakar, A. (2014). Experimental performance evaluation of a stand-alone point-focus parabolic solar still. Desalination, 352, 1-17.

[2] Hiba Qasim, Ali Sh. Baqir, Hassan Hadi, " Effects of Air Bubble Injection on the Efficiency of a Flat Plate Solar Collector: An Experimental Study for the Open Flow System " , Journal of Engineering and Applied Sciences, March 2020, 15(7):1703-1708, DOI: 10.36478/jeasci.2020.1703.1708

[3] Ahmad Hashim, Ali Sh. Baqir, Ali Majeed, "Study the effect of twisted tapes on thermal performance solar collector with using curvature vortex generators ",Technology Reports of Kansai University, August, 2020, Volume 62, Issue 07, pp, 3631-3643.

[4] Ali Sh. Baqir, Hameed B. Mahood, Alsadair Campbell, Mudher Sabah, "Heat transfer measurement in a three-phase spray column direct contact heat exchanger for utilisation in energy recovery from low-grade sources ",Energy Conversion and Management, 126 (2016) 342–351, http://dx.doi.org/10.1016/j.enconman.2016.08.013.

[5] Hasan Hadi, Ali Sh. Baqir, Hiba Qasim, "Effect of Air Bubble Injection on the Thermal Performance of a Flat Plate Solar Collector ",Thermal Science and Engineering Progress 17(1):100476, DOI: 10.1016/j.tsep.2019.100476

[6] Muna Ali Talib, Ahmed hammodi, Hameed B. Mahood, Ali Sh. Baqir, "Experimental study on the heat transfer enhancement in externally finned helical and shell tube heat exchanger ",AIP Conference Proceedings 2386(1):040040, DOI: 10.1063/5.0067670

[7] Saif S. Hasan, Hameed B. mahood, Ali Sh. Baqir, " Air bubble injection technique for enhancing heat transfer in a coiled tube heat exchanger: An experimental study ",AIP Conference Proceedings 2386(1):40019, DOI: 10.1063/5.0066887

[8] Saif S. Hasan, Hameed B. Mahood, Ali Sh. Baqir, "Improvement of Thermal Performance of Coiled Tube Heat Exchanger Utilizing Air Bubble Injection Technique ",IOP Conference Series Earth and Environmental Science 877(1):012040, DOI: 10.1088/1755-1315/877/1/012040

[9] Saif S. Hasan, Ali Sh. Baqir, Hameed B. Mahood, "The Effect of Injected Air Bubble Size on the Thermal Performance of a Vertical Shell and Helical Coiled Tube Heat Exchanger ",Energy Engineering: Journal of the Association of Energy Engineers 118(6):1595-1609, DOI: 10.32604/EE.2021.017433

[10] https://ourworldindata.org/

[11] Shindell, D., & Smith, C. J. (2019). Climate and air-quality benefits of a realistic phase-out of fossil fuels. Nature, 573(7774), 408-411.

[12] Noor, I. E. (2021). Waste Heat Driven Membrane Distillation for Industrial Wastewater Treatment.

[13] Skouras, G. N. (2018). Design and Analysis of a Parabolic Trough Solar Concentrator.

[14] L.C. Spencer, A comprehensive review of small solar-powered heat engines: part I. A history of solar-powered devices up to 1950, Sol. Energy. 43 (1989) 197–210. doi:10.1016/0038-092X(89)90019-4.

[15] solar resource maps and GIS data, Online access to: high-resolution solar data, (n.d.). https://solargis.com/maps-and-gis-data/download/world

[16] solar resource maps and G. Data, Solar resource maps of World, (n.d.). https://solargis.com/maps-and-gis-data/overview

[17] Kazem, H. A., & Chaichan, M. T. (2012). Status and future prospects of renewable energy in Iraq. Renewable and Sustainable Energy Reviews, 16(8), 6007-6012.

[18] Maddocks, A., Young, R. S., & Reig, P. (2015). Ranking the world's most water-stressed countries in 2040.

[19] Pistoia, G., Kalogirou, S., & Storvick, T. (2009). Renewable energy focus handbook.

[20] Ummadisingu, A., & Soni, M. S. (2011). Concentrating solar power–technology, potential and policy in India. Renewable and sustainable energy reviews, 15(9), 5169-5175.

[21] Fan, H., Singh, R., & Akbarzadeh, A. (2011). Electric power generation from thermoelectric cells using a solar dish concentrator. Journal of electronic materials, 40(5), 1311-1320.

[22] Hannun, R. M. (2018). Solar Water Desalination by Using Parabolic Dish in Hot Climate Weather Conditions. University of Thi-Qar Journal for Engineering Sciences, 9(2), 1-8.

[23] Omara, Z. M., & Eltawil, M. A. (2013). Hybrid of solar dish concentrator, new boiler and simple solar collector for brackish water desalination. Desalination, 326, 62-68.

[24] Prado, G. O., Vieira, L. G. M., & Damasceno, J. J. R. (2016). Solar dish concentrator for desalting water. Solar Energy, 136, 659-667.

[25]Hameed, H. G., & Neema, H. A. (2011). EXPERIMENTAL STUDY FOR PRODUCTIVITY ENHANCEMENT OF A PARABOLIC SOLAR CONCENTRATOR SYSTEM. Al-Qadisiya Journal For Engineering Science, 4.[

26] Chaichan, M. T., & Kazem, H. A. (2015). Water solar distiller productivity enhancement using concentrating solar water heater and phase change material (PCM). Case studies in thermal engineering, 5, 151-159.

[27] Chaichan, M. T., Abaas, K. I., & Kazem, H. A. (2016). Design and assessment of solar concentrator distillating system using phase change materials (PCM) suitable for desertic weathers. Desalination and water treatment, 57(32), 14897-14907.

[28] Argun, M. E., & Kulaksız, A. A. (2017). Performance investigation of a new solar desalination unit based on sequential flat plate and parabolic dish collector. International Journal of Green Energy, 14(6), 561-568.

[29] Rafiei, A., Loni, R., Mahadzir, S. B., Najafi, G., Pavlovic, S., & Bellos, E. (2020). Solar desalination system with a focal point concentrator using different nanofluids. Applied Thermal Engineering, 174, 115058.

[30] Bahrami, M., Avargani, V. M., & Bonyadi, M. (2019). Comprehensive experimental and theoretical study of a novel still coupled to a solar dish concentrator. Applied Thermal Engineering, 151, 77-89.

[31] Chaouchi, B., Zrelli, A., & Gabsi, S. (2007). Desalination of brackish water by means of a parabolic solar concentrator. Desalination, 217(1-3), 118-126.

[32] Srithar, K., Rajaseenivasan, T., Karthik, N., Periyannan, M., & Gowtham, M. (2016). Stand alone triple basin solar desalination system with cover cooling and parabolic dish concentrator. Renewable Energy, 90, 157-165.

[33] Poonia, S., Singh, A. K., & Jain, D. (2020). Design development and performance evaluation of concentrating solar thermal desalination device for hot arid region of India. Desalination and Water Treatment, 205, 1-11.

[34] Babaeebazaz, A., Gorjian, S., & Amidpour, M. (2021). Integration of a Solar Parabolic Dish Collector with a Small-Scale Multi-Stage Flash Desalination Unit: Experimental Evaluation, Exergy and Economic Analyses. Sustainability, 13(20), 11295.

[35] Al_qasaab, M. R., & ABD AL-WAHİD, W. A. (2021). Enhancement the solar distiller water by using parabolic dish collector with single slope solar still. Journal of Thermal Engineering, 7(4), 1000-1015.

[36] Thakur, A. K., Sathyamurthy, R., Velraj, R., Lynch, I., Saidur, R., Pandey, A. K., ... & Kabeel, A. E. (2021). Sea-water desalination using a desalting unit integrated with a parabolic trough collector and activated carbon pellets as energy storage medium. Desalination, 516, 115217.

[37] Kabeel, A. E., Dawood, M. M. K., Ramzy, K., Nabil, T., & Elnaghi, B. (2019). Enhancement of single solar still integrated with solar dishes: An experimental approach. Energy conversion and management, 196, 165-174.

[55] Abed, F. M., Kassim, M. S., & Rahi, M. R. (2017). Performance improvement of a passive solar still in a water desalination. International Journal of Environmental Science and Technology, 14(6), 1277-1284.

[38] Gupta, B., Shankar, P., Sharma, R., & Baredar, P. (2016). Performance enhancement using nano particles in modified passive solar still. Procedia Technology, 25, 1209-1216.

[39]Al-Amir Khadim, M. A., Al-Wahid, W. A. A., Hachim, D. M., & Sopian, K. (2021). Experimental Study of the Performance of Cylindrical Solar Still with a Hemispherical Dome. Smart Science, 9(1), 30-39.

[40]Fadhel, H., Abed, Q. A., & Hachim, D. M. (2021). An Experimental Work on the Performance of Single Solar Still with Parabolic Trough Collector in Hot Climate Conditions. Journal homepage: http://iieta. org/journals/ijht, 39(5), 1627-1633.

[41]Arun, C. A., & Sreekumar, P. C. (2018). Modeling and performance evaluation of parabolic trough solar collector desalination system. Materials Today: Proceedings, 5(1), 780-788.

[42]Elashmawy, M. (2017). An experimental investigation of a parabolic concentrator solar tracking system integrated with a tubular solar still. Desalination, 411, 1-8.

[43]Kedar, S. A., Bewoor, A. K., Murali, G., Kumar, R., Sadeghzadeh, M., & Issakhov, A. (2021). Effect of Reflecting Material on CPC to Improve the Performance of Hybrid Groundwater Solar Desalination System. International Journal of Photoenergy, 2021.

[44]Gupta, B., Shankar, P., Sharma, R., & Baredar, P. (2016). Performance enhancement using nano particles in modified passive solar still. Procedia Technology, 25, 1209-1216.

[45] Sharshir, S. W., Peng, G., Elsheikh, A. H., Edreis, E. M., Eltawil, M. A., Abdelhamid, T., ... & Yang, N. (2018). Energy and exergy analysis of solar stills with micro/nano particles: a comparative study. Energy Conversion and Management, 177, 363-375.

[46] Chen, W., Zou, C., Li, X., & Liang, H. (2019). Application of recoverable carbon nanotube nanofluids in solar desalination system: An experimental investigation. Desalination, 451, 92-101.

[47] Shanmugan, S., Essa, F. A., Gorjian, S., Kabeel, A. E., Sathyamurthy, R., & Manokar, A. M. (2020). Experimental study on single slope single basin solar still using TiO2 nano layer for natural clean water invention. Journal of Energy Storage, 30, 101522.

[48] Hannun, R. M., & Koban, R. M. (2022). The Use of a Parabolic Solar Concentrator in Nasiriya city, Iraq. Journal of Petroleum Research and Studies, 12(1), 332-349.

[49] Ghazouani, K., Skouri, S., Bouadila, S., & Guizani, A. (2016). Thermal study of solar parabolic concentrator. In International Conference on Recent Innovations in Civil & Mechanical Engineering IOSR Journal of Mechanical and Civil Engineering (pp. 2278-1684).

[50] Aidan, J. (2014). Performance evaluation of a parabolic solar dish cooker in Yola, Nigeria. IOSR J. Appl. Phys., 6, 46-50.

[51] Wu, S. Y., Xiao, L., Cao, Y., & Li, Y. R. (2010). A parabolic dish/AMTEC solar thermal power system and its performance evaluation. Applied Energy, 87(2), 452-462.

[52] Alarcón, J. A., Hortúa, J. E., & Lopez, A. (2013). Design and construction of a solar collector parabolic dish for rural zones in Colombia. Tecciencia, 7(14), 14-22.

[53] Ngo, L. C., Bello-Ochende, T., & Meyer, J. P. (2012). Exergetic analysis and 108ptimization of a parabolic dish collector for low power application. In Proceedings of the postgraduate symposium (pp. 22-23).

[54] Bellel, N. (2011). Study of two types of cylindrical absorber of a spherical concentrator. Energy Procedia, 6, 217-227.

[55] S. Pavlovic, A. M. Daabo, E. Bellos, V. Stefanovic, S. Mahmoud and R. K. Al-Dadah. "Experimental and numerical investigation on the optical and thermal performance of solar parabolic dish and corrugated spiral cavity receiver." Journal of cleaner production 150 (2017): 75-92.

[56] R. M. Hannun, S. E. Najim and M. H. Khalaf. "The Parameters Change with Different Operation Conditions of Solar Chimney Power Plant Model." Basrah Journal for Engineering Science 14.2 (2014): 189-199.

APPENDIXES

Appendix (A): Heat loss from heat exchanger

$Aa=\frac{\pi}{4}\mathbf{1.58^2}$ =1.96m^2

$\lambda=\frac{A_a-A_t}{A_a}$(shadow heat exchanger)

A_t=0.2(πdL)=0.2(π*0.09*0.166)=0.00938 m^2

$\lambda=\frac{1.96-0.00938}{1.96}$ =0.9952

ρ=0.9 (Reflectivity of dish surface)

τά=0.97(Black body)(Transmittance–absorptance product)

γ=1(Intercept factor of the receiver)

η_o= ρ τά γ λ = 0.9*0.97*0.9952*1 = 0.868

$Q_s=I_b . A_a$ (Solar energy reflected on a parabolic dish)

$Q_{abs}= \eta_o * Q_s$

$Q_{rad.1}=\varepsilon_{abs}*\sigma*A_{abs.1}*(T_{abs}^4 - T_{amb}^4)$

$A_{abs}=\frac{\pi}{4}0.09^2$=0.0063 m^2

ε_{abs}=0.97

σ= 5.67 × 10^{-10} W/m^2.K^4

$Q_{rad.2}=\varepsilon_{abs}*\sigma*A_{abs.2}*(T_{abs}^4 - T_{amb}^4)$

$A_{abs.2}$=π*L*d = π *0.166*0.101 =0.0526 m^2

Where d: Diameter of the heat exchanger after insulation.

$Q_{conv.1}=A_{abs}*h_{air}*(T_{abs} - T_{amb})$

$h=2.8+(3*V_{wind})$

$Q_{loss}=Q_{rad1}+Q_{rad.2}+ Q_{rad.3}+Q_{conv.1}+Q_{Conv.2}+ Q_{Conv.3}$

$Q_{rad.1}$=0.97*5.67*10^{-8} *0.00636*($396.92^4 - 292.4^4$) =6.125 W

$Q_{rad.2}$=0.04*5.67*10^{-8}*0.0526(335.4^4-292.4^4) = 0.637 W

$Q_{rad.3}$=0.04*5.67*10^{-8}*0.008(335.4^4-292.4^4) =0.096W

h=2.8+(3*1.3) = 6.7

$Q_{conv.1}$=0.00636*6.7*(396.92-292.4) =4.453 W

$Q_{conv.2}$=0.0526*6.7(335.4-292.4) =15.154W

$Q_{conv.3}$=0.008*6.7*(335.4-292.4) =2.3048W

Q_{loss}=6.125+0.637+4.453+15.154+0.096+2.3048 =28.34 W (from 9:00-10:00)

Q_{useful} =1039.482-26.369 =1013.113

Table (A-1): Heat loss for the experiment conducted on 3/17/2022(Fins without nano filling)

Time	solar intensity(W/m^2)	Q_s(W)	Q_{abs}	Q_{loss}(W)	Q_{useful}(W)
09:00-10:00	651	1275.96	1107.53	28.34	1079.19
10:00-11:00	700	1372	1190.89	29.791	1161.10
11:00-12:00	795	1558.2	1352.51	27.58	1324.93
12:00-13:00	823	1613.08	1400.15	30.508	1369.64
13:00-14:00	767	1503.32	1304.88	31.322	1273.55
14:00-15:00	685	1342.6	1165.37	26.68	1138.69

Table (A-2): Heat loss for the experiment conducted on 24/4/2022(Fins without nano filling**)**

Time	solar intensity(W/m^2)	Q_s(W)	Q_{abs}	Q_{loss}(W)	Q_{useful}(W)
09:00-10:00	695	1362.2	1182.39	20.695	1161.69

10:00-11:00	750	1470	1275.96	23.471	1252.49
11:00-12:00	841	1648.36	1430.78	28.913	1401.867
12:00-13:00	875	1715	1488.62	22.197	1466.423
13:00-14:00	771	1511.16	1311.69	23.195	1288.495
14:00-15:00	689	1350.44	1172.18	27.348	1144.83

Table (A-3): Heat loss for the experiment conducted on 3/5/2022(Fins without nano filling**)**

Time	solar intensity(W/m^2)	Q_s(W)	Q_{abs}	Q_{loss}(W)	Q_{useful}(W)
09:00-10:00	707	1385.72	1202.80	22.83	1182.99
10:00-11:00	766	1501.36	1303.18	19.551	1283.63
11:00-12:00	869	1703.24	1478.41	20.57	1439.92
12:00-13:00	886	1736.56	1507.33	23.69	1483.64
13:00-14:00	833	1632.68	1417.17	18.573	1398.59
14:00-15:00	732	1434.72	1245.34	17.796	1227.54

Table (A-4): Heat loss for the experiment conducted on 13/5/2022(Fins without nano filling**)**

Time	solar intensity(W/m^2)	Q_s(W)	Q_{abs}(W)	Q_{loss}(W)	Q_{useful}(W)
09:00-10:00	741	1452.36	1260.65	18.196	1242.45
10:00-11:00	801	1569.96	1362.73	20.288	1342.44
11:00-12:00	880	1724.8	1497.13	25.89	1471.24
12:00-13:00	911	1785.56	1549.87	24.872	1524.99
13:00-14:00	827	1620.92	1406.96	28.88	1378.08
14:00-15:00	747	1464.12	1270.86	16.968	1253.89

Table (A-5): Heat loss for the experiment conducted on 18/3/2022) Fins with nano filling)

Time	solar intensity(W/m^2)	Q_s(W)	Q_{abs}(W)	Q_{loss}(W)	Q_{useful}(W)
09:00-10:00	659	1291.64	1121.14	17.25	1103.89
10:00-11:00	707	1385.72	1202.80	18.61	1184.19
11:00-12:00	799	1566.04	1359.32	21.715	1337.605
12:00-13:00	825	1617.00	1403.56	22.18	1378.68
13:00-14:00	772	1513.12	1313.39	18.94	1294.45
14:00-15:00	685	1342.60	1165.38	20.52	1144.86

Table (A-6): Heat loss for the experiment conducted on 25/4/2022) Fins with nano filling)

Time	solar intensity(W/m^2)	Q_s(W)	Q_{abs}(W)	Q_{loss}(W)	Q_{useful}(W)
09:00-10:00	696	1364.16	1184.09	20.356	1163.73
10:00-11:00	756	1481.76	1286.17	24.338	1261.83
11:00-12:00	845	1656.2	1437.58	27.46	1410.12
12:00-13:00	880	1724.8	1497.13	30.66	1466.47
13:00-14:00	775	1519	1318.49	23.321	1295.17
14:00-15:00	690	1352.4	1173.88	27.635	1146.25

Table (A-7): Heat loss for the experiment conducted on 6/5/2022) Fins with nano filling)

Time	solar intensity(W/m^2)	Q_s(W)	Q_{abs}(W)	Q_{loss}(W)	Q_{useful}(W)
09:00-10:00	711	1393.56	1209.61	15.11	1194.50

10:00-11:00	772	1513.12	1313.39	18	1295.39
11:00-12:00	875	1715	1488.62	20.409	1468.211
12:00-13:00	891	1746.36	1515.84	13.973	1501.87
13:00-14:00	840	1646.4	1429.08	22.854	1406.22
14:00-15:00	734	1438.64	1248.74	18.12	1230.62

Table (A-8): Heat loss for the experiment conducted on 14/5/2022) Fins with nano filling)

Time	solar intensity(W/m^2)	Q_s(W)	Q_{abs}(W)	Q_{loss}(W)	Q_{useful}(W)
09:00-10:00	738	1446.48	1255.54	23.351	1232.19
10:00-11:00	811	1589.56	1379.74	24.974	1354.76
11:00-12:00	885	1734.6	1505.63	27.199	1478.431
12:00-13:00	913	1789.48	1553.27	32.743	1520.53
13:00-14:00	830	1626.8	1412.06	26.478	1385.58
14:00-15:00	745	1460.2	1267.45	27.786	1239.67

Appendix (B): Calibration curves.

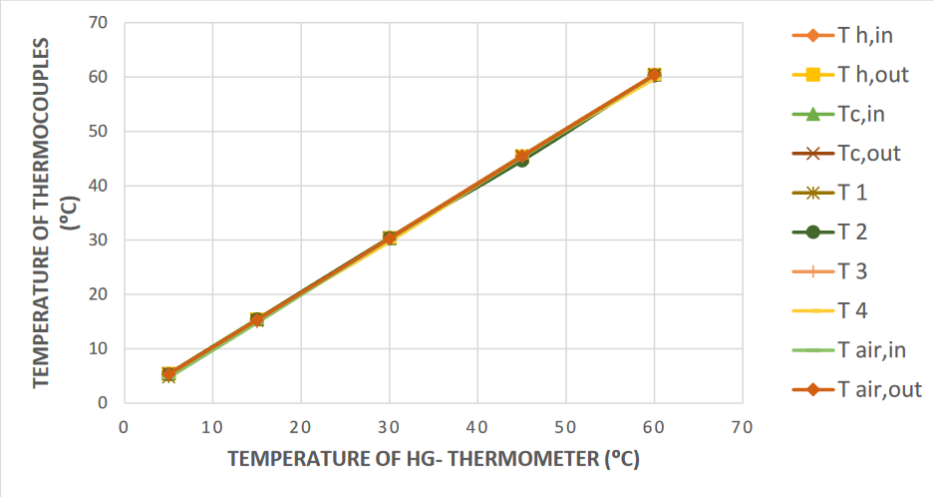

Fig. B-1: Calibration curve of thermocouples.

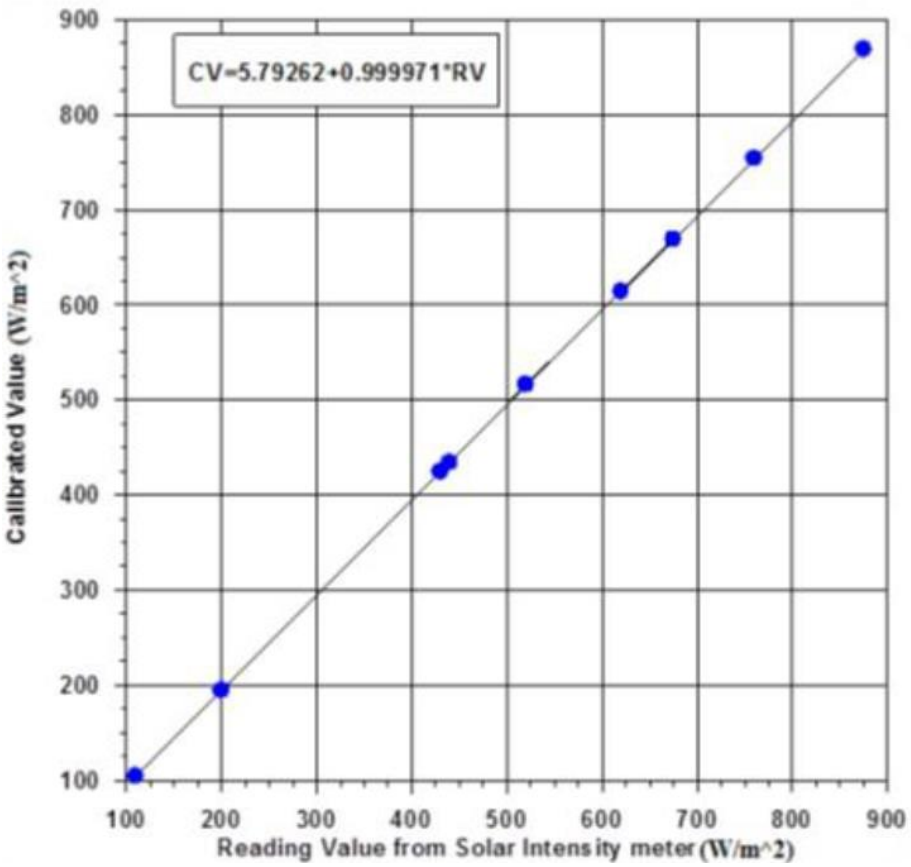

Fig. B-2: Calibration of solar power meter

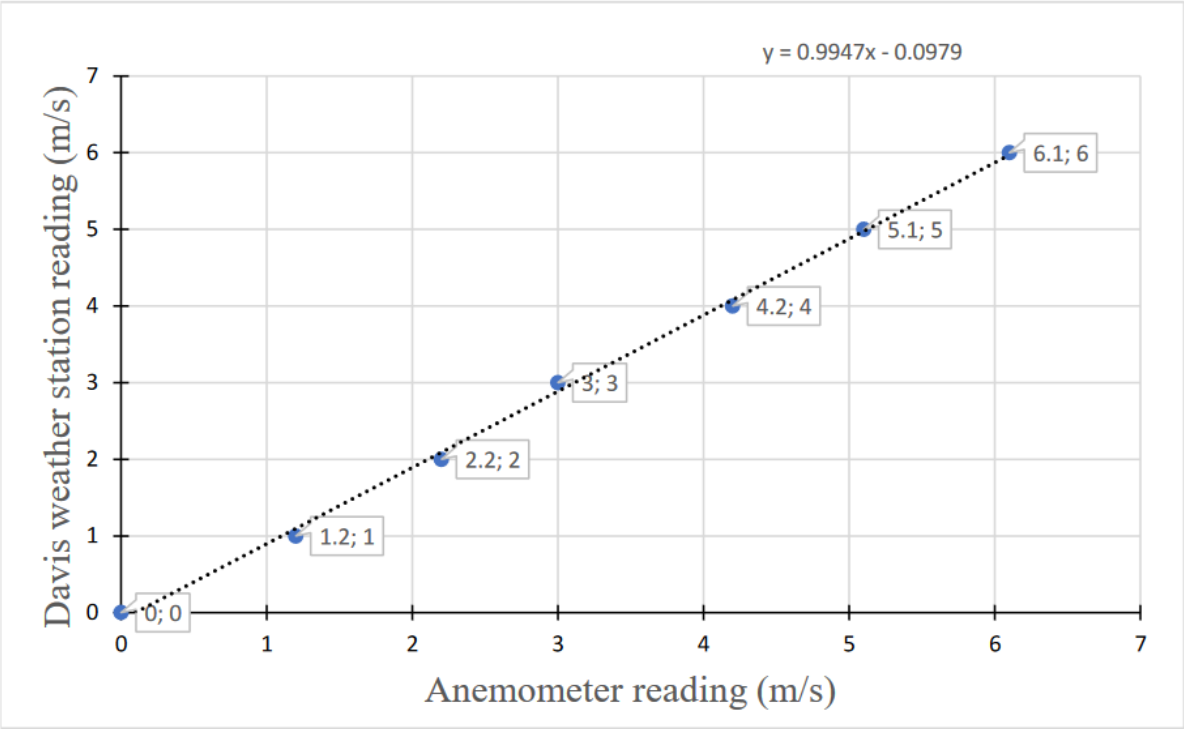

Fig. B-3: Anemometer calibration

Appendix (C): List of Publications

1. Water desalination by parabolic concentrator:A review.

1st International Conference on Achieving the Sustainable Development Goals

(6th – 7th) June 2022 in Istanbul- Turkey

Final Acceptance Letter

Manuscript Number: 157

Dear: Ahmed Raheem Qaida

Co-Authors: Ali Shakir Baqir and Montadhar Almoussawi

Congratulations!

It's a great pleasure to inform you that, after the peer review process, your manuscript entitled

(Water desalination by parabolic concentrator: A review)

had been **ACCEPTED** for participating in the **1st International Conference on Achieving the Sustainable Development Goals,** and considered for publication in **(AIP Conference proceeding).**

Thank you for your valuable participation in the ICASDG2022 conference.

Prof. Dr. Ahmed G. Wadday
ICASDG2022 Scientific Committee Chair | AIP Conference Proceeding Editor
6th – 7th June 2022 | Istanbul | Turkey

2. Experimental study of the use of solar parabolic dish concentrators in distillation of brackish water in Iraq.

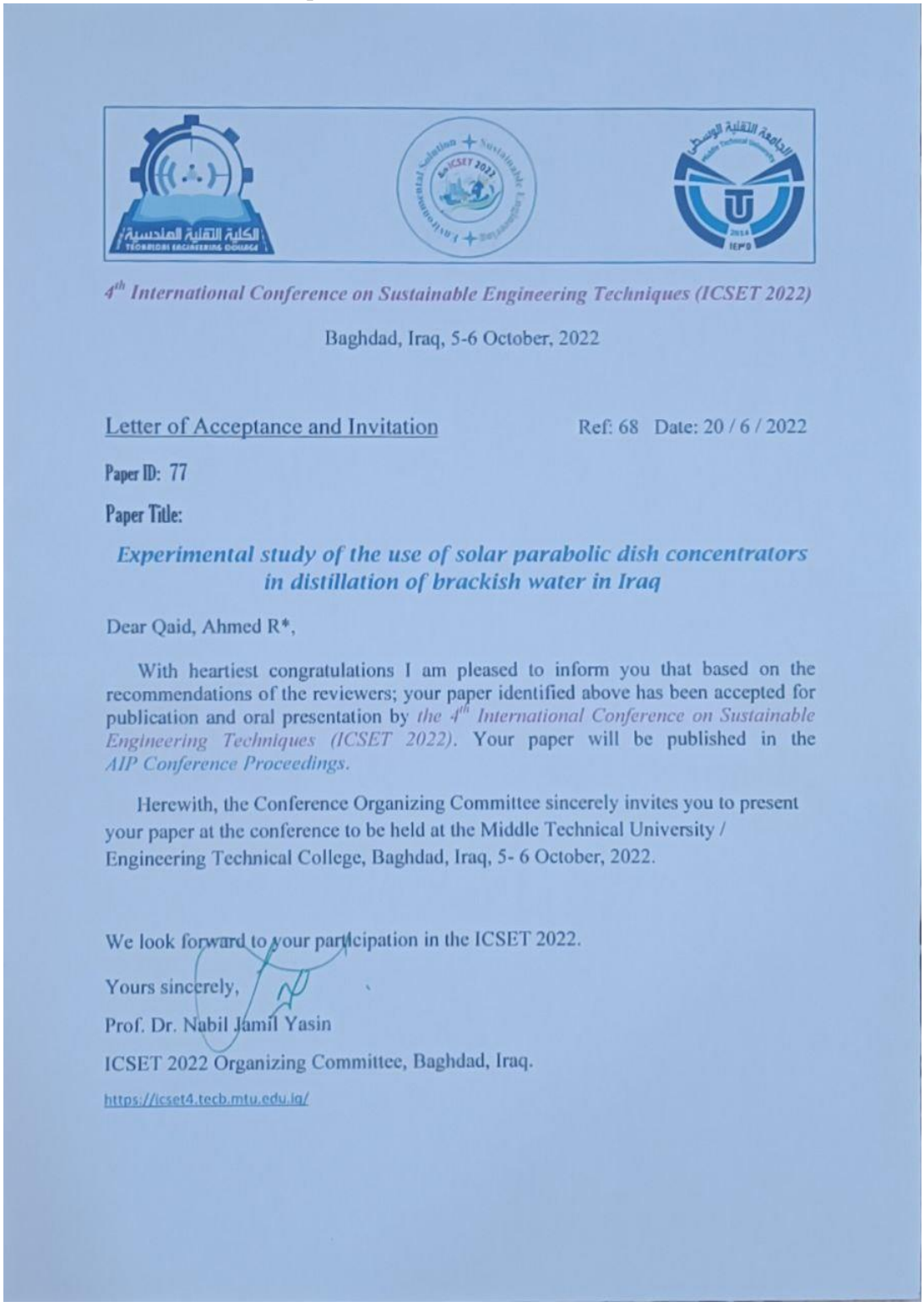

4th International Conference on Sustainable Engineering Techniques (ICSET 2022)

Baghdad, Iraq, 5-6 October, 2022

Letter of Acceptance and Invitation Ref: 68 Date: 20 / 6 / 2022

Paper ID: 77

Paper Title:

Experimental study of the use of solar parabolic dish concentrators in distillation of brackish water in Iraq

Dear Qaid, Ahmed R*,

With heartiest congratulations I am pleased to inform you that based on the recommendations of the reviewers; your paper identified above has been accepted for publication and oral presentation by *the 4th International Conference on Sustainable Engineering Techniques (ICSET 2022)*. Your paper will be published in the *AIP Conference Proceedings*.

Herewith, the Conference Organizing Committee sincerely invites you to present your paper at the conference to be held at the Middle Technical University / Engineering Technical College, Baghdad, Iraq, 5- 6 October, 2022.

We look forward to your participation in the ICSET 2022.

Yours sincerely,

Prof. Dr. Nabil Jamil Yasin

ICSET 2022 Organizing Committee, Baghdad, Iraq.

https://icset4.tecb.mtu.edu.iq/

الخلاصة

تعتبر الطاقة الشمسية أهم مصادر الطاقة البديلة في بلدنا العراق , ويمكن الاستفادة من هذه الطاقة سواء من خلال استخدام الالواح الشمسية لتوليد الطاقة الكهربائية أو من خلال الاستفادة من المحتوى الحراري المصاحب للطاقة الشمسية .وأحدى طرق الاستفادة من الطاقة الشمسية هي استخدام مركزات الطاقة الشمسية كمركز طبق القطع المكافئ.تهدف الدراسة الحالية الى تقطير المياه بأستخدام الطاقة الشمسية من خلال أستخدام مركز طبق القطع المكافئ الشمسي , كذلك العمل على تحسين إنتاجية منظومة تقطير المياه الشمسية من خلال استخدام مبادل حراري مبتكر يحتوي على زعانف داخلية لزيادة المساحة السطحية المعرضة للانتقال الحراري .أيضاً تم ابتكار أسلوب جديد لزيادة الانتقال الحراري وتسريع عملية تحول المياه الى بخار داخل المبادل الحراري من خلال استخدام حشوة المادة النانوية (MWCT), حيث يعتبر هذا العمل الأول من نوعه في العالم في أستخدام الحشوات النانوية.

في هذه التجربة تم أستخدام نموذجين من المبادلات الحرارية الأول يحتوي على زعانف داخلية من الالمنيوم ,والثاني يحتوي على زعانف داخلية تحتوي على حشوة نانوية من مادة انابيب الكاربون النانوية(MWCT) ذات الموصلية الحرارية العالية .أظهرت التجارب أن استخدام الحشوة النانوية ساهم بشكل كبير في زيادة إنتاجية منظومة تقطير المياه الشمسية , حيث بلغ معدل نسبة الزيادة في الإنتاجية بين النموذجين للايام التي أجريت فيها التجارب 57.67%.أن أقصى إنتاجية تم الحصول عليها بأستخدام النموذج الأول من المبادل الحراري ذو الزعانف الداخلية (بدون حشوة نانوية) كانت 10.17 لتر وكان عندها متوسط شدة الاشعاع الشمسي (W/m^2 817.8) وبمعدل ساعات عمل لمنظومة التقطير مقدارهُ 6 ساعات , حيث بدءت التجارب عند الساعة 9:00صباحاً وتوقفت في الساعة 15:00مساءاً .بينما بلغت أقصى إنتاجية لمنظومة التقطير عند استخدام النموذج الثاني من المبادل الحراري (زعانف ذات حشوة نانوية) 6.11 لتر وبمعدل ساعات عمل مقدارهُ 6ساعات , وكانت عندها متوسط شدة الاشعاع الشمسي ($820.33\ W/m^2$).أيضاً أظهرت النتائج أن استخدام الصوف الزجاجي كمادة عازلة للمبادل الحراري ساهم بشكل كبير في تقليل الفقد الحراري , حيث أن الفقد الحراري لم يتجاوز 2% من مجمل الطاقة التي يمتصها سطح غطاء المبادل الحراري.

دراسة عملية لتأثير ملئ الزعانف بحشوات نانوية المستخدمة في المبادل الحراري على

رسالة مقدمة الى

قسم هندسة تقنيات ميكانيك القوى

كجزء من متطلبات نيل درجة الماجستير في

هندسة تقنيات ميكانيك القوى/ الحراريات

تقدم بها

أحمد رحيم قائد

ماجستير في هندسة تقنيات ميكانيك القوى

اشراف

الاستاذ الدكتور

علي شاكر باقر

الأستاذ المساعد الدكتور

منتظر عبودي الموسوي

1444

جمهورية العراق

وزارة التعليم العالي والبحث العلمي

جامعة الفرات الاوسط التقنية

الكلية التقنية الهندسية/النجف

دراسة انتاج مياه مقطرة قليلة الملوحة /مياه البرك بأستخدام مبادل حراري شمسي معدل بأستخدام طلاء بالجسيمات النانوية

أحمد رحيم قائد

ماجستير في هندسة تقنيات ميكانيك القوى

1444